Chapter 22

Nose, Larynx, and Trachea

Ronald A. Herbert[1], Kyathanahalli S. Janardhan[2], Arun R. Pandiri[1], Mark F. Cesta[1] and Rodney A. Miller[3]

[1]National Institute Of Environmental Health Sciences, Research Triangle Park, NC, USA, [2]Integrated Laboratory Systems Inc., Research Triangle Park, NC, USA, [3]Experimental Pathology Laboratories, Inc., Research Triangle Park, NC, USA

Chapter Outline

1. INTRODUCTION

The upper respiratory tract (nose, pharynx, and larynx) and trachea are morphologically complex and have multiple functions. Although specific attention is focused on these tissues in inhalation studies, treatment-related effects sometimes occur in the nose following exposure to chemicals administered by other routes, such as gavage dosing. Because of the varied anatomic features of the nasal passages and the encasement of the nose within the bones of the maxilla, special attention to collection, fixation, trimming, and sectioning is required to obtain uniform sections. Optimal decalcification, rinsing, and processing are critical for obtaining well-stained sections of the nose for histopathological evaluation. Anatomical landmarks for trimming and careful embedding must be used to consistently obtain the desired sections. These landmarks are illustrated and described in Section 2. Typically, three or four levels of the nose, three levels of the larynx, and one section of the trachea are examined. This chapter provides a brief outline of the morphology of the nose, larynx, and trachea and descriptions of spontaneous and treatment related lesions observed in these tissues in toxicity and carcinogenicity studies.

2. NORMAL UPPER RESPIRATORY TRACT

2.1. Embryology

Between days 10−15 of gestation, the structures of the nasal passages develop from bilateral, oval thickenings of the surface ectoderm, the nasal placode. Proliferation of the mesenchyme at the margins of the placode produces a depression (the nasal pit), which deepens to form the primary nasal cavity. The first microvilli on respiratory epithelium appear around day 14, and by day 18, cilia are evident. The olfactory epithelium develops from ectoderm of the olfactory placode in the roof of the nasal passages. Primitive neuroepithelial cells become neuroblasts and then esthesioneurocytes, which are thought to differentiate into sustentacular cells and olfactory neurons. By day 18 of gestation, the olfactory epithelium exhibits clear differentiation of sensory and sustentacular cells and resembles that in the adult rat.

The larynx and trachea develop from the laryngotracheal groove in the ventral wall of the pharynx and the foregut. The anterior trachea and developing larynx are independent of the pharynx by day 13 or 14. The connective tissue, cartilage, and smooth muscle of these structures develop from the splanchnic mesenchyme surrounding the foregut. The endoderm lining the laryngotracheal tube gives rise to the epithelium and glands of the larynx and trachea. Cilia develop in tracheal epithelial cells approximately 2 days later than in the nasal cavity, and secretory cells appear on days 19−20. The mucociliary epithelium continues to develop during the postnatal period.

2.2. Anatomy and Histology

2.2.1. Nasal Cavity

The structure of the nasal passages is best appreciated by the combined processes of observation during dissection, histologic examination, and inspection of nasal casts (Morgan and Monticello, 1990; Morgan et al., 1989; Schreider and Raabe, 1981). The nasal passages consist of two major compartments separated by a septum with three well-developed sets of turbinates, the nasoturbinates, maxilloturbinates, and ethmoid turbinates (Figure 22.1), that project into the lumen of each compartment (Harkema et al., 2006). The septal window in the caudoventral portion of the nasal cavity provides a direct connection between the left and right nasal passages and the nasopharyngeal duct. The septal window is the point of convergence for both air and mucus streams. There are four main routes for inspiratory airflow through the dorsal, middle, ventral, and lateral meatuses (Figure 22.1) (Morgan et al., 1989). Nasal airflow pattern is one of numerous factors influencing the distribution of nasal lesions in toxicology studies (Morgan and Monticello, 1990). The lateral meatus has a characteristic medially curved profile ventrally and a
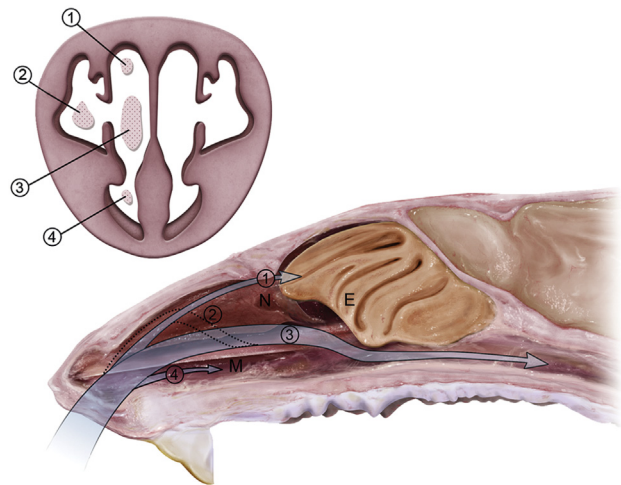

FIGURE 22.1 Illustrations of nasal cavity showing the ethmoid turbinates (E), nasoturbinates (N) and maxilloturbinates (M) and four principal routes of air flow during inspiration. 1. Dorsal meatus, 2. Lateral meatus, 3. Middle meatus, and 4. Ventral meatus. *Modified from Morgan, K.T., Monticello, T.M., Patra, A.L., Fleishman, A., 1989. Preparation of rat nasal airway casts and their application to studies of nasal airflow. In: Crapo, J.D., Smolko, E.D., Miller, F.J., Graham, J.A., Hayes, W.A. (Eds.), Extrapolation of Dosimetric Relationships for Inhaled Particles and Gases. Academic Press, Inc., San Diego, California, pp. 45−58.*

curved lateral recess dorsally, which reflect its anatomical association with the roots of the incisor teeth.

The bilaterally symmetric nasopalatine ducts pass through incisive canals of the hard palate connecting nasal and oral cavities. These ducts are about 0.5 mm in diameter in adult F344 rats and may provide a passageway for nasal secretions or air. These ducts have valve-like flaps on the buccal aspect to prevent passage of material from the oral cavity into the nose.

The microscopic anatomy of the nasal cavity varies extensively along its length. Nasal lesions tend to be site specific due to airflow, regional deposition of inhaled toxicants and chemicals, and regional tissue sensitivity or susceptibility to these agents (Morgan and Monticello, 1990). In toxicologic studies, it is essential to sample and evaluate the nasal cavity in relation to the regional differences. Three sections are routinely examined microscopically in studies sponsored by the National Toxicology Program. However, modifications in the number of levels sectioned may be necessary, depending on the degree of detail needed for a particular study (Mery et al., 1994). Specific palatal landmarks are used to obtain the necessary sections (Figure 22.2). Level I is trimmed immediately posterior to the upper incisor teeth; Level II, through the level of the incisive papilla anterior to the first palatial ridge; Level III, through the middle of the second molar teeth. Using these landmarks, some variation will still be observed. A difference of millimeters at a particular level will alter the amount and shape of nasoturbinates and teeth, the location of ducts and accessory glands, and the types of epithelium in the section.
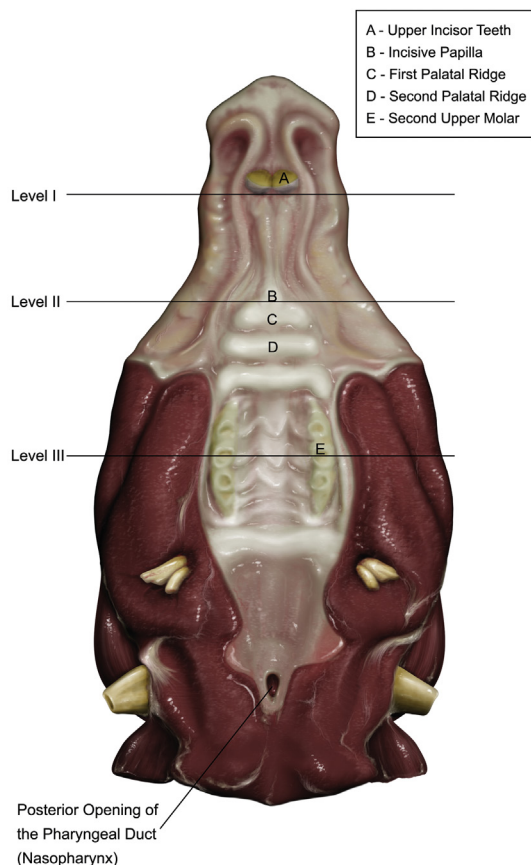
In the optimal section, the mucosa of Level I consists primarily of respiratory and squamous epithelia (Figure 22.3). Transitional epithelium lines the lateral aspects of Level I. If sections of Level I are slightly posterior to that shown in Figure 22.3, olfactory epithelium will be present in the dorsal meatus. The nasolacrimal duct appears nearest to the lumen of the nasal cavity in Level I.

In Level II, three types of epithelium (squamous, respiratory, and olfactory) are present (Figure 22.4). The roots of the incisor teeth are prominent, and the nasolacrimal duct is lateral to the incisor tooth in Level II. A portion of the incisive duct is present in this section.

The most posterior section, Level III, contains the olfactory region in which the ethmoid turbinates are most prominent (Figure 22.5). The left and right sides of the nasal passage are separated by the delicate nasal septum in the dorsal two-thirds of the nasal cavity. The two sides communicate ventrally via the septal window where they merge into a single midline nasopharyngeal meatus that extends to the nasopharynx via the nasopharyngeal duct.

The total surface area of the nasal passages of a 16-week-old F344 rat is approximately 1340 mm² (Gross et al., 1982); various morphometric data on the nasal cavity are presented in other publications (Parent, 2015). Approximately 50% of the nasal passages is lined by sensory olfactory neuroepithelium, 46% by the respiratory and transitional epithelium, and 3.5−4% by squamous epithelium. The septal olfactory organ (Organ of Masera), an isolated patch of olfactory epithelium surrounded by

A - Upper Incisor Teeth
B - Incisive Papilla
C - First Palatal Ridge
D - Second Palatal Ridge
E - Second Upper Molar

FIGURE 22.2 Drawing of the ventral surface of the skull showing landmarks for the three levels of nasal sections.

(A) **(B)**

— **Transitional Epithelium**
— **Respiratory Epithelium**
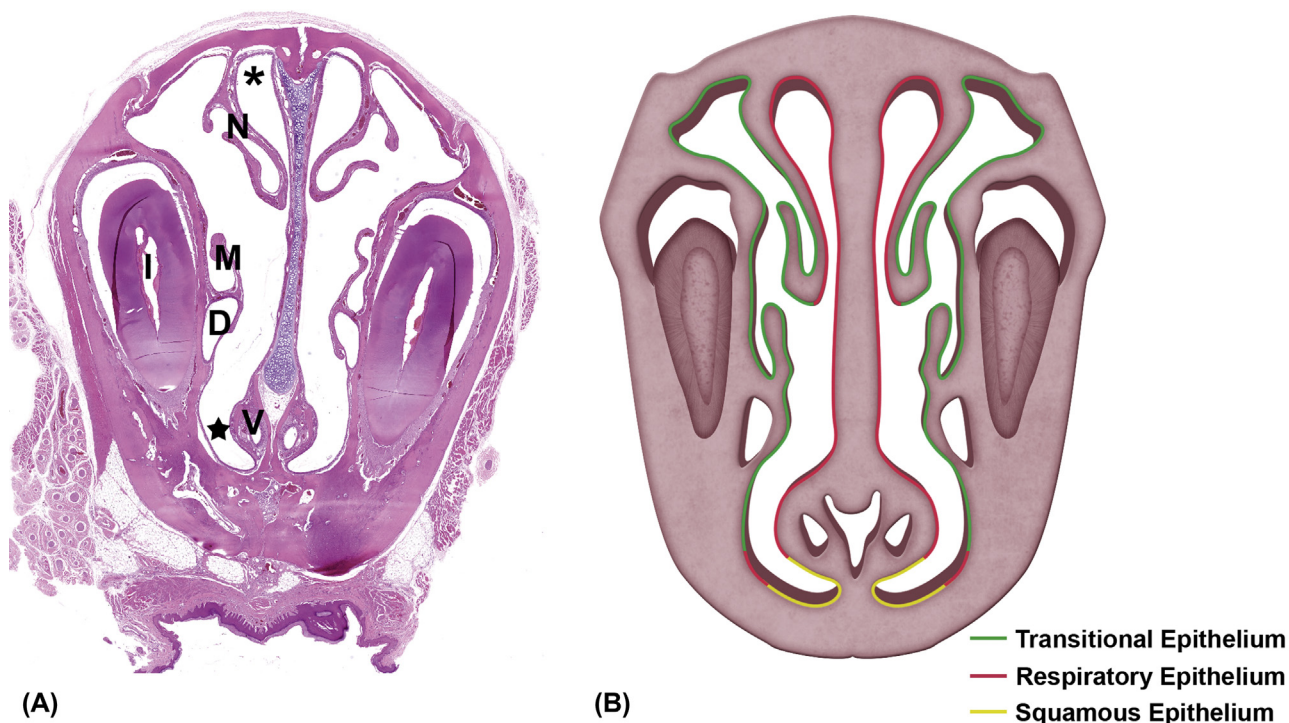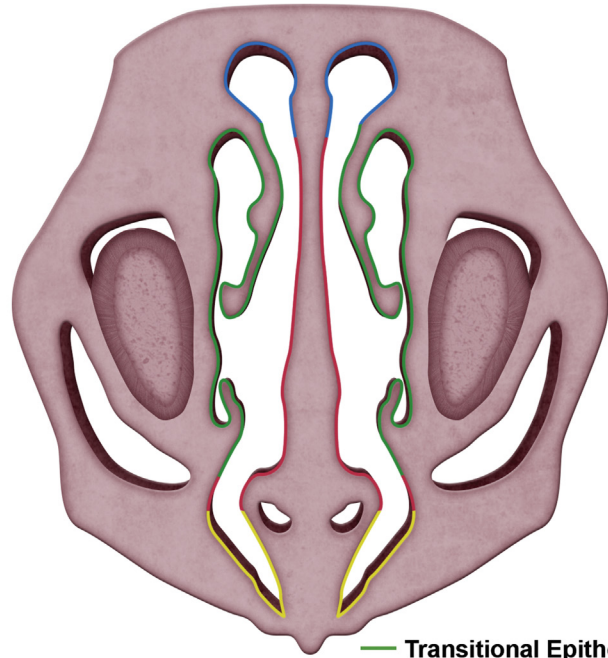— **Squamous Epithelium**

FIGURE 22.3 Photomicrograph of the Level 1 section (A) showing the nasoturbinates (N) and maxilloturbinates (M) with lateral hooks and nasolacrimal duct (D) medial to medioventral to the incisor (I) tooth. Vomeronasal organ (V) is at the base of nasal septum. Dorsal meatus (asterisk) and ventral meatus (star) are also shown. Illustration (B) demonstrates the types of epithelium normally present in Level 1 sections.

FIGURE 22.4 Photomicrograph of the Level 2 section (A) showing nasoturbinates (N) and maxilloturbinates (M) which no longer have characteristic lateral hooks. Nasolacrimal ducts (D) are lateral to the incisor (I) teeth and incisive ducts (ID) are at the base of the septum (S), ventral to the vomeronasal organ (V). Dorsal meatus (asterisk) and ventral meatus (star) are also shown. (B) Illustration of the types of epithelium normally present in Level 2 sections.

Legend (Figure 22.4B):
— Transitional Epithelium
— Respiratory Epithelium
— Squamous Epithelium
— Olfactory Epithelium
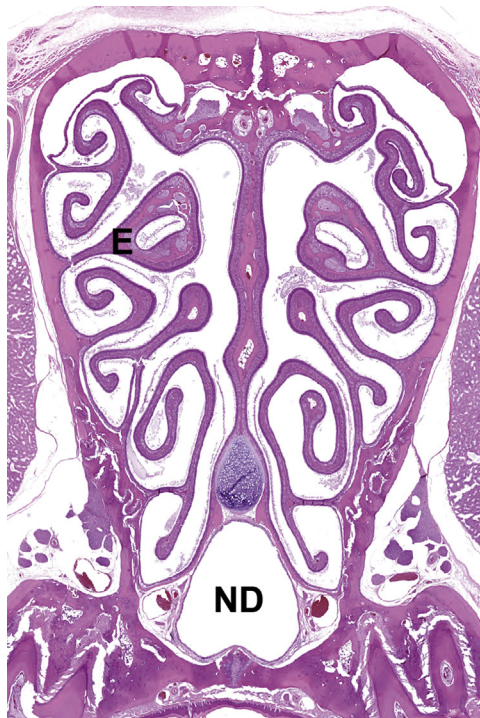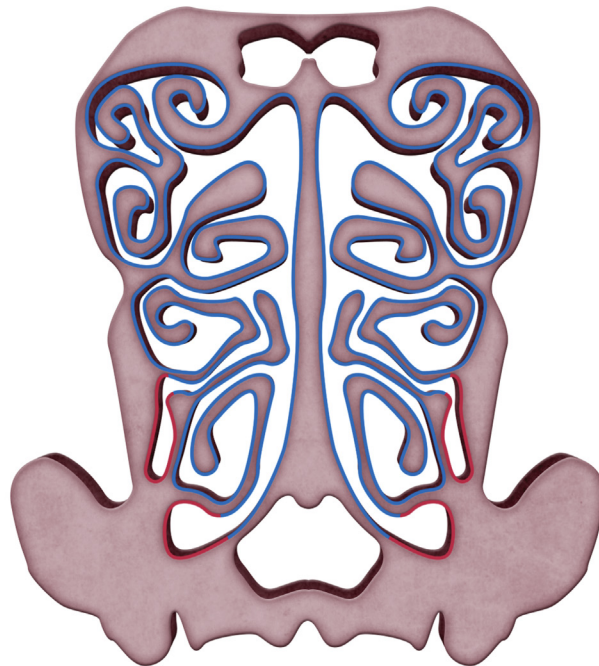
FIGURE 22.5 Photomicrograph of the Level 3 section (A) showing extensive scrolls of the ethmoid turbinates (E) and nasopharyngeal duct (ND). (B) Illustration of the types of epithelium normally present in Level 3 sections.

Legend (Figure 22.5B):
— Transitional Epithelium
— Respiratory Epithelium
— Squamous Epithelium
— Olfactory Epithelium

respiratory epithelium at the base of the nasal septum near the entrance to the nasopharyngeal duct, occupies nearly 2% of the surface area (Bojsen-Møller, 1975; Katz and Merzel, 1977; Weiler and Farbman, 2003). In addition to these epithelial types, the mucosa lining the nasal passages shows highly specific regional features with respect to physiology and biochemistry.

The nares have a spiral profile, and the nasal vestibule (the portion of the nasal cavity enclosed by cartilage) is completely lined by lightly keratinized, stratified squamous epithelium which functions to protect the underlying tissues from potentially toxic gases and vapors. This epithelium is composed of a single layer of basal cells that rest on a basal lamina, and several layers of squamous epithelial cells that progressively flatten towards the lumen of the vestibule. The squamous epithelium lining the nasal vestibule extends along the floor of the ventral meatus through the nasopalatine (incisive) ducts to merge with the squamous epithelium of the oral mucosa.

Respiratory epithelium is a pseudostratified ciliated cuboidal to columnar epithelium that extends from the margins of the squamous epithelium of the vestibule to the nasopharynx via the nasopharyngeal duct. It covers most of the lateral walls, most of the medial aspects of maxilloturbinates, most of the medial aspects of the naso-turbinates, and the anterior and ventral portions of the ethmoid turbinate, where it forms a complex zone of interdigitation with the olfactory epithelium.

The nasal respiratory epithelium consists of six morphologically distinct cell types (Monteiro-Riviere and Popp, 1984; Uraih and Maronpot, 1990): ciliated columnar, nonciliated columnar, mucous (goblet), brush, cuboidal, and basal cells. These cell types are unevenly distributed along the mucosal surface and rest on a basal lamina of reticular and collagen fibrils (Figure 22.6). The epithelium has a wide range of site-specific characteristics, including differences in epithelial height, density of ciliated cells and goblet cells, and enzyme activity. Along the nasal septum, the respiratory epithelial cells are evenly distributed from proximal to caudal sites; the epithelium is highly ciliated, and contains numerous goblet cells (Figure 22.7). In contrast, the epithelium lining the lateral meatuses and tips of the turbinates (transitional epithelium) is nonciliated, sparsely ciliated, or have short microvilli (Figure 22.8).

The lamina propria in the respiratory epithelial region is a highly vascularized, loose, fibroelastic connective tissue that contains many mucous and serous glands (Bojsen-Møller, 1964; Katz and Merzel, 1977; Uraih and Maronpot, 1990). The glands in the anterior half of the nasal septum (anterior septal glands) are tubuloalveolar glands comprising numerous solitary acini and a single long duct that empties into the vestibule. The secretions are primarily serous. The posterior septal glands, ventral to the junction between the respiratory epithelium and the septal olfactory organ, and near the bony encasement of the vomeronasal organ, have a mucous secretion that empties into the vomeronasal organ. The posterior septal glands can be clearly distinguished from the anterior septal glands by periodic acid-Schiff (PAS) staining of the posterior glands. The lamina propria of the turbinates and lateral wall also contains tubular and compound acinar glands whose ducts open directly into the maxillary sinus or nasal lumen.

Swell bodies are cavernous venous plexuses in the lamina propria of the respiratory epithelial region that dilate to alter airflow in the two halves of the nasal passage (Bojsen-Moller and Fahrenkrug, 1971; Uraih and Maronpot, 1990). The largest swell bodies are located on the lateral wall between the naso- and maxilloturbinates, with smaller swell bodies on the maxilloturbinates (Figure 22.9) and nasal septum.
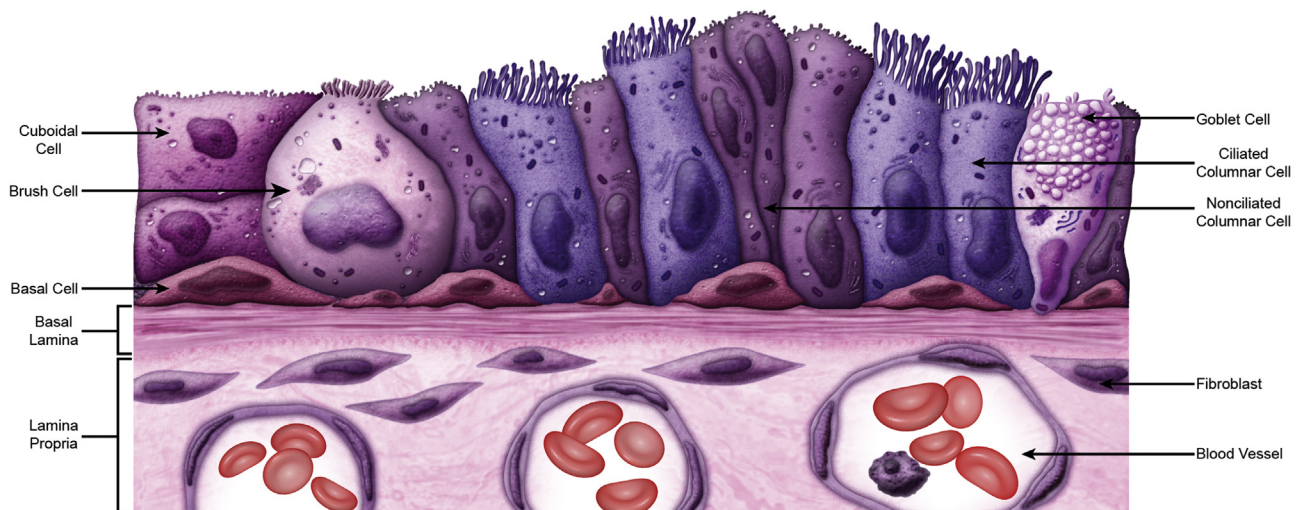

FIGURE 22.6   Illustration of the six different cell types of the respiratory epithelium and relationship to lamina propria.
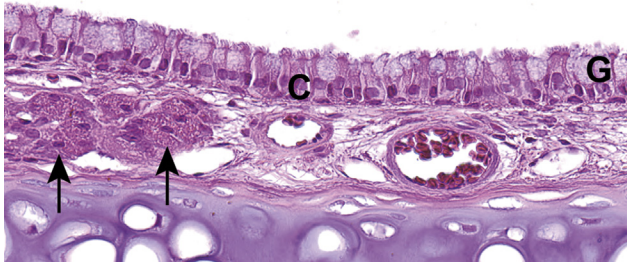
FIGURE 22.7   Photomicrograph of respiratory epithelium on the nasal septum showing ciliated cells (C), goblet cells (G), and submucosal glands (arrows).
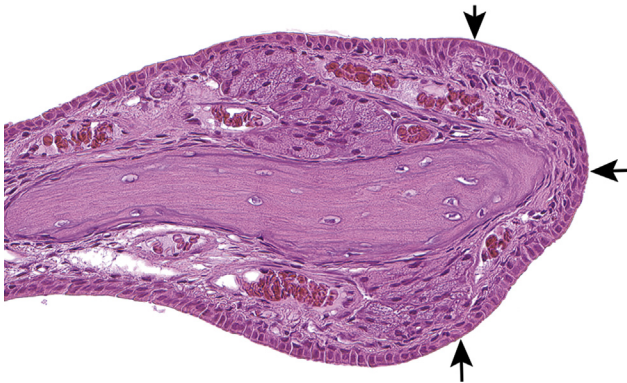

FIGURE 22.8   Tip of the nasoturbinate covered by cuboidal transitional epithelium (arrows).
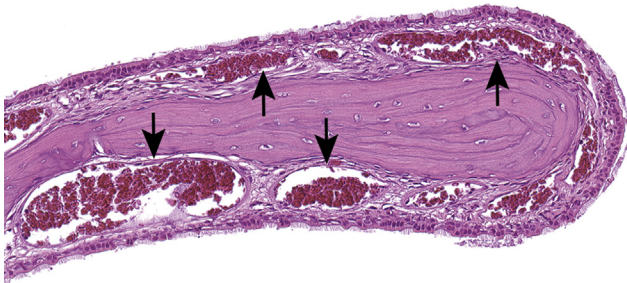

FIGURE 22.9   Swell bodies consist of prominent vascular spaces (arrows) in the mucosa of the maxilloturbinate.

Transitional type respiratory epithelium is located in a narrow region in the proximal nasal cavity distal to the squamous epithelium, and proximal to the ciliated respiratory epithelia, and lines the tips and lateral aspects of the naso- and maxilloturbinates and the lateral walls of nasal meatuses (Harkema et al., 2006). The transitional epithelium is thin (one to two cells thick), cuboidal to low columnar, nonciliated, has surface microvilli, and rests on a single layer of basal cells (Figure 22.8). The lamina propria is similar to that beneath the respiratory epithelium.

Olfactory epithelium covers the upper posterior one-third of the nasal septum, much of the dorsal meatus including the attachment of the nasoturbinates, portions of posterior lateral nasal wall, and the ethmoid turbinates (Katz and Merzel, 1977). Olfactory epithelium is pseudostratified and comprising three epithelial cell types—olfactory sensory neurons (neuroepithelium), sustentacular (supporting) cells, and basal cells (Figures 22.10 and 22.11) (Mendoza, 1993; Vollrath et al., 1985). The sensory neurons are bipolar, and interposed between the sustentacular cells. The nuclei and perikaryon of the olfactory neurons are in the middle third of the epithelial layer. An apical dendritic process extends above the surface of each epithelial cell to form a bulbous swelling, the olfactory vesicle. The olfactory vesicle has 10−15 basal bodies that give rise to long, nonmotile, sensory cilia that are approximately 50 microns in length and 0.1−0.3 microns in diameter (Harkema et al., 2006; Jenkins et al., 2009; Menco, 1997; Naguro and Iwashita, 1992). These cilia intertwine with each other and with surface microvilli to provide an extensive surface area for reception of odorants. An axon originates from the base of each olfactory neuron and passes through the basal lamina to join axons from adjacent neuronal cells to form nonmyelinated nerve fascicles and bundles in the lamina propria. The axons from the olfactory nerves traverse perforations in the cribriform plate to synapse with neurons forming the outer olfactory nerve layer of the olfactory bulb.

The columnar sustentacular (supporting) epithelial cells that surround the olfactory sensory neurons, span the entire thickness of the olfactory epithelium from the airway surface to the basal lamina. The nuclei of the sustentacular cells are aligned in a single row along the apical one third of the olfactory epithelium. The supranuclear portion of the cell is broad whereas the portion of the cell below the nucleus is thin and forms foot-like processes that attach to the basal lamina. The cytoplasmic processes of the sustentacular cells surround and support the sensory neurons. Their apical surfaces are lined by numerous long microvilli that intertwine with the cilia of the olfactory neurons along the surface of the epithelium (Naguro and Iwashita, 1992; Nomura et al., 2004). The dendrites of sensory cells and supranuclear portion of the supporting cells can easily be recognized ultrastructurally; the supporting cells contain a well-developed smooth endoplasmic reticulum whereas the dendrites contain microtubules, mitochondria and sparse smooth endoplasmic reticulum (Mendoza, 1993).

Two types of basal cells, horizontal and globose, are described in the olfactory epithelium (Graziadei and Graziadei, 1979). These cells are morphologically similar to basal cells in the respiratory epithelium but have extended cytoplasmic processes that often sheathe the axon processes of olfactory neurons. The horizontal basal cells rest on the basal lamina and have elongated nuclei. The globose basal cells are oval to round cells with a round nucleus and are located above the horizontal basal cells. The basal cells are generally considered the
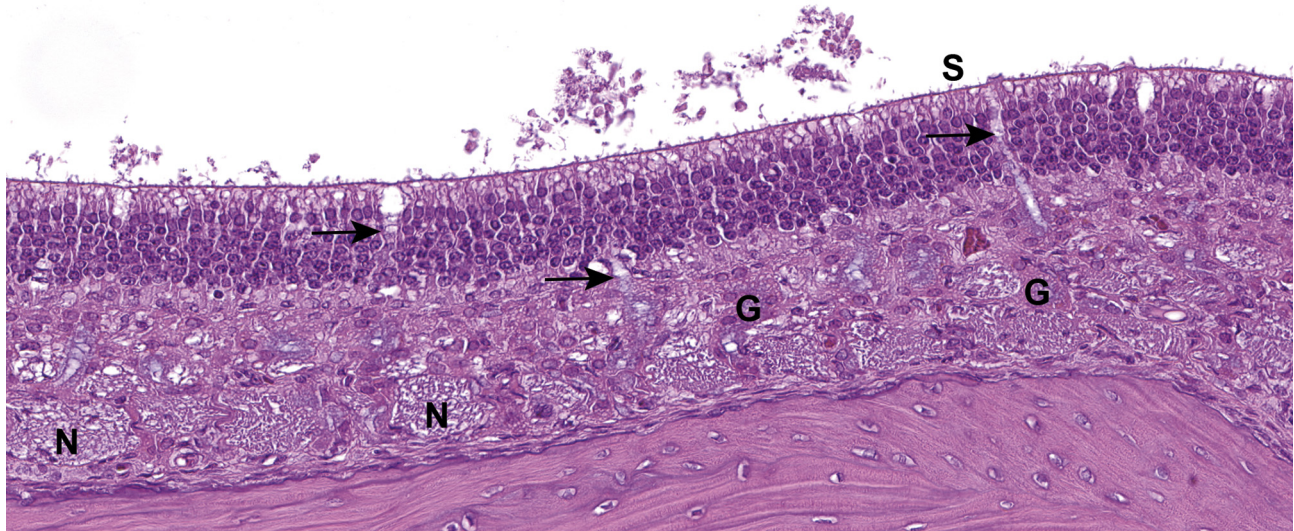
FIGURE 22.10   Photomicrograph of the olfactory epithelium showing nerve bundles (N) and submucosal glands (G) in the lamina propria. Ducts (arrows) of the glands extend through the olfactory epithelium and open on the luminal surface (S).
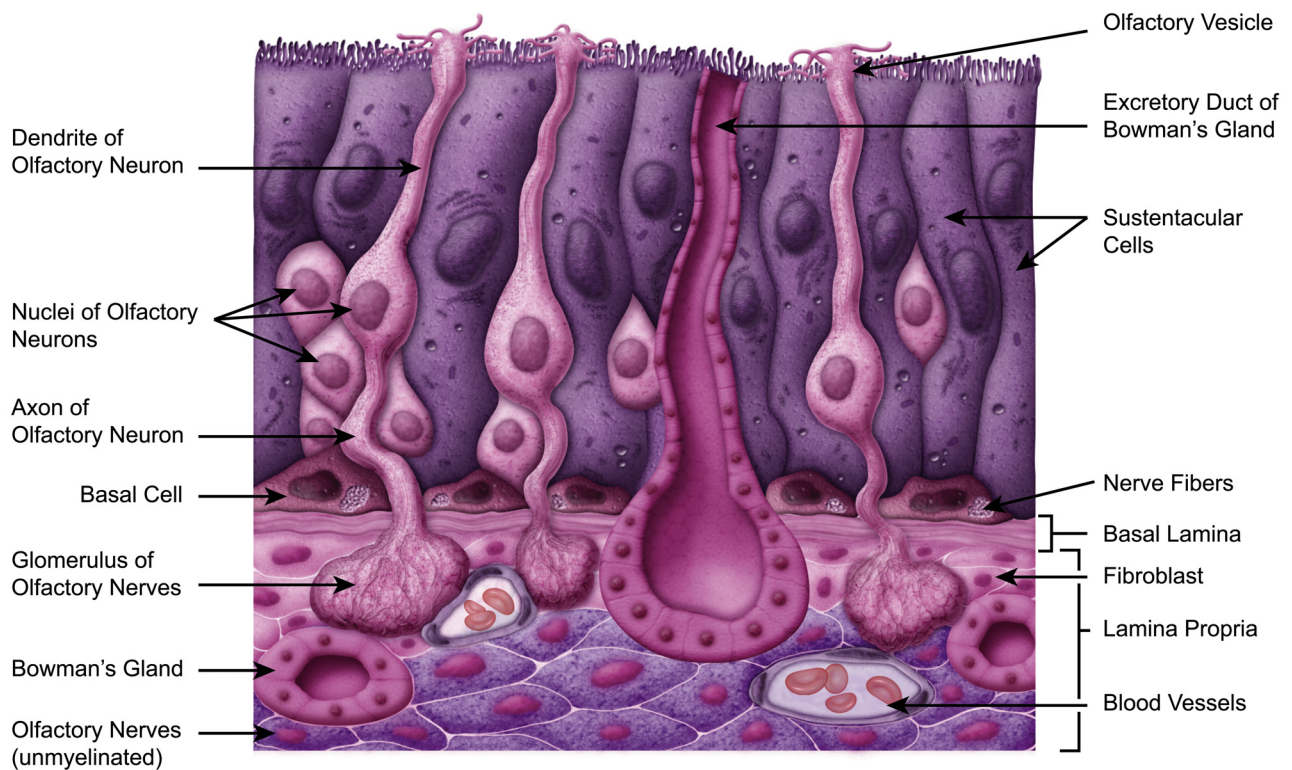
FIGURE 22.11   Illustration of the olfactory epithelium showing various cells and glands that comprise this complex epithelium.

progenitor cells for the regenerating olfactory neuroepithelium (Huard and Schwob, 1995; Jang et al., 2014). Olfactory neurons, in contrast to other neurons, are capable of regeneration, having a 28- to 30-day turnover rate (Harkema and Morgan, 1996).

The lamina propria of the olfactory region contains prominent nerve bundles, blood vessels, and submucosal glands (Bowman's glands). The glands are of simple tubular type composed of small compact acini interspersed among the olfactory nerve bundles (Figures 22.10 and 22.11). Ducts of the submucosal glands traverse the basal lamina at regular intervals, extend through the olfactory epithelium, and open on the luminal surface of the olfactory mucosa (Nomura et al., 2004). These glands, which

may contain both serous and mucus-producing cells, may be important in olfactory epithelial regeneration.

Discrete focal aggregates of nasal-associated lymphoid tissue (NALT) are present within the submucosa at the caudoventral aspect of the left and right nasal passages adjacent to the opening to the nasopharyngeal ducts (Cesta, 2006; Spit et al., 1989). These focal lymphoid aggregates are covered by a specialized lymphoepithelium composed of ciliated cuboidal cells, low numbers of mucous cells, and numerous nonciliated cuboidal cells (microfold cells or M cells) that lack or contain short irregular microvilli (Corr et al., 2008). The M cells are similar to those of the gut- and bronchus-associated lymphoid tissues (GALT and BALT). Most of the nasal secretions pass over this area on their way to the nasopharynx. NALT is considered to play a central role in regional mucosal immunity of the upper respiratory tract. M cells function in the uptake and translocation of antigen from the surface of the nasal epithelium to the submucosal lymphoid aggregates. B- and T-lymphocytes have a distinct zonal distribution within NALT with a predominance of B-lymphocytes, and a high CD4:CD8 ratio in T-lymphocyte zones (Cesta, 2006; Harkema et al., 2006).

2.2.2. Vomeronasal Organ

The vomeronasal (Jacobson's) organ consists of paired tubular diverticula within the vomer bone in the ventral portion of the nasal septum. It is an auxiliary olfactory sense organ in mammals involved in the flehmen response to pheromone detection. The diverticula are discrete chemoreceptor structures. One side of each diverticulum is lined by tall, ciliated, columnar epithelium, and the opposite side by neuroepithelium similar to that of the olfactory region, however, basal cells are absent (Mendoza, 1993) (Figures 22.3, 22.4, 22.12). The epithelial components of this organ follow a spiral course in the long axis of the nose. The sensory neurons of the vomeronasal organ have olfactory vesicles that lack the long cilia of the olfactory epithelium, but have numerous long microvilli (Harkema and Morgan, 1996; Mendoza, 1993; Vaccarezza et al., 1981). Axons of the neurons extend posteriorly and aggregate to form the vomeronasal nerves which synapse in the accessory olfactory bulbs.

2.2.3. Nasolacrimal Ducts

The paired nasolacrimal ducts carry lacrimal secretions from the eye to the nasal cavity, and originate as oval openings near the edge of the medial canthus of the eyelids. Each duct extends cranio-ventrally along the lateral surface of the lacrimal bone, through the infraorbital fissure, and enters the osseous nasolacrimal canal, where it is seen in histological sections of the nasal passage. Initially the duct is small and circular, but in the middle portion, the diameter increases and the appearance is
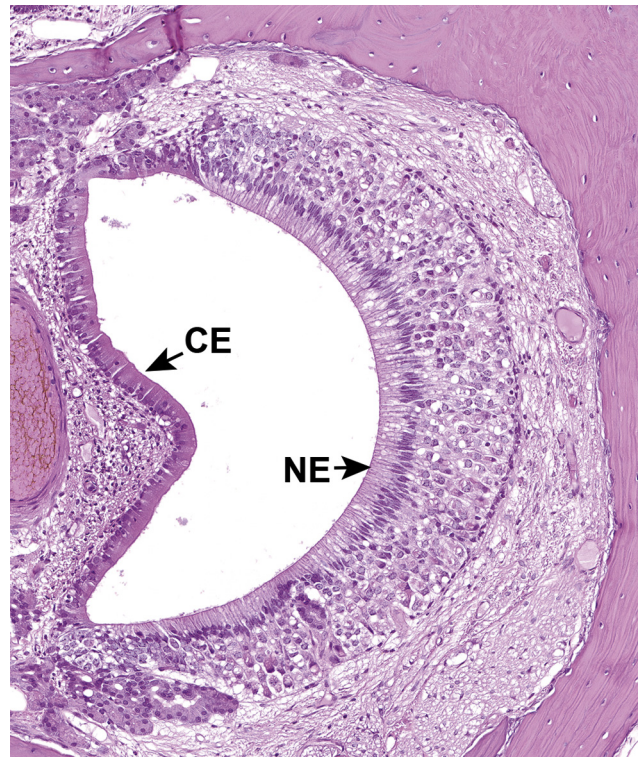

FIGURE 22.12 Photomicrograph of the vomeronasal organ showing neuroepithelium (NE) and ciliated epithelium (CE).

more oblong and saccular. The diameter again decreases before the duct enters the ventrolateral nasal vestibule medial to the root of the incisor tooth approximately 2 mm caudal to the nares.

The location of the nasolacrimal ducts in the histology sections varies depending on the level being examined, as does the lining epithelium which varies from squamous to low cuboidal. In Level I, the duct appears ventral or medial to the root of the incisor tooth (Figure 22.3) and is lined by squamous epithelium. In Level II, the duct, lined by cuboidal to squamous epithelium, is lateral to the root of the incisor tooth and appears as an oblong, saccular structure (Figure 22.4).

2.2.4. Maxillary Sinuses

The rat has one pair of paranasal sinuses (the maxillary sinuses) located in the lateral wall of the nasal cavity. The maxillary sinuses are lined by a ciliated columnar epithelium with few goblet cells. The lamina propria surrounding the sinuses contains prominent glands (Steno's glands) that extend deep into the connective tissue of the lateral wall ventral to the ostium of the maxillary sinus. The ducts of the glands open into the nasal vestibule.

2.2.5. Larynx

The larynx is situated between the pharynx and the proximal end of the trachea and has the primarily mechanical

function of preventing food from entering the trachea during swallowing. The larynx also functions as an organ of phonation. The larynx is bilaterally symmetrical, comprising a cartilaginous framework of three single cartilages (epiglottis, thyroid, and cricoid), two paired cartilages (arytenoid and cuneiform) and a U-shaped cartilage at the ventral depression of larynx, that enclose the laryngeal cavity (Hebel and Stromberg, 1976; Smith, 1977). The cavity extends from the anterior end of the larynx caudally to the entrance to the trachea. It is subdivided into three compartments (the vestibule, left and right ventricles, and the infraglottic cavity) by two pairs of laterally situated folds—the ventricular folds and the vocal folds or cords. The epiglottis is leaf-shaped and composed largely of elastic cartilage. A small laryngeal saccule is present at the base of the epiglottis. Intrinsic and extrinsic striated muscles insert on the laryngeal cartilages to control movement and function.

The laryngeal cavity is lined by regionally specific epithelia (Renne et al., 1992). The epithelium on the anterior and upper posterior surface of the epiglottis, the upper half of the anterior laryngeal surface, a portion of the ventricular folds, and the true vocal cords are nonkeratinized, stratified, squamous epithelium. Most of the remainder of the laryngeal cavity is lined by pseudostratified, ciliated, columnar epithelium with a nonciliated, columnar epithelium intervening between the squamous and ciliated

epithelia. In the ventral portion of the larynx, the epithelial cells have inconspicuous microvilli or no cilia. Specific sites in the transition zone are more susceptible to injury, by inhaled toxicants, and are frequently the first sites that exhibit lesions. The most frequent site of exposure-induced lesions is the epithelium at the base of the epiglottis. Other sensitive sites are the medial aspects of the vocal processes of the arytenoid cartilages that are lined by squamous epithelium, and the medial laryngeal recess or ventral pouch (Lewis, 1981, 1991; Renne and Gideon, 2006).

The lamina propria of the larynx contains serous and mucous glands that vary in composition by location. The glands of the epiglottis are mostly mucous cells with few serous cells, while those in the other parts of the larynx are a mixture of serous and mucous cells.

Specific methods have been developed for precise and consistent sectioning at defined anatomical sites to facilitate accurate evaluation of the larynx, and comparisons between exposure groups and studies. Sections of the larynx should be prepared from at least three defined levels. Level I should be taken through the base of the epiglottis, to include the arytenoid cartilages (Figure 22.13). At this level, the larynx is lined dorsally by nonkeratinized, stratified squamous epithelium (Figure 22.13). This epithelium transitions to a mix of non- or sparsely ciliated flattened, to oval, cuboidal, or columnar (respiratory type) epithelium lining the lateral surfaces and the base
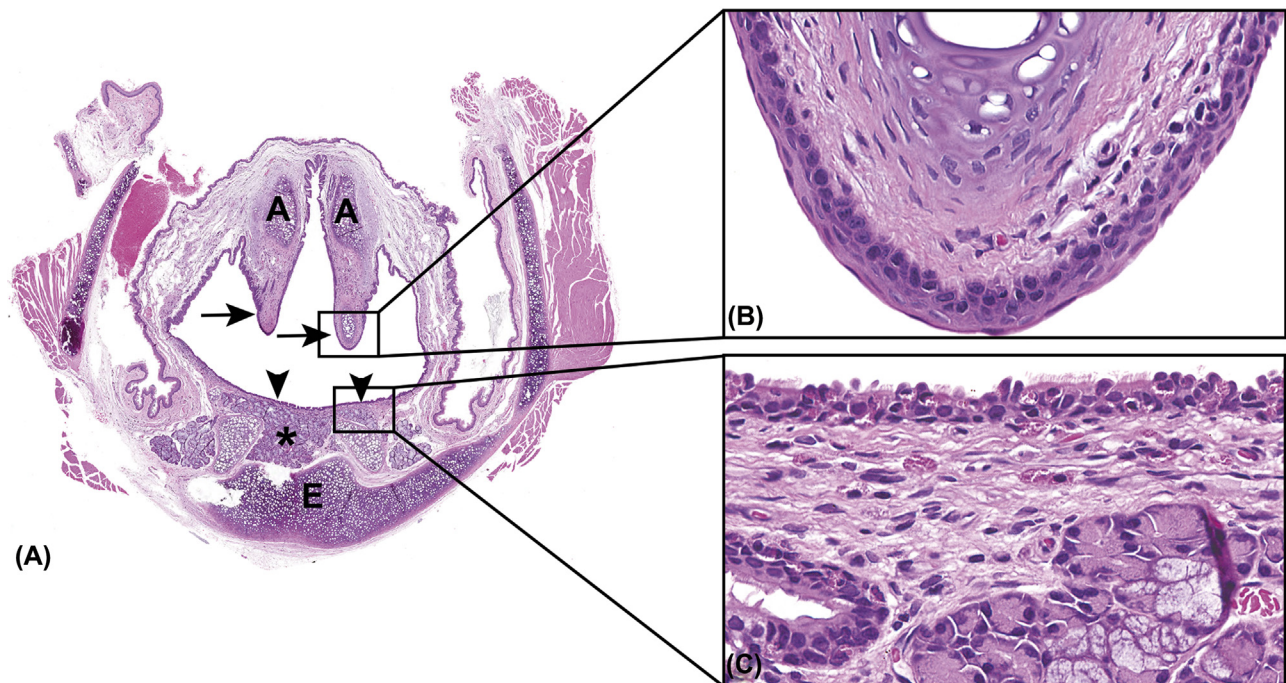

FIGURE 22.13 Photomicrograph of the Level I section of the larynx that contains the base of the epiglottis (E), and the arytenoid cartilages (A). At this level, the arytenoid cartilages are lined by nonkeratinized, stratified squamous epithelium (arrows) that transitions to a mix of non- or sparsely-ciliated, flattened, to oval, cuboidal, or columnar (respiratory type) epithelium lining the lateral surfaces and the base of the epiglottis (arrowheads). Seromucous glands (asterisk) are present beneath the ventral epithelium on the midline and are an important point of reference for accurate sectioning through Level I. The lining epithelia of arytenoid cartilages and base of the epiglottis are magnified in (B) and (C), respectively.

of the epiglottis ventrally (Figure 22.13). In this section, aggregates of seromucous glands are present beneath the ventral epithelium on the midline and are an important point of reference for accurate sectioning of Level I (Figure 22.13). Level II should include the ventral pouch, lined primarily by a mixture of cuboidal and ciliated columnar epithelial cells, and the vocal processes of the arytenoid cartilages, which are lined by two to three rows of nonkeratinized squamous epithelium or nonciliated, cuboidal and/or sparsely ciliated, low columnar epithelial cells (Figure 22.14). Level III should include the caudal larynx with the caudoventral extensions of the vocal processes, and the vocal folds which are lined by a mixture

of nonciliated, cuboidal and ciliated, low columnar epithelial cells (Figure 22.15).

2.2.6. Trachea

The trachea is the longest extrapulmonary conducting airway of the respiratory system. It is a hollow tubular structure formed by 24 C-shaped hyaline cartilages joined at the ends by bands of smooth muscle (Hebel and Stromberg, 1976). The trachea originates at the caudal end of the larynx and extends into the thoracic cavity, bifurcating distally at the carina to form the primary, extrapulmonary, airways of the lungs.
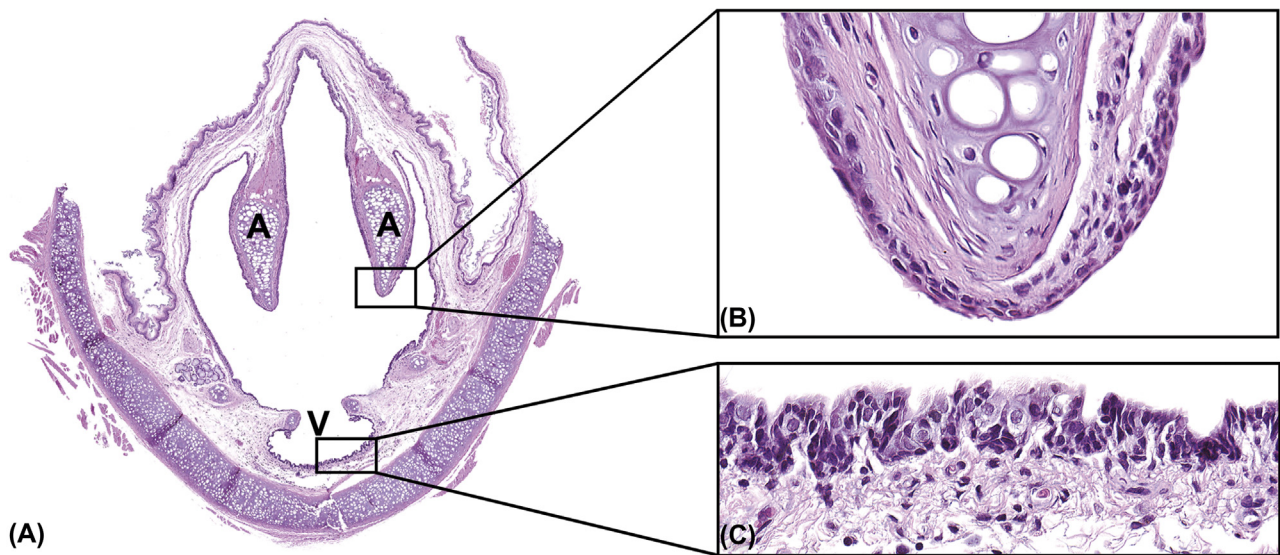

FIGURE 22.14   Photomicrograph of the Level II section of the larynx (A) that contains the ventral pouch (V), lined by a mixture of cuboidal and ciliated columnar epithelial cells, and the vocal processes of the arytenoid cartilages (A), which are lined by 2 to 3 rows of nonkeratinized squamous epithelium. Epithelia lining the arytenoid cartilage and ventral pouch are magnified in (B) and (C), respectively.
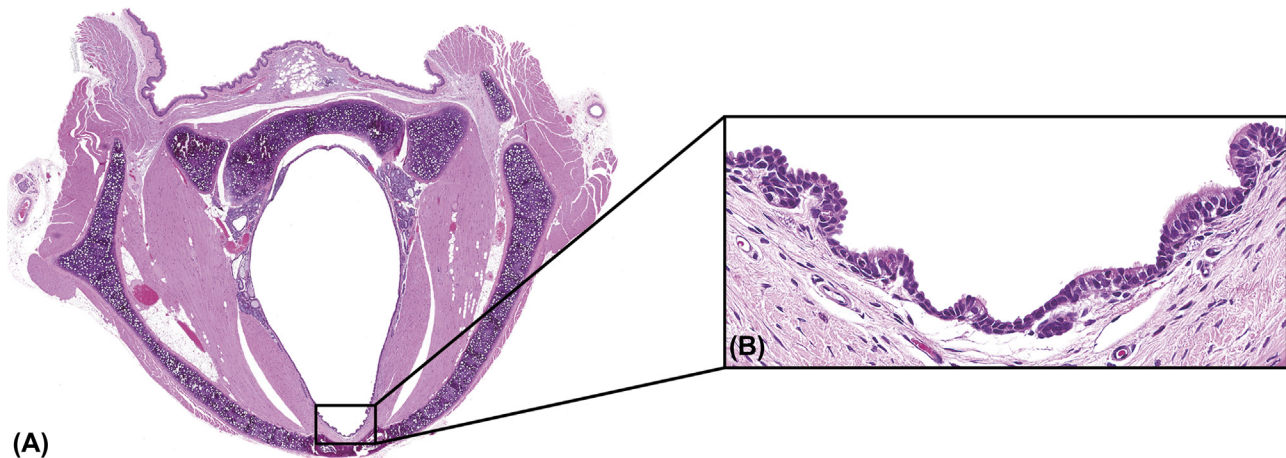

FIGURE 22.15   Photomicrograph of the Level III section of the larynx (A). The mucosa is lined by a mixture of nonciliated, cuboidal, and ciliated, low columnar epithelial cells. (B) Magnified view of the epithelium lining the mucosa.
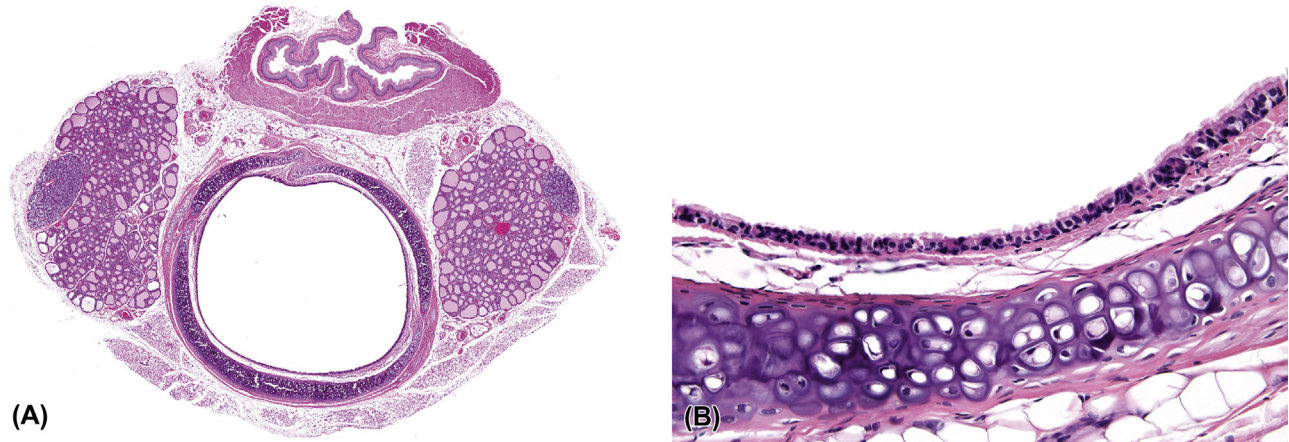
(A)

(B)

FIGURE 22.16   Photomicrograph of a normal trachea (A). The epithelium is primarily pseudostratified, columnar and consists of ciliated, nonciliated cells and basal cells. (B) Magnified view of the lining epithelium.

The epithelium of the trachea is similar to that of the respiratory epithelium of the nasal cavity and the distal larynx. It is mostly pseudostratified columnar and consists of ciliated, nonciliated, and basal cells (Jeffery and Reid, 1975; Marin et al., 1979) (Figure 22.16). In the proximal trachea, the majority of cells are nonciliated (basal, goblet, and neurosecretory cells). The number of ciliated cells increases as the trachea nears its bifurcation. Basal epithelial cells are similar to those of the nasal cavity and larynx. Club cells [previously known as Clara cells (Winkelmann and Noack, 2010)] have not been reported in the rat trachea (Plopper et al., 1983; Reynolds et al., 2015).

The lamina propria consists of an inner layer of fibrous connective tissue, rich in lymphocytes and blood vessels, and an outer layer of longitudinally arranged elastic fibers (fibroelastic membrane). The submucosa consists of loose connective tissue that supports the seromucous (mainly serous) glands whose ducts open on the epithelial surface. Glands are numerous in the upper trachea; few occur below the level of the thyroid and essentially no glands are present in the lower third of the trachea.

2.3. Physiology

The nasal passages are functionally complex with primary functions that include conditioning of inhaled and exhaled air, olfaction, chemoreception, and metabolism. As the primary site of entry for inhaled air, the nasal passages function to warm, humidify (moisten), and filter the inspired air in preparation for entry into the lungs. Conditioning of the air also prevents excessive drying of the mucosal surfaces and facilitates absorption of olfactory stimuli. Inspired air is cleansed by the absorption and/or metabolism of toxic and irritant gases and vapors and filtering of particulates of various sizes. The short

coarse hairs of the external nares eliminate larger inhaled particulates whereas smaller particulates, toxic gaseous and chemical impurities are trapped in the seromucous layer that covers the mucosal surfaces and are effectively removed by the mucociliary apparatus.

The respiratory epithelium is covered by a continuous blanket of mucus (epiphase), which has clearly defined flow patterns and region-specific flow rates. The mucous blanket floats on a layer of fluid (hypophase) and is moved along by the action of cilia. Cilia in the nose have region specific lengths and beat frequencies. Mucus in the anteriodorsal portion of the nose of the rat flows as a counter-current system with respect to the inspired air. The counter-current exchange system maintains a concentration gradient between the two fluids in order to maximize movement from one fluid to the other. The complex mucus streams converge on the nasopharyngeal duct to pass into the pharynx and are subsequently swallowed along with any trapped materials. In addition to clearing particulate material from the upper respiratory tract, as the medium in which olfactory molecules are dissolved, mucus prevents excessive transudation of fluid from tissues into the lumen and inward osmotic passage of water condensed on the surface during expiration, and facilitates the sense of smell.

The sense of smell is important for acquisition of food and recognition of enemies, territory, and members of same species for sexual and nonsexual interaction. There are specialized organs in the nasal cavity concerned with olfaction including the olfactory neuroepithelium, vomeronasal organ, septal olfactory organ, and olfactory nerves (fila olfactoria). The septal olfactory organ is a functioning part of the chemosensory system and primarily has an alerting function, providing information relevant to odor stimulus assessment. The vomeronasal organ may also play an important role in the sucking reflex in the young

and reproduction in the adult through recognition of pheromones and affecting release of hormones from the pituitary. Unlike the respiratory epithelium, the olfactory epithelium has high levels of cytochrome P-450 enzymes, which are considered important in metabolism and removal of odorants. The high metabolic capacity of submucosal glands may contribute to the development of some chemically induced lesions in the olfactory epithelium. Submucosal glands of the maxillary sinus also have extensive metabolic capacity and are specific target cells for some chemicals that require metabolism to proximate carcinogens.

The function of the larynx is primarily mechanical. During swallowing, the epiglottis closes the opening of the trachea to prevent swallowed food and liquids from entering the trachea. The larynx also functions as an organ of phonation. The intrinsic and extrinsic muscles that insert on the laryngeal cartilages control function and work in concert to regulate movement of the cartilages. The extrinsic laryngeal muscles position and stabilize the larynx. The intrinsic muscles regulate tension in the vocal folds, and open and close the entrance to the trachea. During inspiration, the epiglottis is closely opposed to the soft palate, leaving the entrance to the larynx open. As air passes through the larynx, the vocal folds vibrate producing sound waves. The pitch of the sound produced is regulated by the diameter, length, and tension in the vocal folds. The tension is controlled by the contraction of muscles that change the relative positions of the thyroid and arytenoid cartilages.

3. CONGENITAL LESIONS

Congenital lesions of the nasal structures, larynx, and trachea are rare. Deviation of the nasal septum is occasionally observed. Perforation of the septum is occasionally found in the ventral portion, but this may be the result of a resolved inflammatory lesion or injury rather than a congenital lesion.

4. DEGENERATIVE, REGENERATIVE, AND ADAPTIVE LESIONS

In toxicology studies, lesions classified as degenerative may result from aging, physical trauma, or exposure to noxious agents. These may include the initial insult followed by inflammatory, reparative, adaptive, or metaplastic lesions, or proliferative lesions that are not generally considered preneoplastic, or a component of the morphological continuum to neoplasia. Any region of the upper respiratory tract may be affected; however, the mucosal epithelia are most commonly affected. The respiratory or transitional epithelium lining the dorsal, medial, and lateral aspects of the nasal cavity are initially affected following exposure to irritant gases, aerosols, and vapors. The extent of the lesions depends on the nature and duration of the insult. The accessory nasal structures (Bowman's and Steno's glands, nasolacrimal duct, vomeronasal organ), larynx, trachea, and associated submucosal glands are less often affected. Degenerative lesions of the basement membranes, submucosal connective tissue, vessels, nerves, and bone are also occasionally observed. The base of the epiglottis is a sensitive target area of the larynx; the trachea is affected less often than the other sites.

Degenerative lesions are uncommon in control rats, and when observed, are often age-related, or the result of injury associated with physical trauma (foreign bodies) or infectious agents. Degenerative lesions are more frequently the sequel to the toxic effects of inhaled vapors, aerosols, or particulates, or to the systemic effects of ingested/injected compounds and/or their metabolites.

4.1. Nasal Cavity

4.1.1. Squamous Epithelium

The stratified squamous epithelium of the nasal cavity is relatively resistant to injury by inhaled toxicants; as such, spontaneous and exposure-related lesions in the squamous epithelium of the vestibule and nasal passages are uncommon. However, focal erosion or ulceration of the squamous epithelium of the ventral septum and ventral aspect of the vestibule may be seen when exposed to sufficiently high concentrations of irritant gases.

4.1.2. Respiratory Epithelium

Degenerative changes are most common in the respiratory epithelium and may manifest as one or more changes that include small irregular cytoplasmic vacuoles, increased cellular eosinophilia, swelling and rounding up of normally cuboidal/columnar cells, loss of cilia, cellular blebbing, loss of cell-to-cell contact, variable loss of epithelial cells, and disorganization of the epithelium (Figure 22.17).
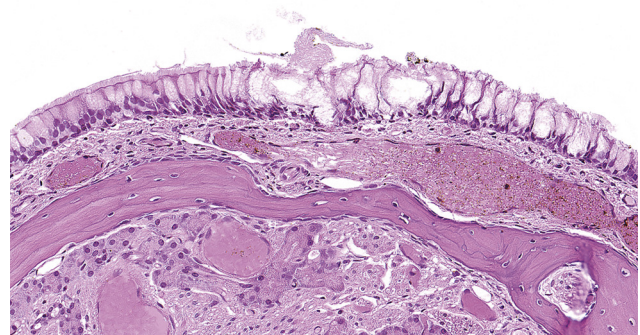

FIGURE 22.17 Degenerative changes in the respiratory epithelia in the nasal cavity. The cells are vacuolated and swollen.
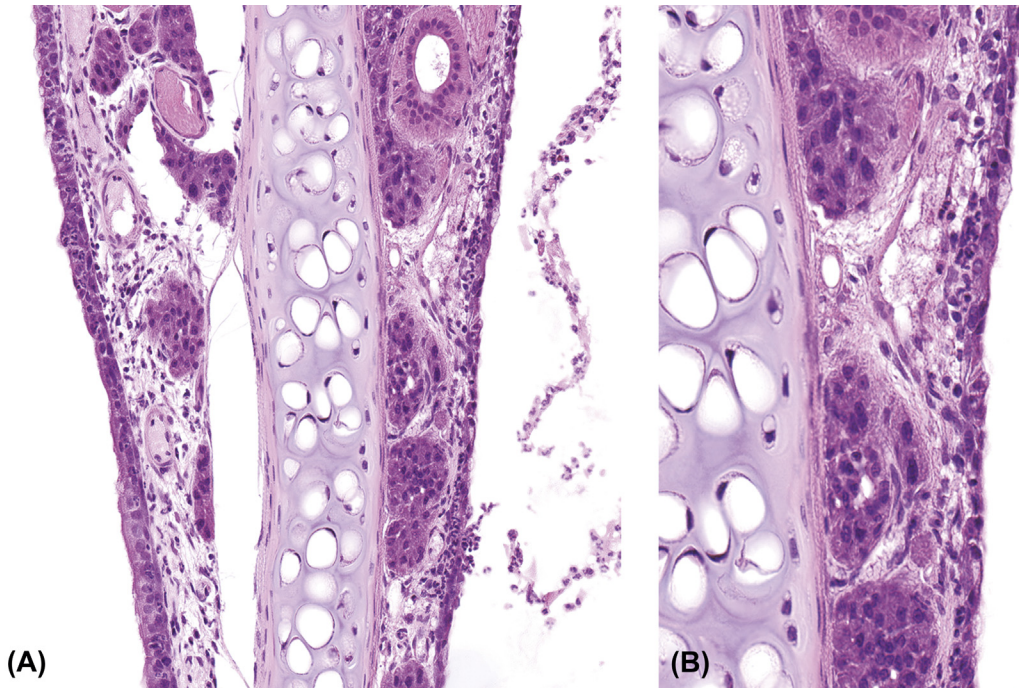
(A)

(B)

FIGURE 22.18 Atrophy of the respiratory epithelium (A) lining the nasal septum (compare this to Figure 22.7). The epithelium is thin and not pseudostratified; ciliated and mucous cells are not apparent. (B) Magnified view of the atrophic respiratory epithelium.

Epithelial degeneration is less common in the submucosal glands. Degeneration may be accompanied by mucosal inflammation and variable exudation into the nasal passages. Degenerative lesions that result from exposure to chemicals of low toxicity or irritancy, or to low concentrations of more potent chemicals, may be subtle and difficult to detect. Such mild lesions may manifest only as loss of cilia and slight flattening or rounding of normally cuboidal/columnar cells. Some areas normally have few cilia, and nonciliated epithelial cells are normally present in the respiratory type epithelium, which may make lesions detection difficult. When the epithelium of the submucosal glands is affected, glandular dilation and accumulation of secretory material in the ducts may be observed. Atrophy of the respiratory epithelium may occur secondary to degeneration. The affected epithelium appears thin and may not be pseudostratified (Figure 22.18). The transitional and respiratory epithelia of the lateral wall of the nose in Level I are the sites most sensitive to inhaled irritants.

A commonly observed lesion in the respiratory epithelium is accumulation of $2-10\ \mu m$ diameter, homogenous, brightly eosinophilic or hyaline globules in the cytoplasm of nonciliated cells of the respiratory epithelium, and of the submucosal glands and their ducts (Figure 22.19). Hyaline droplet accumulation is a common spontaneous change in aging rats and the droplets are often increased in number and size with exposure to some irritant chemicals. As a spontaneous change, hyaline droplet accumulation is particularly common at the junction of respiratory and olfactory epithelia, but frequently occurs at several sites or throughout the nasal mucosa (especially ventrally) with inhalation exposure to a variety of compounds and chemicals. The significance of exposure-related exacerbation of this change in inhalation studies is uncertain, but is thought to be a nonspecific, adaptive or protective response to chronic inhalation exposure to chemical irritants and frequently accompanies epithelial hyperplasia. The globules are located in the sub- or supranuclear cytoplasm and are thought to be secretory in nature. In mice, the hyaline droplets are reported to contain Ym1/2 chitinase proteins in mice (Ward et al., 2001).

In toxicology studies, necrosis, erosion, and ulceration of the respiratory epithelium are most commonly observed following exposure to irritant chemicals or toxicants. These lesions are infrequently observed in untreated control rats or rats raised under barrier conditions, and if observed, are most likely associated with physical (foreign bodies) or infectious (bacterial or fungal) agents. Necrosis of the respiratory and glandular epithelia (Figure 22.20) may occur with or without exfoliation; it may result in erosion or ulceration. Necrosis may extend to the turbinate bone when severe. Erosions are characterized by exfoliation of the superficial epithelium only (Figure 22.21). Ulceration is characterized by complete loss of the epithelium and basement membrane with
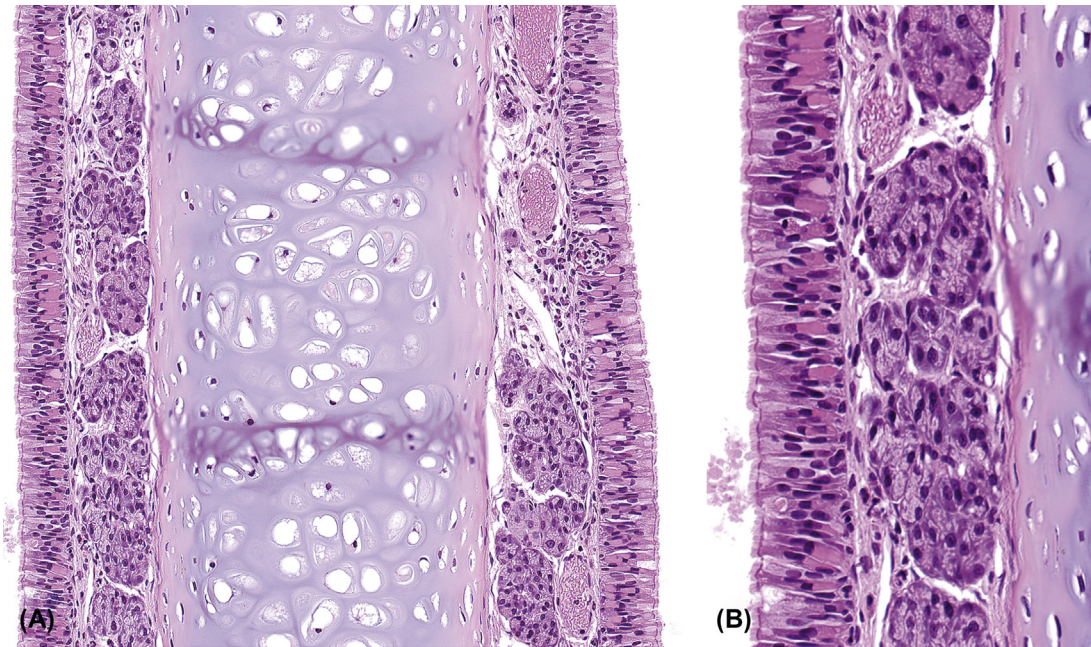
FIGURE 22.19 Hyaline droplet accumulation (A). The cytoplasm of the respiratory epithelium contains homogeneous, eosinophilic hyaline droplets. (B) Magnified view of the respiratory epithelium showing hyaline droplets in the cytoplasm.

FIGURE 22.20 Necrosis of the respiratory epithelium (asterisk). There is loss of cellular detail, exfoliation and inflammation.
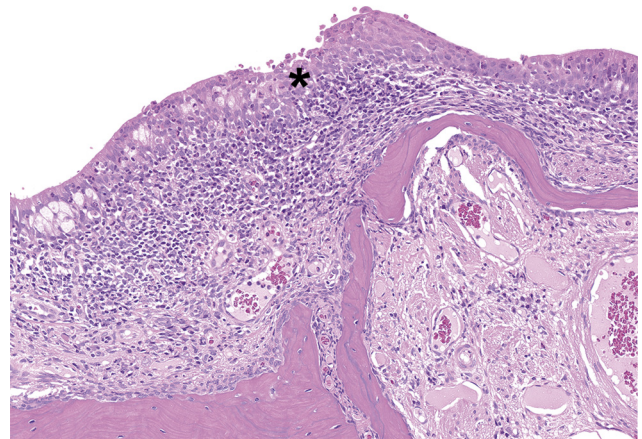

FIGURE 22.21 An erosion in the respiratory epithelium. Only superficial epithelial cells have exfoliated (asterisk).

exposure of the underlying submucosa (Figure 22.22). Ulceration or necrosis may be accompanied by edema and inflammation of the lamina propria and submucosa. Involvement of the turbinates may be associated with atrophy, hypertrophy, or remodeling of the underlying bone, or with adhesions (synechiae) to the lateral wall or other turbinates.

Repeated or prolonged damage to the respiratory epithelium may result in reparative, proliferative, or adaptive changes. During the early reparative response, the adjacent undamaged epithelium rapidly proliferates and migrates to form a thin cell layer to partially or completely cover the affected area. The lost or damaged epithelium may be replaced by a single layer of flattened to low cuboidal regenerating cells (Figure 22.23) or, in cases of continued injury, with two or more layers of seemingly undifferentiated polyhedral cells. These foci of regenerating cells may progress to squamous metaplasia
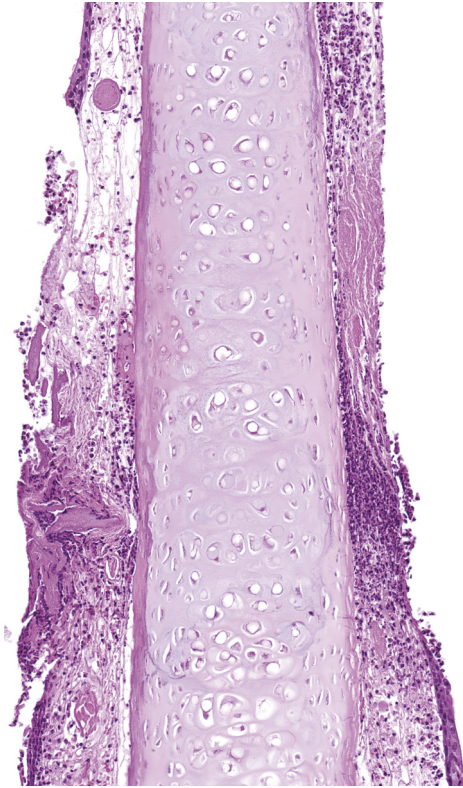
FIGURE 22.22   An ulcer in the respiratory epithelium. The ulcer is characterized by the complete loss of epithelium and basement membrane with exposure of the underlying submucosa.

with persistent or repeated injury (Figure 22.24). In mild cases of squamous metaplasia, the cells are nonkeratinized and may be difficult to distinguish from undifferentiated regenerating cells. More advanced squamous metaplasia is characterized by three or more layers of well-differentiated squamous epithelial cells with relatively prominent cell boundaries, intercellular bridges, and moderately abundant eosinophilic cytoplasm; some advanced lesions may have variable amounts of keratinization.

Hyperplasia of respiratory epithelium is a common response to mucosal injury. In some instances, several layers of disorganized, flattened to cuboidal cells may replace the normal epithelium. More typically, the respiratory epithelium is thickened due to increased numbers of cells, and may have an irregularly undulating, folded, or rugose appearance caused by invagination of the hyperplastic epithelium; formation of intraepithelial "pseudocrypts" or "pseudoglands" may be present (Figure 22.25). Hyperplasia and hypertrophy of the secretory mucous (goblet) cells frequently accompany respiratory epithelial cell hyperplasia. Goblet cells are larger and more abundant and the epithelium may have a glandular appearance (Figure 22.26). Clusters of goblet cells surrounding extruded mucus in the epithelium may give the appearance of intraepithelial crypts and may coalesce to form mucous cysts.
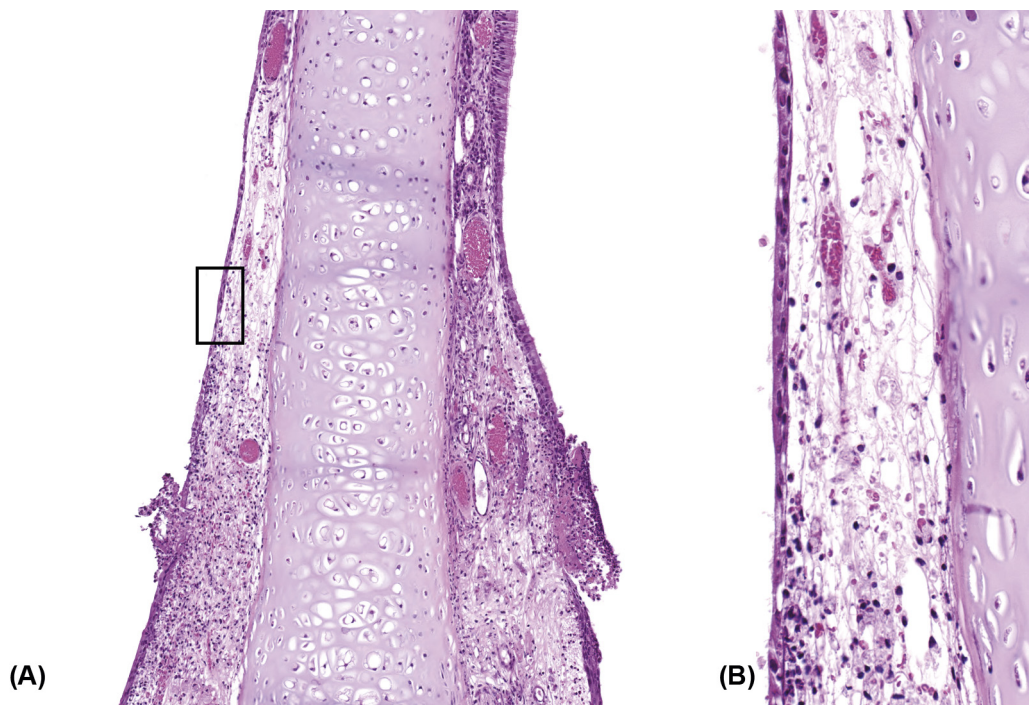

(A)

(B)

FIGURE 22.23   Regeneration of the respiratory epithelium (A). The mucosa is lined by a thin layer of flattened regenerating epithelial cells. There is necrosis and inflammation in the adjacent epithelium and submucosa. (B) Higher of magnification of boxed area in (A) shows a thin layer of regenerating epithelium.
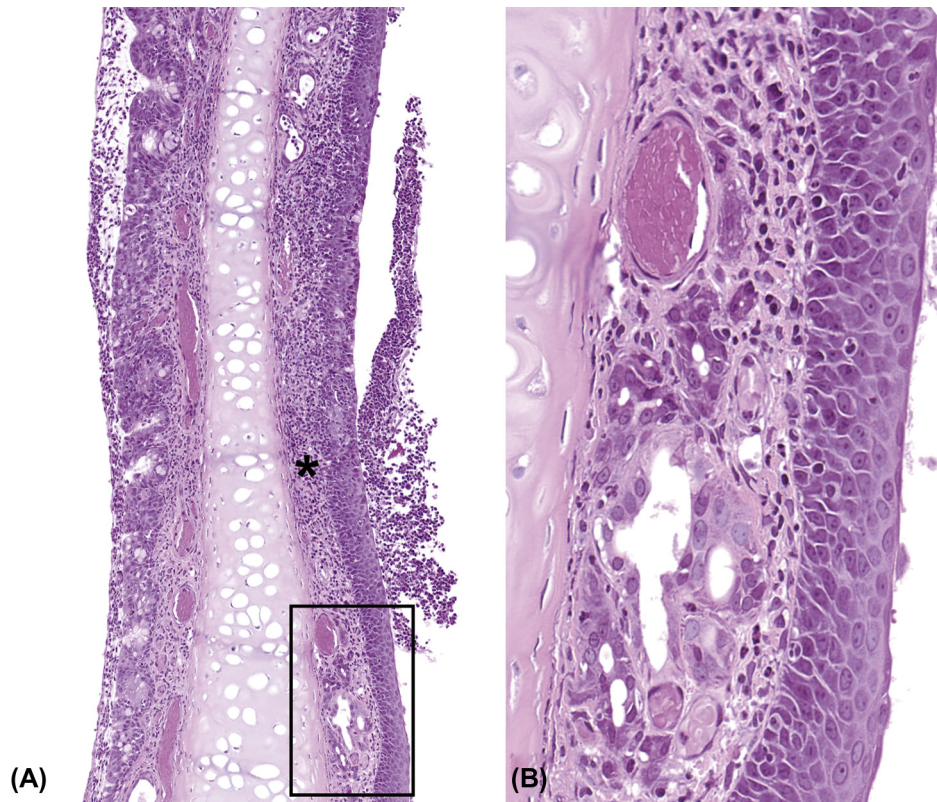
FIGURE 22.24 Squamous metaplasia of the respiratory epithelium (A). The affected epithelium (asterisk), is replaced by stratified squamous epithelium. (B) Higher magnification of (A) (box) demonstrates well-differentiated, metaplastic squamous epithelium with prominent cell borders.

Severe degenerative and necrotic lesions of the nasal epithelium, particularly following exposure to highly irritant agents, may result in necrosis of the septal cartilage and turbinates. Extensive necrosis may result in rupture and perforation of the nasal septum (Figure 22.27).

Dilation of the submucosal glands may occur concurrently with the lesions discussed above, but may also occur as a spontaneous age-related change. Affected glands are variably dilated and may be empty or contain variable amounts of pale eosinophilic to amphophilic secretory material (Figure 22.28).

A variety of other incidental degenerative changes occur in the respiratory epithelium including corpora amylacea, focal mineral and amyloid deposition. Corpora amylacea are small basophilic to amphophilic, laminated bodies in the epithelium, lamina propria, or lumen of submucosal glands (Figure 22.29). Mineral appears as focal irregular, basophilic deposits in the epithelium or lamina propria (Figure 22.30).

4.1.3. Olfactory Epithelium

The degenerative and regenerative lesions and squamous metaplasia in the olfactory epithelium, and associated glands, may be morphologically similar to those in the respiratory epithelium. These lesions are rare and spontaneous in aged and control rats, but are common following inhalation exposure to irritants. Degeneration and necrosis are perhaps the most frequently observed changes following exposure to toxic gases, aerosols, and vapors. The sensory neurons are most susceptible to injury, and are usually the first cells affected. The sustentacular cells, and the epithelium of the submucosal glands, tend to be more resistant to injury; however, all cell types of the olfactory epithelium may be affected when the insult is prolonged and the injury severe. Inflammation frequently accompanies degeneration and necrosis as a secondary change, but sometimes is observed as the primary response. Inflammatory cell infiltrates occur primarily in the lamina propria, and become common in the epithelium with increasing severity of the lesions. Cytoplasmic vacuolation and increased intercellular space may be the earliest manifestations of degeneration (Figure 22.31). As the degenerative process progresses, loss of cilia and epithelial cells, and/or disorganization and disruption of the epithelium may occur. Progression of the degenerative changes leads to necrosis and partial to complete exfoliation of epithelial cells (Figure 22.32). Atrophy of the
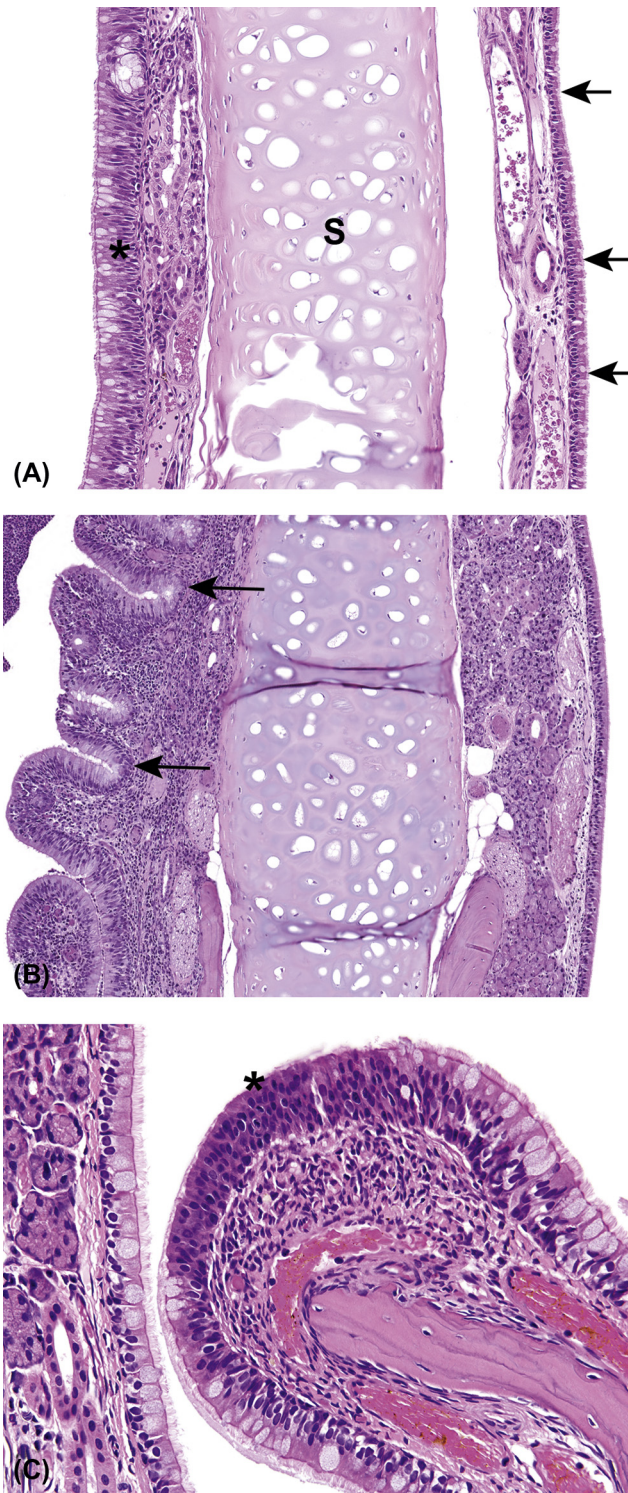
(A)

(B)

(C)

FIGURE 22.25   Hyperplasia of the respiratory epithelium (A). There is increased cellularity and disorganization of the respiratory epithelium (asterisk) compared to the relatively normal respiratory epithelium on the contralateral side (arrows) of the nasal septum (S). (B) Hyperplastic respiratory epithelium with irregular rugose folding of the mucosa and pseudocrypt formation (arrows). (C) Focal respiratory hyperplasia (asterisk) with normal epithelium on contralateral side.

ethmoid turbinates may occur in conjunction with severe epithelial lesions, similar to that of the naso- and maxilloturbinates (Figure 22.33).

The olfactory epithelium has remarkable regenerative capacity (Figure 22.34). Degeneration and necrosis are followed by stages of repair as described for the respiratory epithelium. Complete recovery can occur in four to five weeks. However, regenerative repair may not always be complete; adaptive repair may occur. With more advanced epithelial injury, there may be complete loss of sensory and sustentacular cells and replacement by pseudostratified, columnar epithelium that resembles the respiratory epithelium of the naso- and maxilloturbinates; however, goblet cells are not typically present (Figure 22.35). The term respiratory epithelial metaplasia may be used to describe this change. This metaplastic transformation frequently affects the epithelium of the submucosal glands and their ducts. Prolonged injury to the olfactory epithelium may lead to squamous metaplasia (Figure 22.36). Keratinization of the metaplastic squamous epithelium is uncommon, but may occur with repeated injury.

Focal atrophy of the olfactory epithelium with loss of sensory cells is occasionally seen in untreated, aging rats. However, atrophy is also a frequent consequence of degeneration and necrosis of the olfactory epithelium; it may be extensive after inhalation of certain irritant chemicals. Atrophy is most common in the dorsal meatus at Level II; however, with more severe injury, the ethmoid turbinates are also affected. The affected epithelium is thin primarily due to decreased numbers of sensory cells and, in some instances, sustentacular cells (Figure 22.37). Following more severe injury, sustentacular cells may predominate or there may be complete loss of sensory and sustentacular cells, and the atrophic epithelium may be lined primarily by basal epithelial cells. Atrophy of the olfactory epithelium secondary to degeneration and necrosis is often accompanied by atrophy and sometimes loss of the olfactory nerve axon bundles in the lamina propria.

Accumulation of brightly eosinophilic cytoplasmic globules, similar to those in the respiratory epithelium, is common in small numbers of olfactory sustentacular cells in aging rats (Figure 22.38). As in the respiratory epithelium, the incidence, extent, and severity of this change may increase with exposure to a variety of inhaled toxicants. Occasionally, small intraepithelial mucous crypts are observed in the olfactory epithelium. These consist of mucous cells apparently derived from the ducts of submucosal (Bowman's) glands that traverse the epithelium. In young adult and aging rats, foci of mineral deposition may be present in the basement membrane of the olfactory epithelium (Figure 22.39).
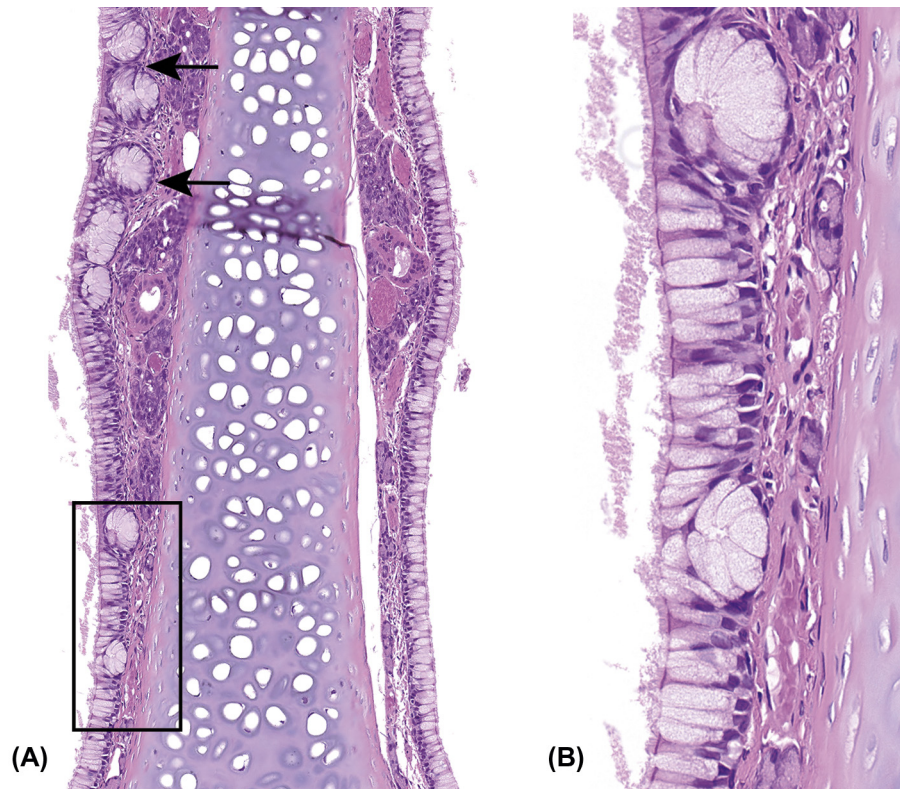
FIGURE 22.26   Goblet cell hyperplasia in the respiratory epithelium (A). There are increased numbers of goblet cells with pseudocrypt formation (arrows). (B) Higher magnification of boxed area in (A).

FIGURE 22.27   Turbinate necrosis and septal perforation. There is loss of turbinates and loss of the septal cartilage and bone has resulted in perforation (asterisk).

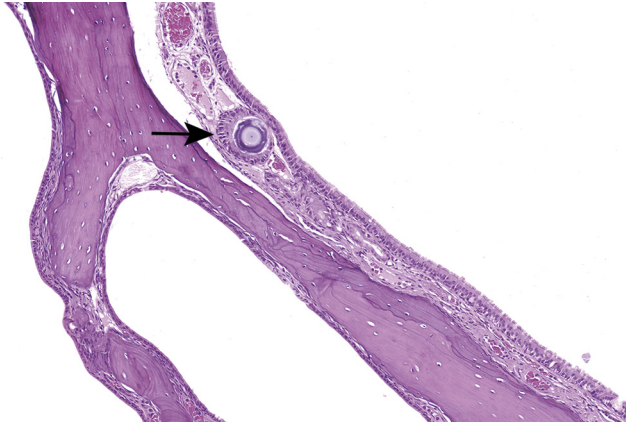**FIGURE 22.28**   Respiratory epithelium, glands—Dilation (asterisks).

FIGURE 22.29   Respiratory epithelium—Corpora amylacea. The submucosa contains a basophilic laminated body (arrow).

4.1.4. Accessory Nasal Structures

Degeneration of the accessory nasal structures may occur in aging rats. Atrophy and dilation of the submucosal (Bowman's) glands of olfactory mucosa (Figure 22.40), although common in aging rats, are more often associated with severe degeneration and necrosis in the olfactory epithelium following inhalation exposure to irritant agents (NTP, 2012). Hyperplasia (Figure 22.41) and squamous metaplasia (Figure 22.42) of the submucosal (Bowman's) gland epithelium often occur in conjunction with induced epithelial changes. Hypertrophy and hyperplasia of mucous cells in submucosal (Bowman's) glands may occur in response to mucosal injury. Degeneration of Steno's glands is uncommon; however chemically induced necrosis and atrophy may occur.
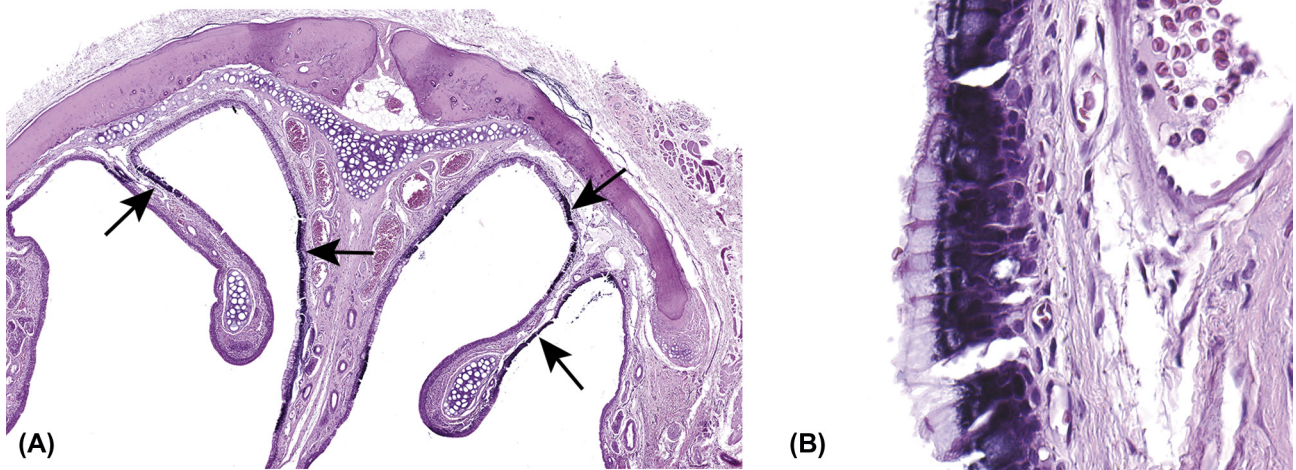

FIGURE 22.30   Respiratory epithelium—Mineral (A). Deposits of mineral are present multifocally (arrows) in the epithelium lining the nasoturbinates and nasal septum. (B) Higher magnification of (A) demonstrating the basophilic mineral deposits.
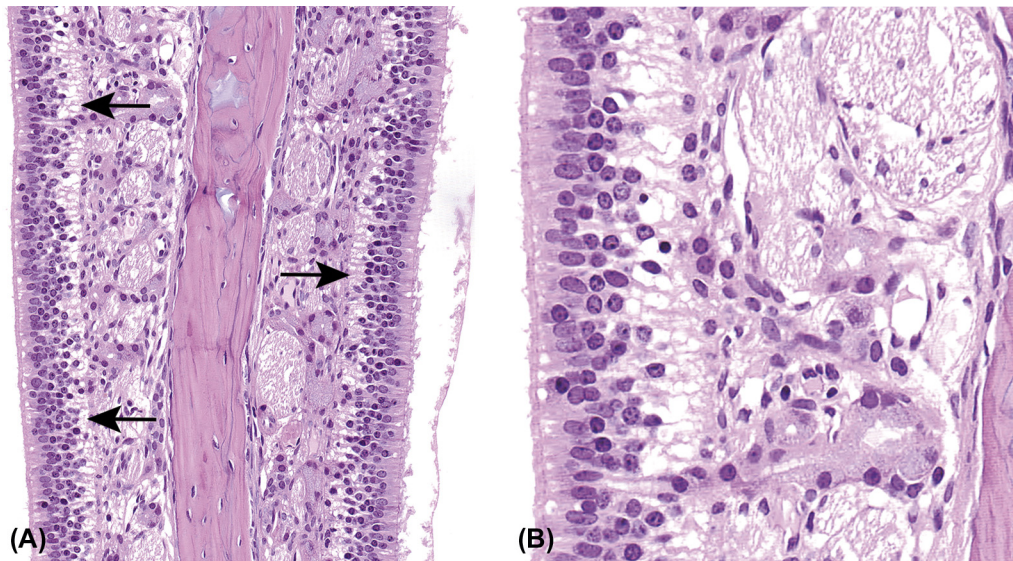

FIGURE 22.31   Degeneration of the olfactory epithelium (A). There is cytoplasmic vacuolation in the olfactory epithelia (arrows). (B) Higher magnification of (A) showing vacuolated olfactory epithelial cells. Compare this to the normal olfactory epithelium in Figure 22.10.
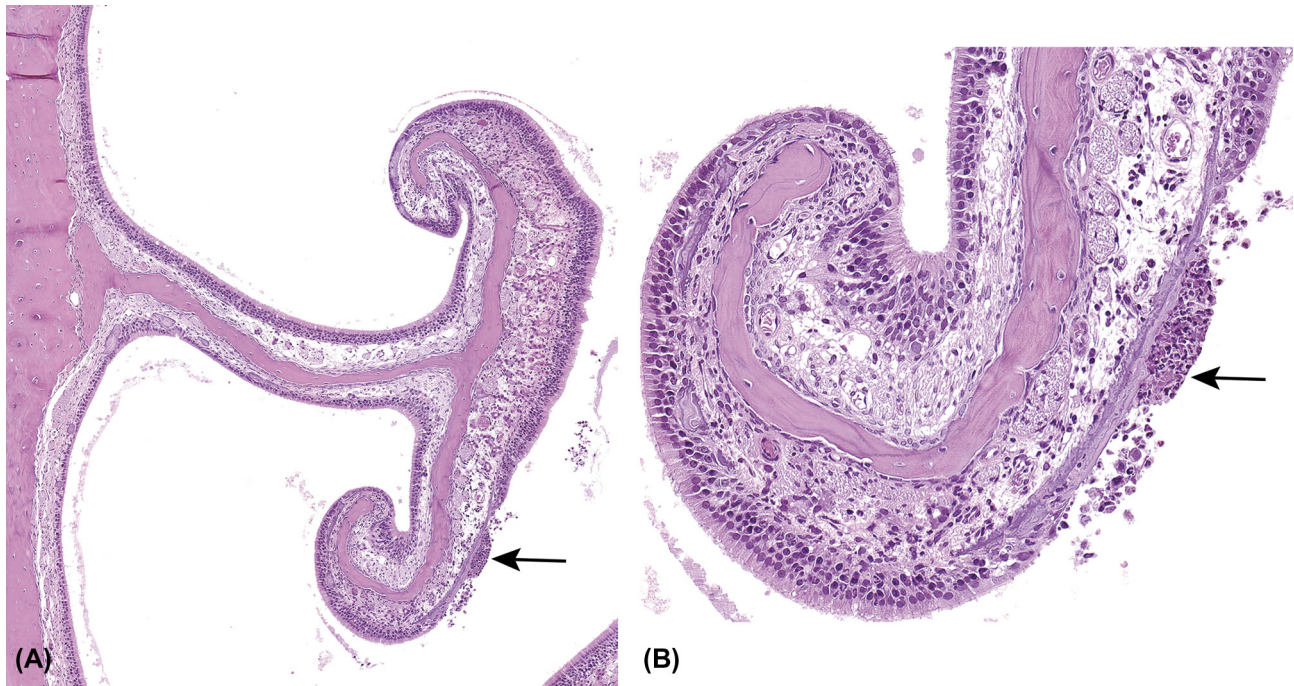
FIGURE 22.32   Necrosis of the olfactory epithelium (A). (B) Higher magnification of Figure. (A). There is loss and exfoliation of necrotic epithelial cells (arrow). Note inflammatory cell within the necrotic epithelium.
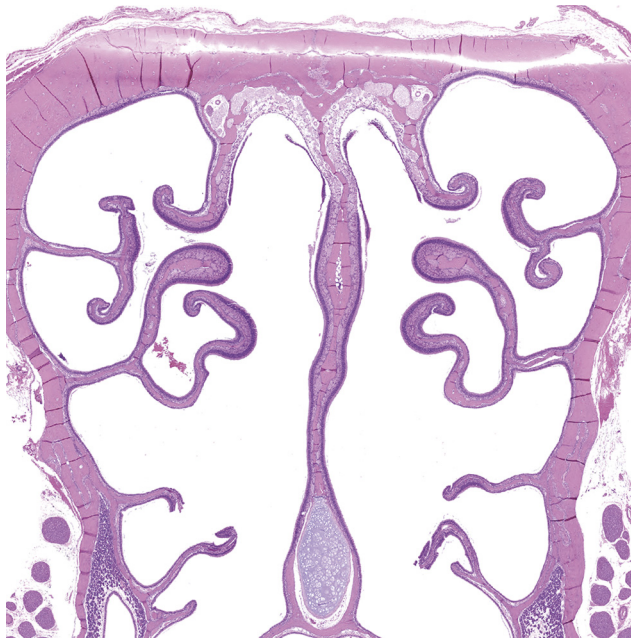

FIGURE 22.33   Atrophy of the ethmoid turbinates. Compare to Figure 22.5. The ethmoid turbinates are short, thin, and blunt and there is increased space in the nasal passages.

Degeneration and necrosis of the nasolacrimal duct epithelium can occur, and is usually associated with inflammation (Figure 22.43). With severe inflammatory lesions, squamous metaplasia may occur. Likewise, degeneration and necrosis, or squamous metaplasia of the vomeronasal organ epithelium, although uncommon, may occur with more severe and extensive lesions in the nasal cavity (Figure 22.44).

4.2. Larynx and Trachea

The lesions observed in the larynx and trachea, and their associated glands, are morphologically similar to those in the nasal passages, and depend on the intensity and duration of inhalation exposure. Necrosis and chronic inflammation of the larynx may result in formation of an inflammatory polyp, often with squamous metaplasia of the overlying epithelial surface. Dilation (ectasia) of the laryngeal or tracheal submucosal glands is a common spontaneous or age-related change (Figures 22.45 and 22.46). However, abnormal glandular dilation may occur in conjunction with marked hyperplasia, squamous metaplasia, or inflammation of the mucosal epithelium; this likely results from blockage of ducts and accumulation of secretory material within the lumens.

Focal mineral deposits may be a background change in the larynx and trachea of aged rats. These deposits are variably sized, deeply basophilic bodies within the epithelium and/or submucosa (Figures 22.47 and 22.48). In general, these deposits have no pathological significance. However, mineral deposition may occur secondary to long-standing inflammation-related degeneration
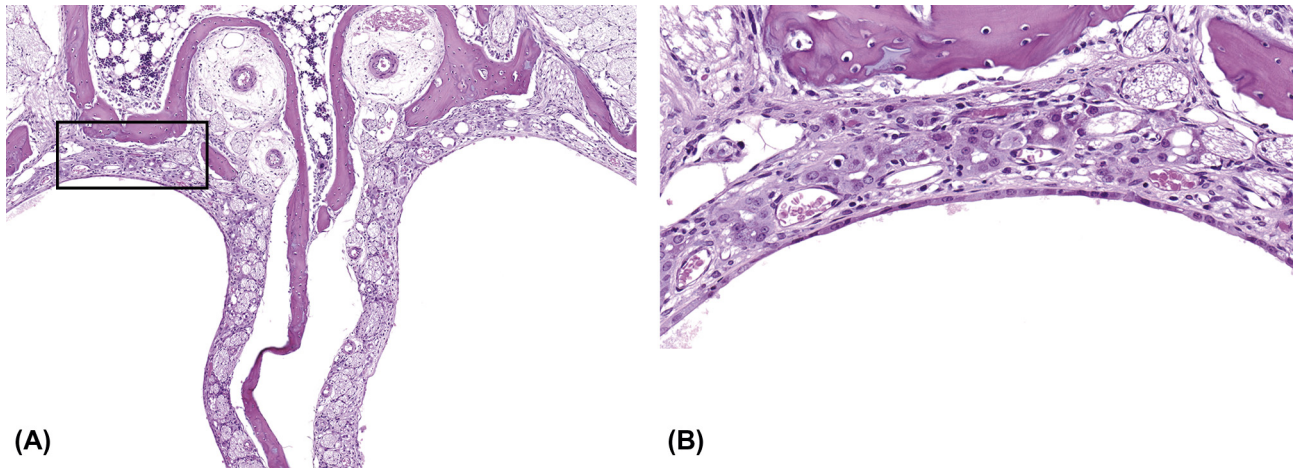
(A)

(B)

FIGURE 22.34   Regeneration of the olfactory epithelium (A). Note thin olfactory epithelium. (B) Higher magnification of boxed area in (A); the olfactory mucosa is lined by a single layer of flat epithelial cells.
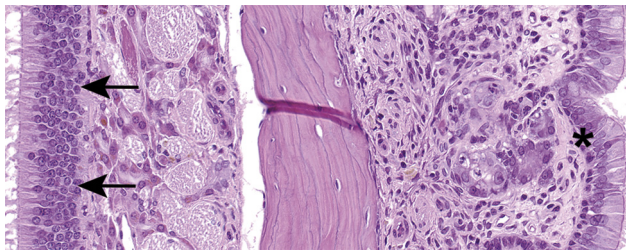

FIGURE 22.35   Respiratory epithelial metaplasia of the olfactory epithelium. Pseudostratified, ciliated, columnar respiratory epithelium (asterisk) has replaced the normal olfactory epithelium. Note the normal olfactory epithelium on the contralateral side (arrows).

and necrosis (dystrophic calcification/mineralization), or it may be an indicator of elevated serum calcium levels (metastatic calcification/mineralization) secondary to end-stage chronic progressive nephropathy or hypoparathyroidism.

5. INFLAMMATORY AND VASCULAR LESIONS

Trauma, inhaled foreign bodies, and injury following exposure to irritant toxicants can elicit inflammatory responses in the nasal cavity of rats. The inflammatory processes may also affect the accessory structures, especially the nasolacrimal duct. Focal, minimal, inflammatory cell infiltrates are common incidental findings in control and exposed rats. Inflammatory cell infiltrates may consist of a mixture of mononuclear cells with neutrophils. Inflammation is characterized by the presence of inflammatory cells in conjunction with one or more of a spectrum of changes that include: vascular congestion, exudation of plasma fluids and proteins (edema), tissue

damage/destruction; accumulation of tissue and inflammatory cell debris; proliferation of fibroblasts (with collagen deposition if long-standing) is indicative of chronic inflammation.

In inhalation exposure studies, the character and intensity of the inflammatory response is often a reflection of the nature of the agent inhaled and the duration of exposure. Mild irritants may result in acute inflammation as the earliest response. Neutrophils are the predominant infiltrating cell type, and minimal to mild edema, congestion, and minimal tissue damage may be apparent. Exposure to highly irritant agents may elicit an early suppurative response, which may persist. With suppurative inflammation, there are considerably more neutrophils, many of which are degenerate. Cellular debris from damaged tissue and degenerate and dead neutrophils, fibrin and protein exudation may be evident. Chronic inflammation signifies a persistent response to injury. There may be a predominance of mononuclear inflammatory cells (macrophages, lymphocytes mostly), with fewer neutrophils, as the response to injury progresses. Evidence of tissue destruction may still be evident, as are attempts at healing, including proliferation of connective tissue (fibrosis) and endothelial cells (neovascularization). Prolonged severe, necrotizing injury with inability of the tissue to repair may elicit chronic active inflammation in which macrophages are still the predominant cell type; however, neutrophils still comprise a large proportion of the inflammatory cells. Granulomatous inflammation occurs in response to inhaled foreign bodies, some infectious agents, or exposure to inhaled agents that are resistant to degradation and clearance. The inflammatory cell infiltrate is predominantly activated macrophages, some of which are epithelioid and multinucleated, accompanied by lymphocytes, plasma cells, and eosinophils.
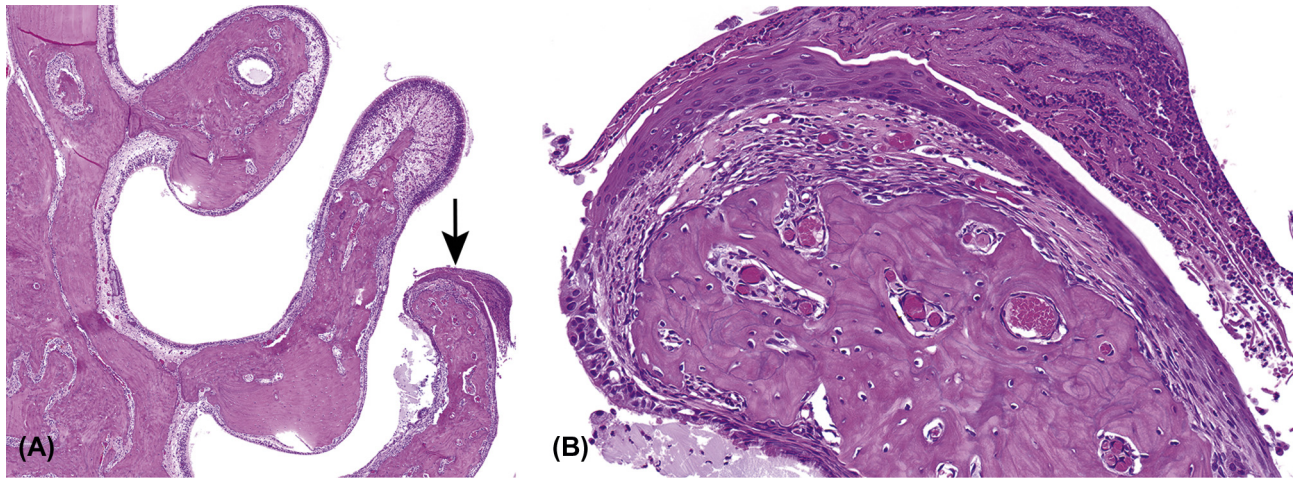
FIGURE 22.36   Squamous metaplasia (arrow) of the olfactory epithelium (A). (B) Higher magnification of (A) shows replacement of normal olfactory epithelium by stratified squamous epithelium.
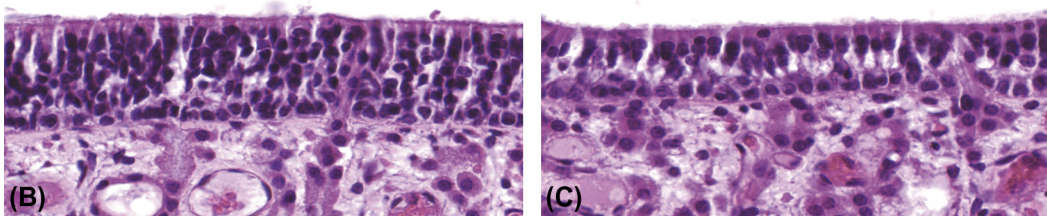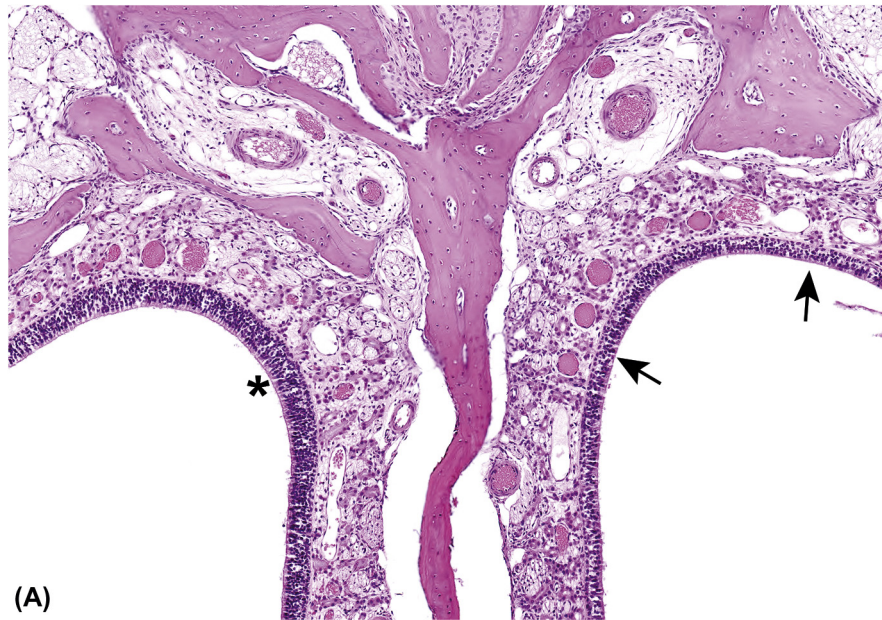

FIGURE 22.37   Atrophy of the olfactory epithelium (arrows) (A). Compare to the normal olfactory epithelium lining the contralateral side (asterisk) and in Figure 22.10. (B) and (C) Higher magnification of normal olfactory epithelium. (C) The atrophic olfactory epithelium is shorter and has decreased number of cells. Note the atrophy and loss of nerve bundles in the submucosa.

Concurrent infectious diseases have the potential to compromise the conduct and interpretation of toxicology studies in laboratory animals.

Mycoplasma pulmonis is the cause of a highly infectious, inflammatory syndrome that affects the nasal passages and sinuses, middle ear, larynx, trachea, bronchi, and lungs. Typically, the infection elicits severe chronic active inflammation, in which neutrophils predominate, but are mixed with significant numbers of macrophages, lymphocytes, and plasma cells. Marked fibrosis occurs in
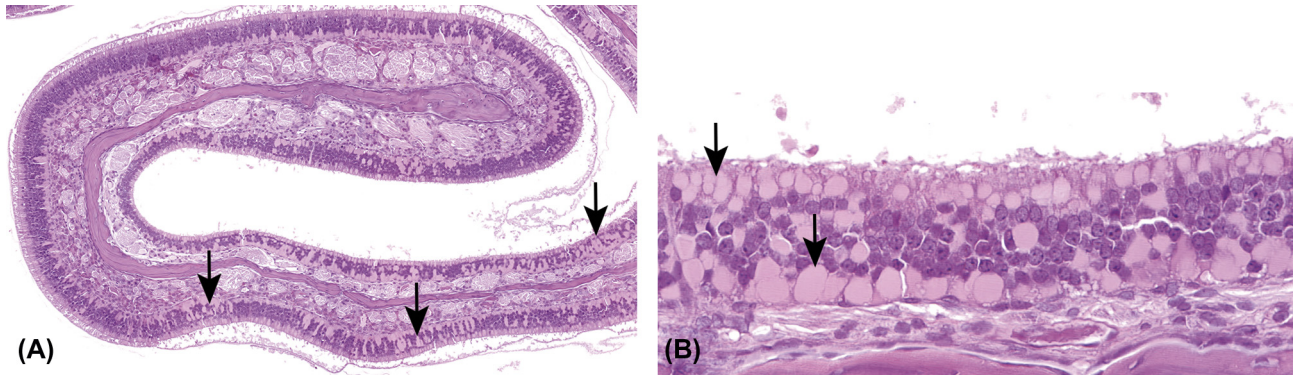
FIGURE 22.38 (A) Olfactory epithelium—Hyaline droplet accumulation in the olfactory epithelium (A). (B) Magnified view showing accumulation of homogeneous, eosinophilic droplets (arrows) in the cytoplasm of olfactory epithelium.
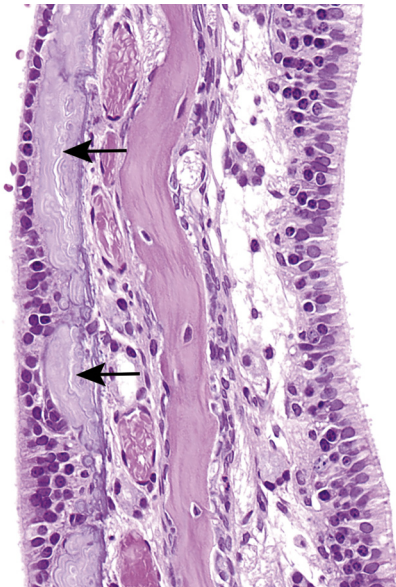
FIGURE 22.39 Mineral in the olfactory epithelium. Basophilic mineral deposits (arrows) are present in the epithelium and basement membrane.
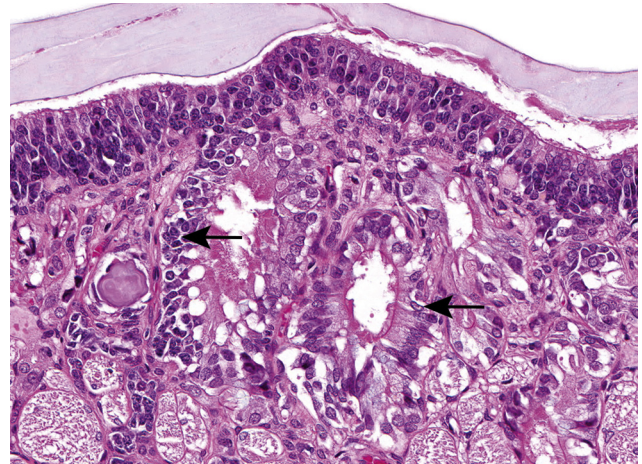
FIGURE 22.41 Hyperplasia of the epithelium of the submucosal glands of the olfactory epithelium (arrows).

FIGURE 22.40 Dilation of submucosal glands of the olfactory epithelium (asterisks).
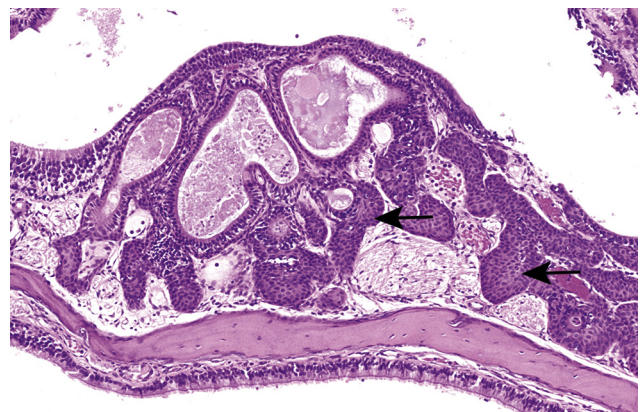
FIGURE 22.42 Squamous metaplasia of the epithelium of the submucosal glands of the olfactory epithelium (arrows).
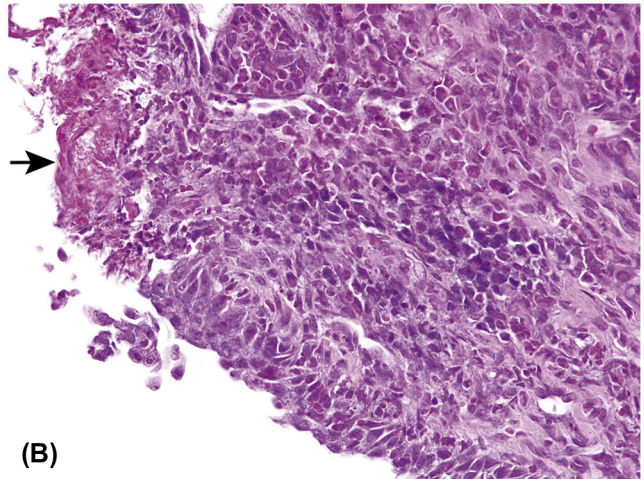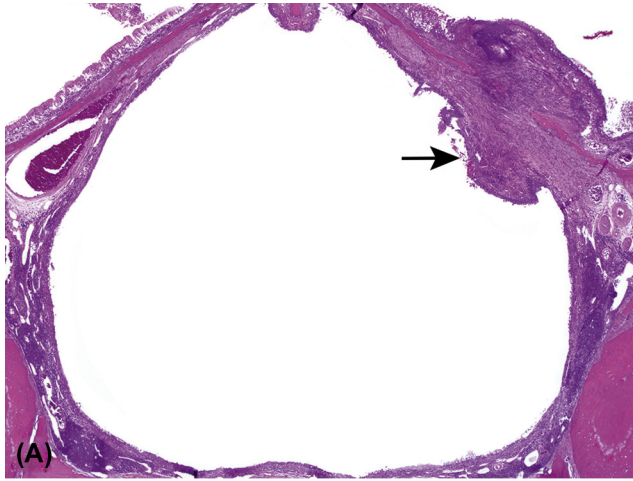
FIGURE 22.43 (A) Inflammation in the nasolacrimal duct with focal necrosis of the epithelium (arrow). (B) Higher magnification of (A).
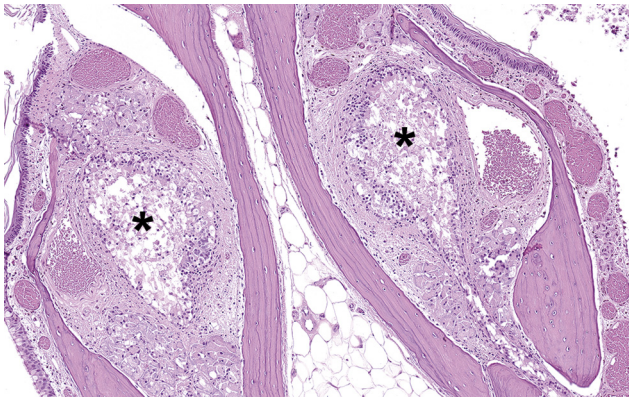
FIGURE 22.44 Necrosis of the epithelium of the vomeronasal organ (asterisks). There is complete, bilateral necrosis of the neuro- and ciliated epithelia. Compare this to normal vomeronasal organ in Figure 22.12.
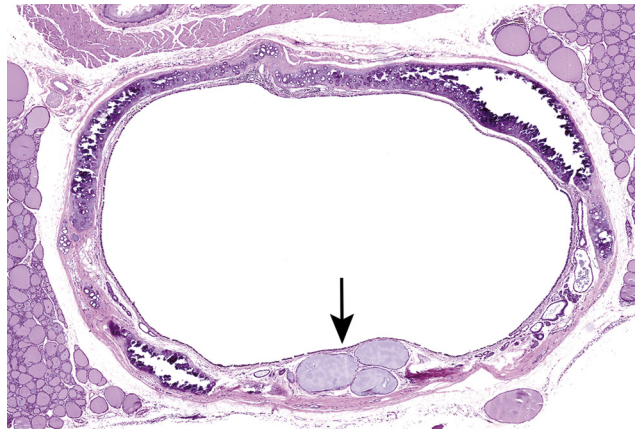
FIGURE 22.46 Trachea, dilation of submucosal glands (arrow).
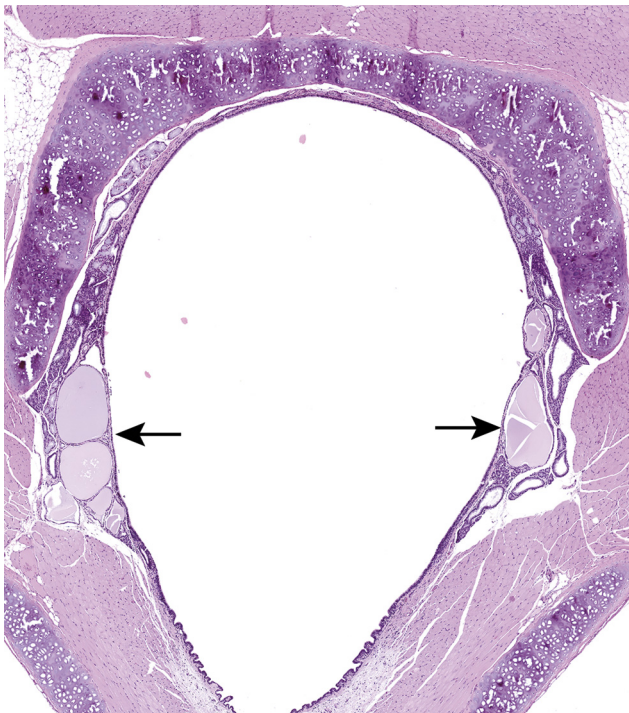
FIGURE 22.45 Larynx, dilation of submucosal glands (arrows).

**FIGURE 22.47** Larynx. Basophilic mineral deposits are present in the epithelium and in the submucosa (arrows).
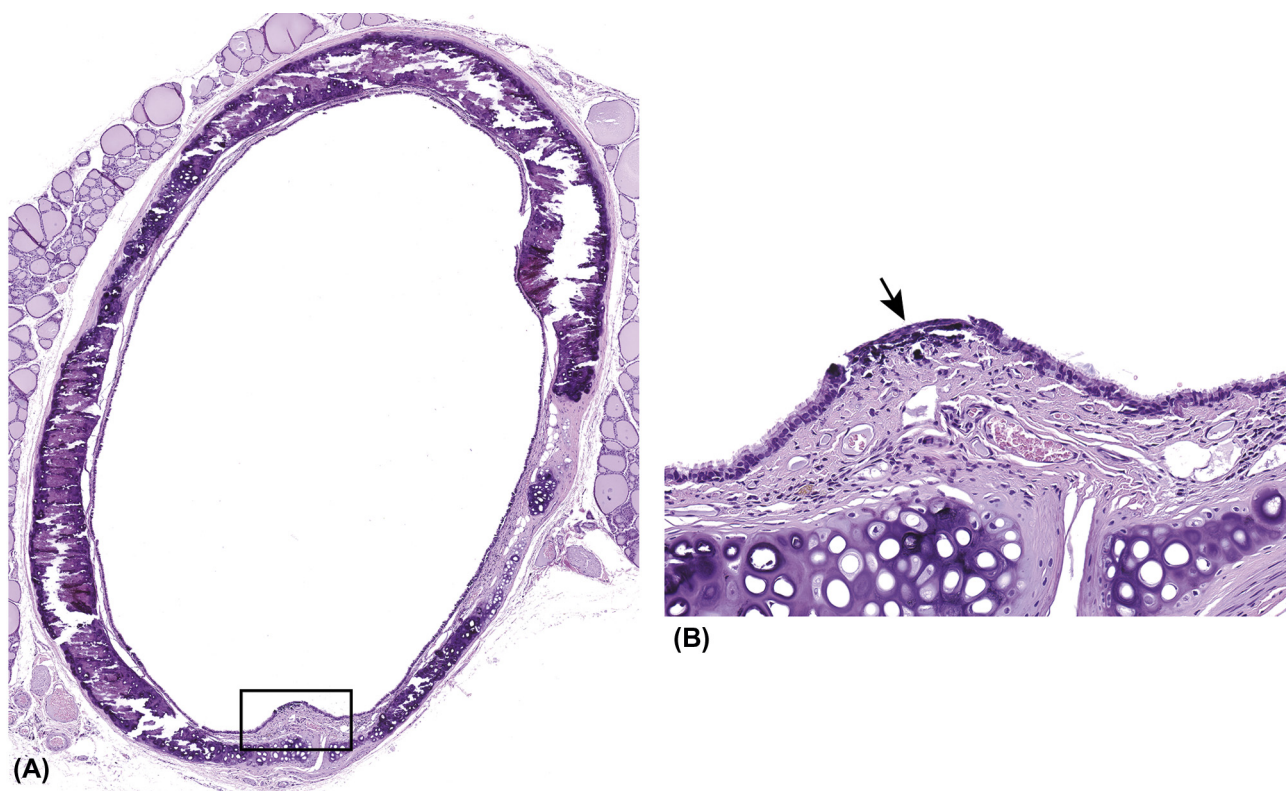
FIGURE 22.48 A focal deposit of mineral (A) is present in the epithelium of the trachea (box). (B) Higher magnification of the boxed area showing basophilic mineral deposit (arrow).

well-established infections. Variable amounts of muco-purulent exudate are present on the mucosal surfaces and in the submusosal glands and ducts, and there is loss of epithelial cell, goblet cell hyperplasia, and accumulations of lymphocytes in the submucosa.

Sendai (paramyxovirus-parainfluenza 1) virus, sialoda-cryoadenitis virus (SDAV), and rat coronavirus, may cause mild to severe inflammation, necrosis, and erosions of the epithelium of the naso- and maxilloturbinates. Infiltrates vary with the stage of infection but are primarily lymphocytic with lesser numbers of lymphocytes and macrophages. Lymphocytic infiltrates are sometimes observed in the nasal submucosa and commonly occur around the nasolacrimal duct with SDAV infections. Sendai virus may act synergistically with *M. pulmonis* to cause a more severe inflammatory response than is caused by either alone.

The lamina propria of the nasal passage contains numerous vessels that may be affected by chemical exposure. Irritants may cause edema of the lamina propria or sometimes an eosinophilic serous exudate with few to no inflammatory cells. Hemorrhage may be observed in the lumens and tissues of the nasal passages, larynx and trachea due to trauma, infection, and inhaled irritant gases, vapors and aerosols. Hemorrhage is commonly

encountered in the nasolacrimal duct after retro-orbital blood collection for hematology. Angiectasis and/or thrombosis is sometimes observed in vasculature of the lamina propria of the nasal septum, turbinates, or lateral wall, usually associated with mononuclear cell leukemia or in debilitated, moribund animals. Congestion may be observed in rats that were found dead or that were euthanized while moribund or debilitated and is related to terminal passive congestion.

6. HYPERPLASTIC AND NEOPLASTIC LESIONS

Hyperplastic and neoplastic lesions of the upper respiratory tract of rats are rarely spontaneous. In acute, subchronic, and chronic inhalation studies, hyperplasia is a common response in the squamous, respiratory, and olfactory epithelia of the nasal cavity, larynx and trachea. The nasal cavity is most commonly affected. It is not always clear whether hyperplasia is a regenerative response or part of a morphologic continuum to neoplasia. In some instances, hyperplasia with disorganization of the epithelium and cellular atypia may represent incipient neoplasia. However, the potential for a particular hyperplastic lesion

to progress or regress, as well as the rate of progression or regression, is unknown.

Spontaneous neoplasms of the nasal cavity, larynx, and trachea are rare in National Toxicology Program (NTP) studies in the F344 rat. Only 19 and 46 neoplasms of the nasal cavity were identified from nearly 13,500 control females and males, respectively. No tumors of larynx and trachea were identified in nearly 3,500 and 13,500 control rats, respectively. However, chemicals given either systemically or by inhalation have been associated with an increased incidence of neoplasms of the nasal cavity. Some chemicals have preferentially induced neoplasms of the olfactory (NTP, 1979), respiratory (NTP, 1985), or squamous epithelium (NTP, 1978), whereas others affect more than one cell type (NTP, 1982a, 1986, 1990, 2000). Fifteen out of a total of 589 toxicology/carcinogenicity studies conducted by the NTP induced neoplasms of the nasal cavity (NTP, 1978, 1979, 1982a, b, 1985, 1986, 1988, 1990, 1993, 1999a, b, 2000, 2008, 2009, 2012).

6.1. Nasal Cavity

6.1.1. Squamous Epithelium

6.1.1.1. Squamous Cell Hyperplasia

Hyperplasia of the stratified squamous epithelium in the anterior portion of the nasal passages is rare as a spontaneous lesion. Even in inhalation studies of irritant or reactive chemicals, proliferative lesions are less common in the squamous than in the respiratory or olfactory epithelia. Hyperplasia of the stratified squamous epithelium occurs in the nasal vestibule, ventral meatus, and the nasolacrimal and incisive ducts and is characterized by focal to diffuse increase in the number of cell layers. Because the thickness of the epithelium varies slightly, depending on location in the vestibule of the nose, it may be difficult to identify subtle lesions or lesions of minimal to mild severity. The hyperplastic epithelium is usually well differentiated; however, the cells in the affected area may have larger nuclei with more prominent nucleoli and more abundant cytoplasm. Minimal to mild hyperkeratosis may present with prolonged exposure. Focal cellular atypia may occur in areas of squamous hyperplasia; it is characterized by cellular and nuclear pleomorphism and increased nucleolar size. These changes may occur with exposure to carcinogens, and may precede the development of squamous cell carcinoma.

6.1.1.2. Squamous Cell Papilloma and Carcinoma

Spontaneous squamous cell neoplasms of the nose are extremely rare, but such neoplasms have been induced in the nasal passages and nasolacrimal ducts of rats exposed to carcinogens by inhalation or other routes. They may arise from stratified squamous epithelium in the vestibule of the nose, but more commonly arise from areas of squamous metaplasia in the respiratory or olfactory epithelia.

Nasal squamous cell papillomas are small, rarely occlusive, and have histological features similar to those of squamous cell papillomas at other sites (Figure 22.49). They are exophytic, sometimes pedunculated masses that typically consist of branching, papillary, or filiform projections of well-differentiated, variably keratinized, stratified squamous epithelium overlying a thin core of connective tissue stroma. The papillary structures of nasal squamous cell papillomas are usually short and show little branching or folding. Occasionally, there may be growth beneath the mucosal surface (inverted or endophytic papilloma; Figure 22.50). Small areas of cellular atypia or dysplasia may be within the epithelium.

Nasal squamous cell carcinomas are most common in the anterior nasal cavity. The growth features and morphological appearance are similar to those of squamous cell carcinomas at other sites. These neoplasms may be well-differentiated or poorly differentiated, and are usually highly invasive; they may efface the surrounding nasal tissue and bones (Figure 22.51). On occasion, they may extend dorsally to invade the brain. Well-differentiated squamous cell carcinomas generally consist of mature, keratinized squamous epithelium that may or may not have distinct intercellular bridges (Figure 22.51). Maturation of the cells within the neoplastic epithelium is dysplastic and

FIGURE 22.49 Squamous cell papilloma (asterisk) arising from the epithelium of the nasal septum occludes the nasal passage.
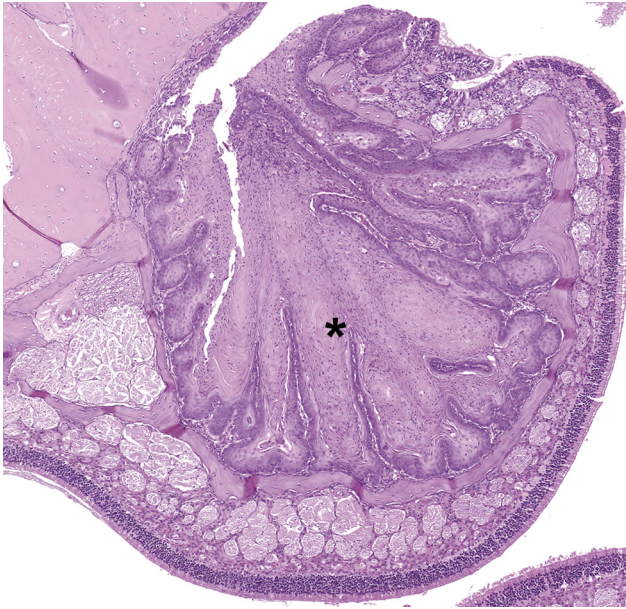
FIGURE 22.50 Inverted squamous cell papilloma arising from the olfactory epithelium.

disorganized. Poorly-differentiated squamous cell carcinomas will generally have marked cellular and nuclear pleomorphism and atypia, increased numbers of abnormal mitotic figures, and the cells lack intercellular bridges. Both histologic types (well-differentiated and poorly differentiated) often contain variable amounts of fibrous tissue.

6.1.2. Transitional, Respiratory and Olfactory Epithelium, and Associated Glands

6.1.2.1. Hyperplasia and Hyperplasia with Atypia (Atypical Hyperplasia, Basal Cell Hyperplasia, Dysplasia)

b. Hyperplasia and Hyperplasia with Atypia (Atypical Hyperplasia, Basal Cell Hyperplasia, Dysplasia) Hyperplasia of the transitional respiratory epithelium lining the lateral walls and lateral aspects of the naso- and maxilloturbinates has a slightly different appearance. In response to injury, 3 or more cell layers of flat epithelial cells, that in some areas may appear squamoidsquamous, replace the normal 1-2 layers of cuboidal, pseudostratified epithelium in these sites (Figure 22.52). Under these conditions, the transitional
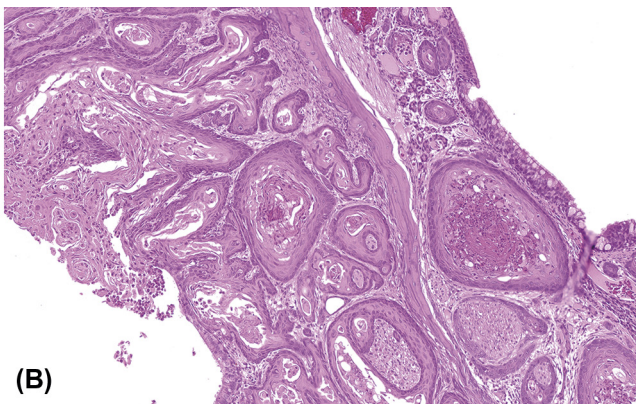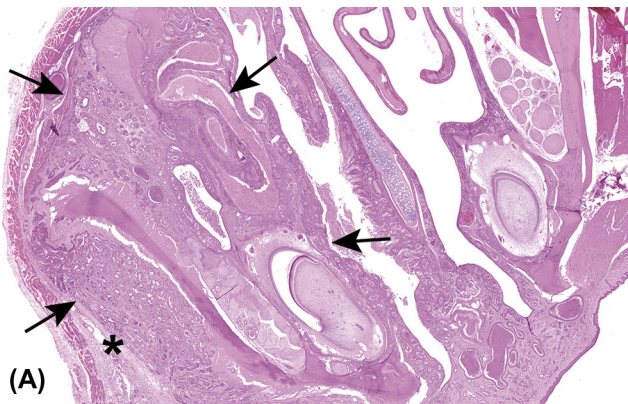

FIGURE 22.51 (A) Unilateral squamous cell carcinoma effacing the nasal cavity (arrows). The neoplastic cells infiltrate the surrounding soft tissue. (B) Magnified view shows neoplastic squamous epithelium with variable amount of keratin.
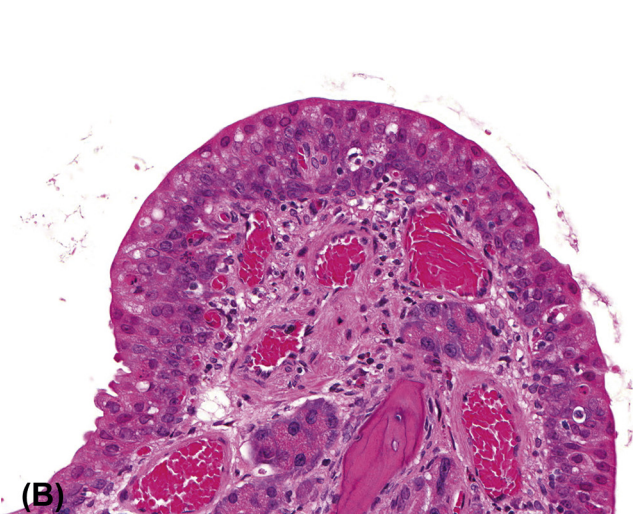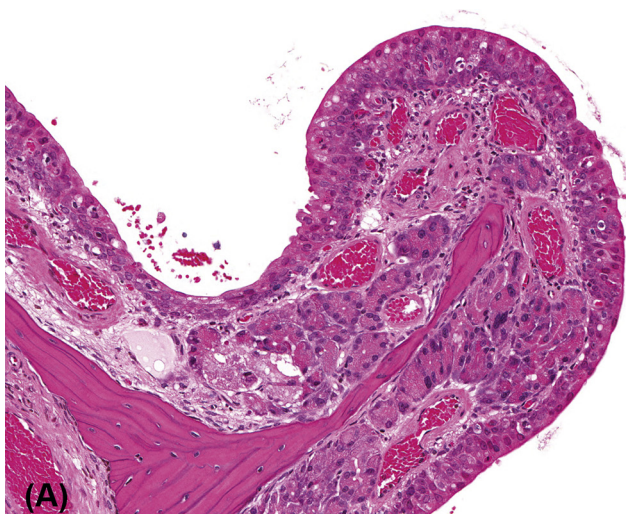

FIGURE 22.52 (A) Transitional epithelium hyperplasia. (B) Note the increased number of cell layers compared to Figure 22.8.
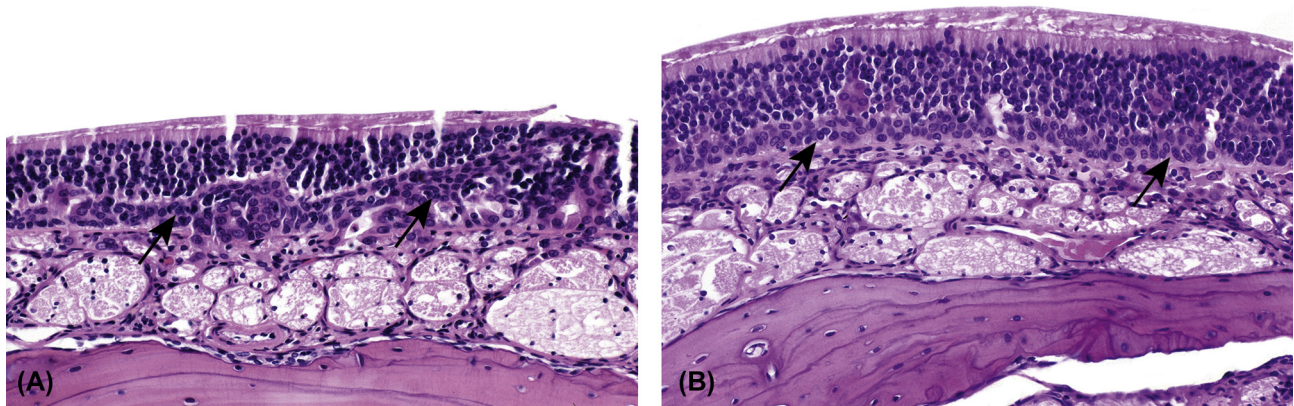
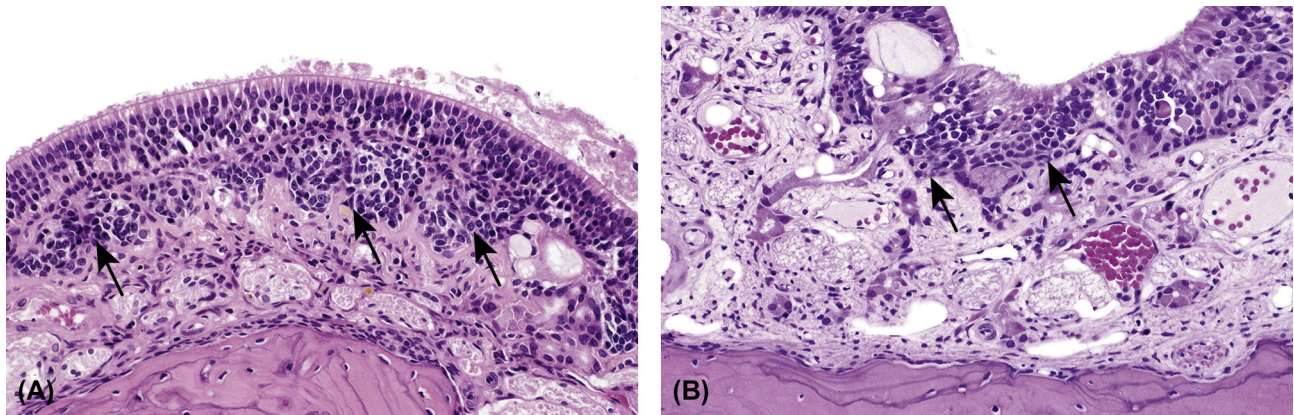**FIGURE 22.53** Basal cell in the olfactory epithelium (arrows).

FIGURE 22.54 Atypical hyperplasia in the olfactory epithelium (arrows)

epithelium, usually devoid of mucous cells, may also develop mucous cell metaplasia.

Olfactory epithelial hyperplasia must be distinguished from respiratory epithelial metaplasia in the olfactory epithelium which is a common adaptive response to injury following inhalation of toxicants. This lesion is also occasionally observed in aged rats as a focal spontaneous change. Respiratory epithelial metaplasia is restricted to the olfactory epithelium of the dorsal meatuses of the Level II section and the ethmoid turbinates, and is characterized by replacement of the olfactory epithelial cells by tall columnar epithelial cells that are morphologically similar to those of the nasal respiratory epithelium (Figure 22.35).

Basal cell hyperplasia is characterized by focal, multifocal, or segmental proliferation of basal cells along the basement membrane of respiratory, transitional, olfactory or squamous epithelia. The basal cells may be relatively uniform or pleomorphic, and frequently occur as small irregular clusters and/or nodular proliferations arising from of the basal epithelium (Figure 22.53). The proliferations are bounded by the basement membrane and do not extend into the subjacent lamina propria.

Cells have scant, often basophilic cytoplasm and nuclei with stippled chromatin.

Focal, multifocal, or more extensive proliferations of poorly-differentiated or pleomorphic epithelial cells (atypical hyperplasia, hyperplasia with atypia) may occur within or in association with respiratory epithelial hyperplasia. Areas of epithelial hyperplasia with cellular atypia should not be mistaken for epithelial regeneration that follows acute epithelial injury. Atypical hyperplasia is diagnosed when proliferating epithelial cells develop below the basement membrane and proliferate in the lamina propria (Figure 22.54); this lesion may be preneoplastic.

6.1.2.2. Adenoma (Adenomatous or Villous Polyp, Villous or Polypoid Adenoma)

Spontaneous and chemically induced adenomas of the nasal cavity are extremely rare. They may arise in the anterior portion from the transitional and respiratory epithelia or from the epithelia of the nasal glands. Adenomas of the respiratory epithelium usually arise from the free margins of the naso- and maxilloturbinates (Figures 22.55
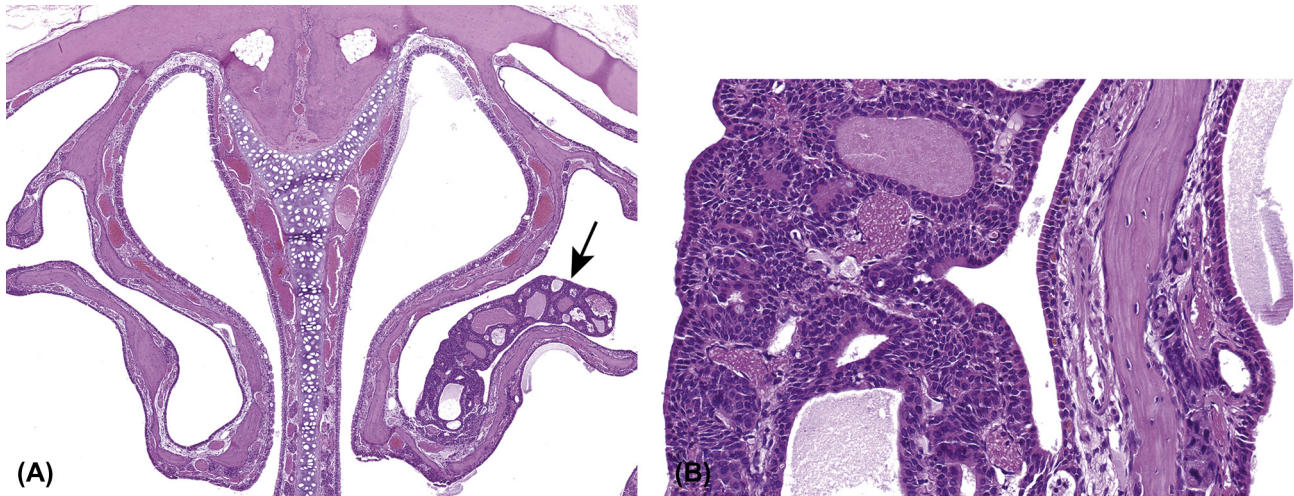
FIGURE 22.55. (A) Adenoma (arrow) arising from the respiratory epithelium of the nasoturbinates (A). (B) Higher magnification of (A) shows the neoplastic cells form irregular glandular structures.
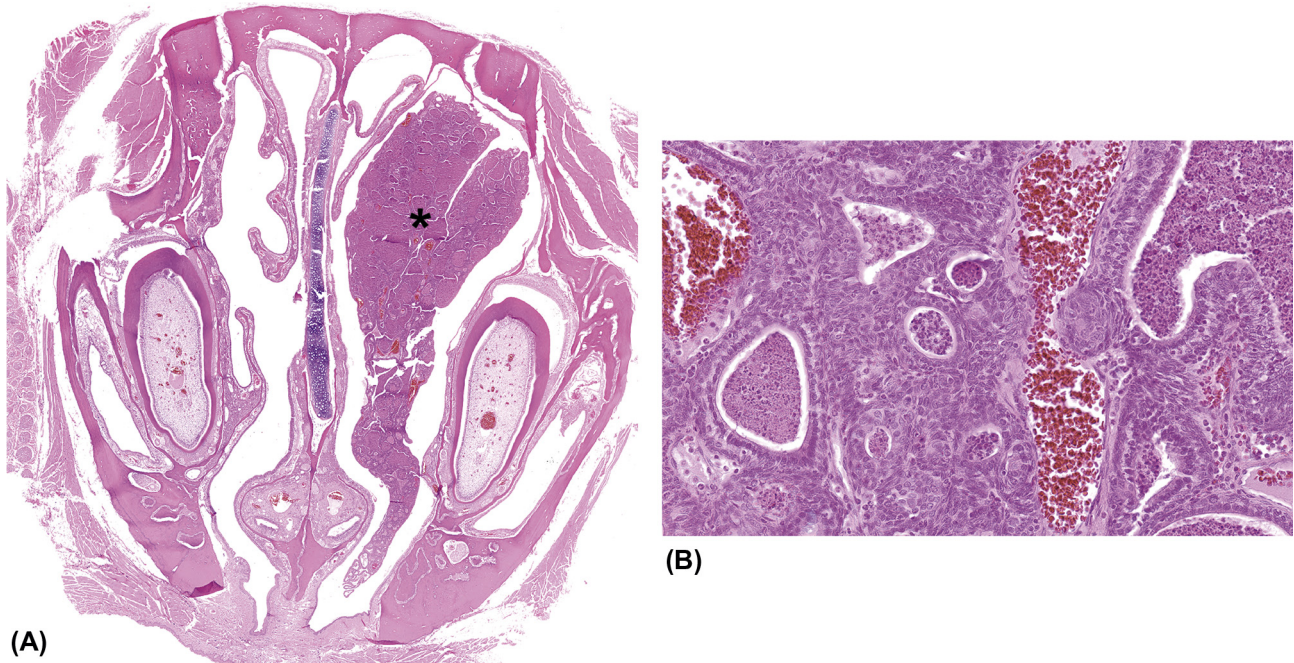
FIGURE 22.56 (A) Adenoma (asterisks) arising from the respiratory epithelium is partially occluding one side of the nasal cavity. (B) Magnified view of the adenoma showing irregular glandular structures.

and 22.56), whereas those arising from the transitional epithelium develop from the lateral walls (Figure 22.57). These adenomas are typically exophytic and extend into the lumen of the nasal passages; however, they are rarely completely occlusive. They may be quite large and attached to the mucosa by a relatively narrow stalk or have a sessile, broad-base of attachment to the mucosa. Adenomas may have a papillary pattern with a few invaginated gland-like structures or tubules, or they may be polypoid with an irregular surface and consist predominantly of tubular or gland-like structures. The villous and glandular structures are lined by simple or pseudostratified epithelium composed of cuboidal to low columnar nonciliated, ciliated and/or secretory cells; however, a few cells may be atypical. Occasionally, the epithelium may have focal areas of squamous epithelium. Endophytic adenomas may be compressive; they consist of acinar or gland-like structures that are separated by scant fibrovascular stroma and lined by nonciliated cuboidal epithelial cells.

(A)

(B)

(C)

FIGURE 22.57   Transitional cell adenoma (asterisk) arising from the lateral wall of nasal cavity (A), (B) and (C). Higher magnification of the adenoma shown in (A).

(A)

(B)

FIGURE 22.58   (A) Adenoma (asterisk) of the submucosal glandular epithelium. (B) Higher magnification of adenoma in (A).

Transitional epithelial adenomas are typically small exophytic masses that arise from the nasoturbinates or the lateral wall between the maxilloturbinates and the naso-turbinates (Figure 22.57); they have been induced by chemicals (NTP, 2012). Neoplastic cells are moderately sized and polygonal with moderate amounts of lightly eosinophilic cytoplasm. Nuclei are also moderately sized and round to oval, with lightly stippled chromatin and one or two prominent basophilic to amphophilic nucleoli.

Adenomas of nasal glands (Figure 22.58) may be mor-phologically indistinguishable from endophytic adenomas; the precise site of origin of the larger neoplasms may be difficult to determine. Small nodules of glandular tissue or solid clusters of cells are within the lamina propria in the region of the septal and submucosal (Bowman's) glands exposed to nasal carcinogens and presumably arise

from these glands. These adenomas are well circumscribed with minimal cellular pleomorphism and atypia.

6.1.2.3. Adenocarcinoma

Spontaneous and chemically induced adenocarcinomas of the nasal cavity are extremely rare. Adenocarcinomas may arise from the transitional (Figure 22.59) and respiratory epithelia (Figure 22.60) of the anterior nasal cavity, the olfactory epithelium, the epithelium of the submucosal glands, or by malignant transformation within adenomas. Their size varies, and the precise epithelial origin of highly invasive expansive adenocarcinomas is often difficult to ascertain, particularly with those neoplasms that grow to occupy both sides of the nasal cavity. Adenocarcinomas that are located in the lateral wall originate from the transitional epithelium. Although transitional cell carcinomas are rare, they can be induced by chemical exposure (NTP, 2012).

Similar to adenomas, adenocarcinomas of the respiratory epithelium may be exophytic or endophytic or may grow by extension along the nasal walls or turbinates. Papillary, glandular, pseudoglandular, or solid growth patterns may occur. Well-differentiated adenocarcinomas may consist of glandular and/or papillary structures composed of cuboidal to columnar epithelial cells surrounded by variable amounts of loosely organized supporting stroma.

Transitional cell carcinomas are expansile and may occlude the nasal cavity. Neoplastic cells are polygonal with eosinophilic cytoplasm and prominent nucleoli. The neoplastic cells tend to be arranged in sheets, or gland-like structures, with a moderately vascular stroma.

Highly malignant adenocarcinomas, of uncertain epithelial origin, are usually poorly differentiated. These neoplasms usually have markedly pleomorphic growth patterns with the cells arranged as poorly formed papillary or glandular structures and/or disorganized cords and sheets. The cells may be cuboidal to columnar, or round to polyhedral, with varying amounts of cytoplasm and hyperchromatic or vesicular nuclei. In some carcinomas the cells are spindle shaped. Numerous mitotic figures and extensive necrosis may be present. Invasion of adjacent tissues, including the bone, may be extensive.

6.1.2.4. Adenosquamous Carcinoma

Adenosquamous carcinomas have histologic characteristics that are morphologically similar to those of adenocarcinomas. However, a significant portion of the neoplasm consists of well- to poorly-differentiated neoplastic squamous epithelium. Squamous components may form keratin pearls (Renne et al., 2009).
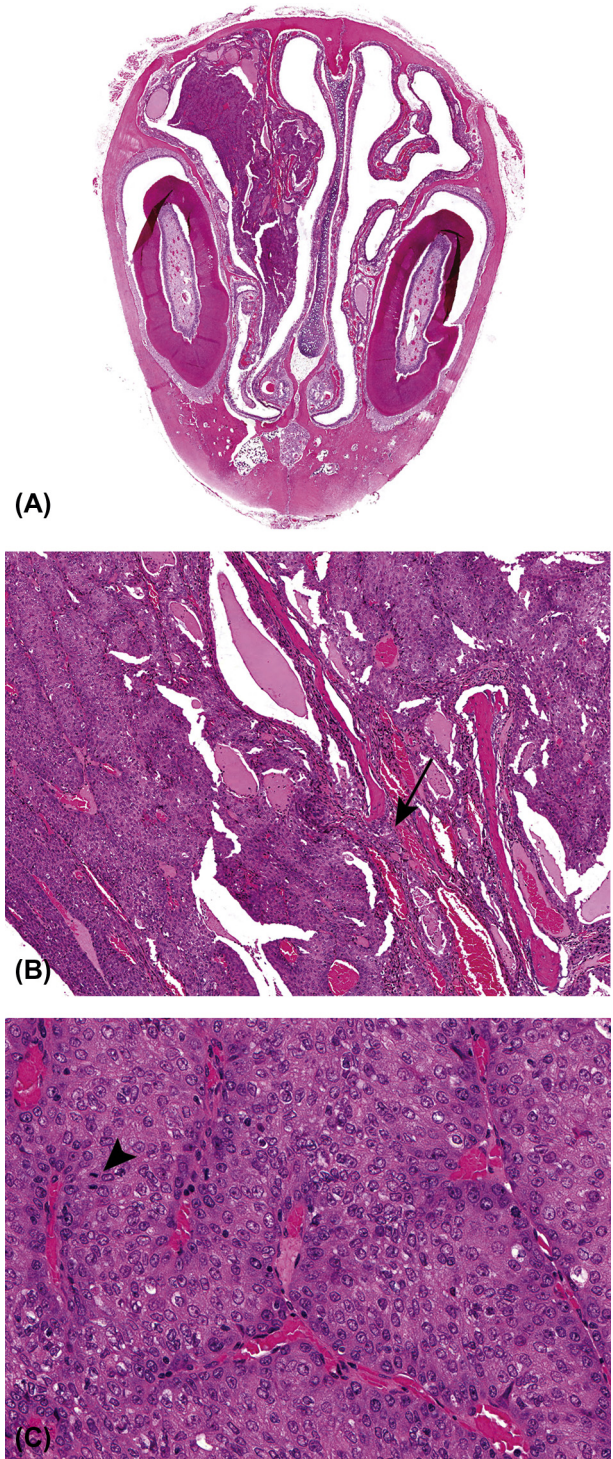
FIGURE 22.59 (A) Transitional cell carcinoma arising on the lateral wall of nasal cavity. (B) and (C) higher magnification of (A). The neoplastic cells invade the underlying tissue including turbinate bone (arrow). The neoplastic are polygonal cells and are arranged in irregular sheets and islands separated by a thin fibrovascular stroma. Occasional mitotic figures are present (arrowhead).
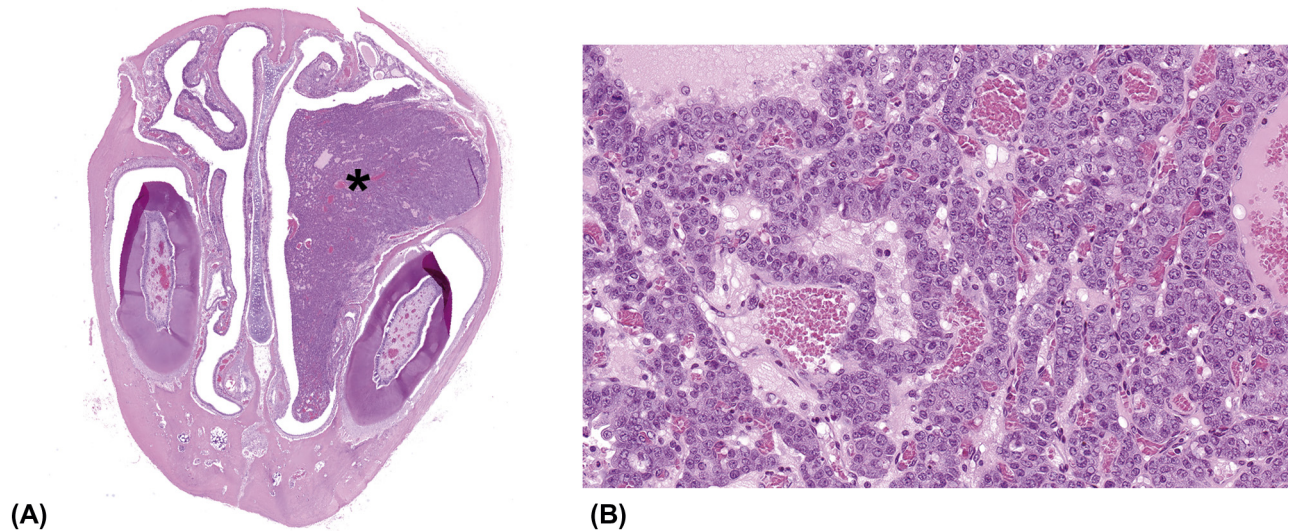
(A)   **(B)**

FIGURE 22.60   Adenocarcinoma (asterisk) arising from the respiratory epithelium (A). The neoplasm completely effaces and occludes one side of the nasal passage. (B) Higher magnification of the A shows relative uniform neoplastic cells that form irregular cords and glandular structures.

6.1.2.5. Olfactory Neuroblastoma

Spontaneous and chemically induced neoplasms of the olfactory epithelium are extremely rare. Exposure related malignant neoplasms have been reported in only one study conducted by the National Toxicology Program. The morphology of these neoplasms can vary considerably making classification based on cell type difficult without application of immunohistochemistry (chromogranin A and synaptophysin) or electron microscopy. A number of terms have been applied to neoplasms of the olfactory neuroepithelium. Esthesioneuroepithelioma has been used for neoplasms that contain "true" rosettes (Flexner-Wintersteiner type with central lumen). Those with pseudorosettes (Homer-Wright type without a true lumen) were called esthesioneuroblastoma. Esthesioneurocytoma was the term used for neoplasms without rosettes but having a neurofibrillary background and lobular pattern. Because of the difficulty in classification, in rodent toxicologic pathology, the general term olfactory neuroblastoma has now been coined for poorly differentiated neoplasms of the olfactory epithelium.

Olfactory neuroblastomas are variably sized and highly invasive. They may be unilateral or bilateral (Figure 22.61). Large masses may obliterate the nasal architecture invading nerves, nasal bones, and the olfactory lobes of the brain through the cribriform plate. Other masses may extend along the mucosa replacing the epithelium of the ethmoid turbinates and nasal septum. The neoplastic cells may be round, polygonal, or spindle-shaped, and arranged in irregular glands, islands, and cords separated by fibrovascular stroma (Figure 22.61). The cells have eosinophilic to amphophilic cytoplasm

with pale oval to polygonal vesicular nuclei and prominent central nucleoli. Dysplastic areas of squamous epithelium, and keratin pearls may be present. Numerous mitotic figures and areas of necrosis are typically present. True rosettes (columnar cells with basally located nuclei and abundant pale cytoplasm surrounding a central lumen) and pseudorosettes (rounded clusters of cells with peripherally located nuclei and cytoplasm converging toward of a poorly defined lumen) may be found.

6.1.2.6. Nasal Polyps

Nasal polyps are relatively uncommon, spontaneous, proliferative, lesions, and are rarely associated with chemical exposure. Polyps are exophytic growths that may be occlusive. They are often free within the nasal passages and conform to the shape of the meatuses. These lesions consist of a core of proliferating loose, vascularized, connective tissue. They are lined by normal, hyperplastic, or metaplastic, mucosal epithelium (Figure 22.62).

6.1.2.7. Mesenchymal Neoplasms

Fibroma (Figure 22.63), fibrosarcoma (Figure 22.64), hemangioma, hemangiosarcoma, chondroma (Figure 22.65), chondrosarcoma (Figure 22.66), osteoma, osteosarcoma, and schwannoma all occur rarely as spontaneous neoplasms of the nasal cavity. They have morphological characteristics of mesenchymal neoplasms at other sites.

6.2. Larynx and Trachea

Spontaneous, age-related lesions are infrequent in the larynx and trachea of rats. However, degenerative,
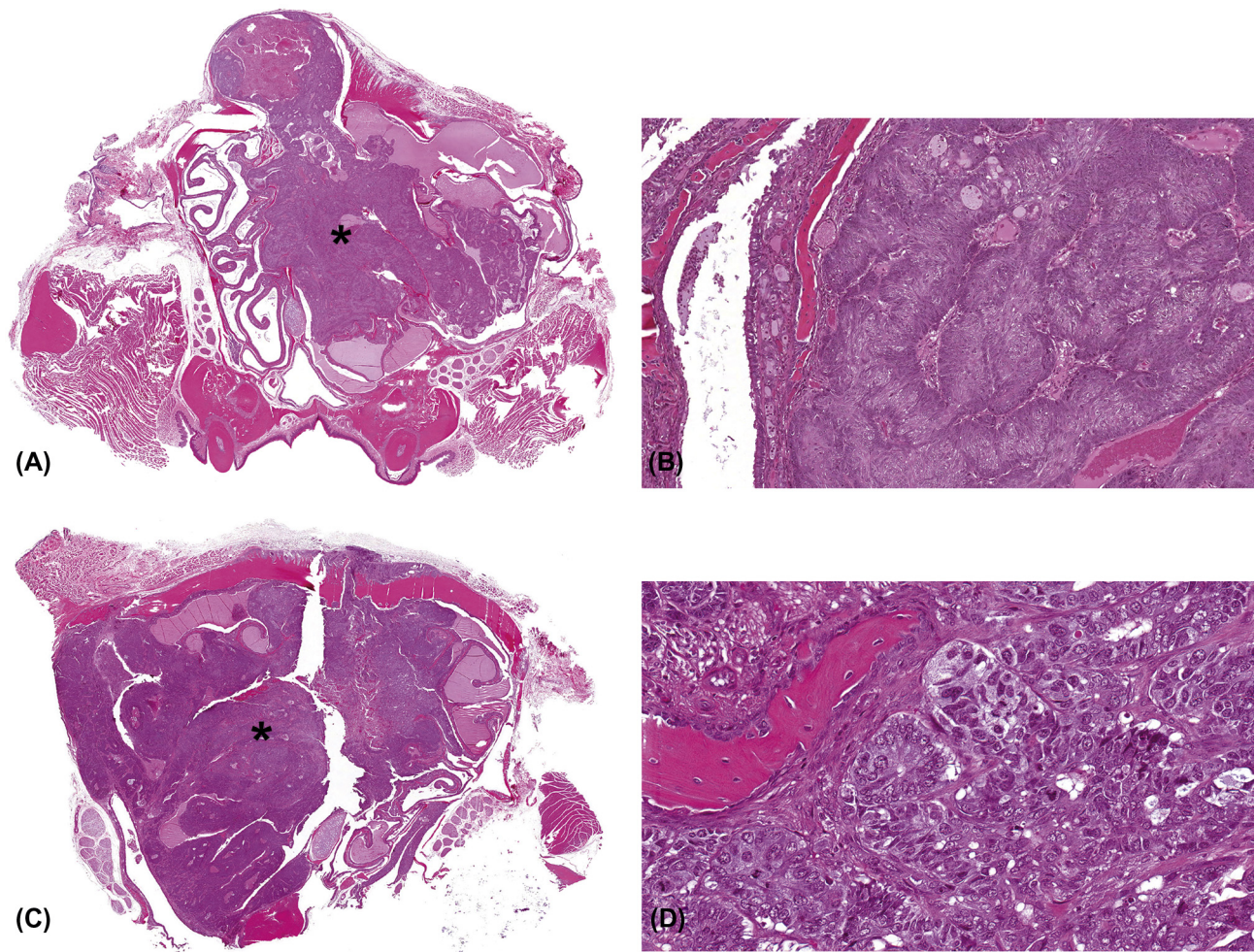
FIGURE 22.61   Olfactory neuroblastoma (A) and (C). Highly invasive neoplasms obliterating the normal architecture (asterisks). (B) and (D) Higher magnifications of (A) and (C). The neoplastic cells form thick, irregular cords (A) and glandular structures (B) separated by fibrovascular stroma.
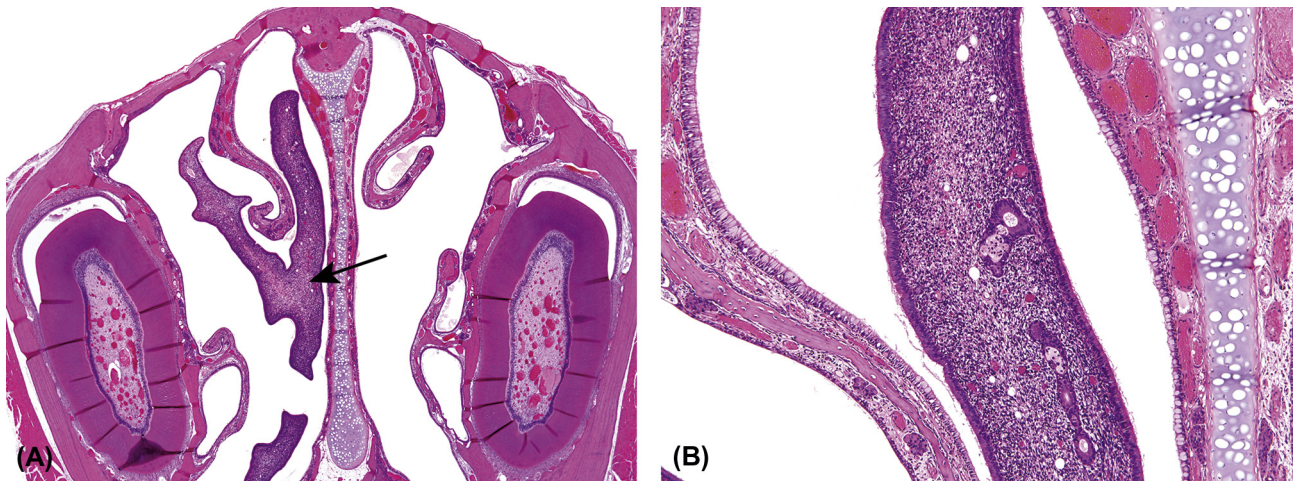
FIGURE 22.62   Epithelial polyp (arrow) partially occludes the nasal passages (A). (B) Higher magnification of (A). The polyp consists of a core loose, vascularized connective tissue lined by ciliated, columnar respiratory type epithelium. The attachment to the mucosa is not present in the section.
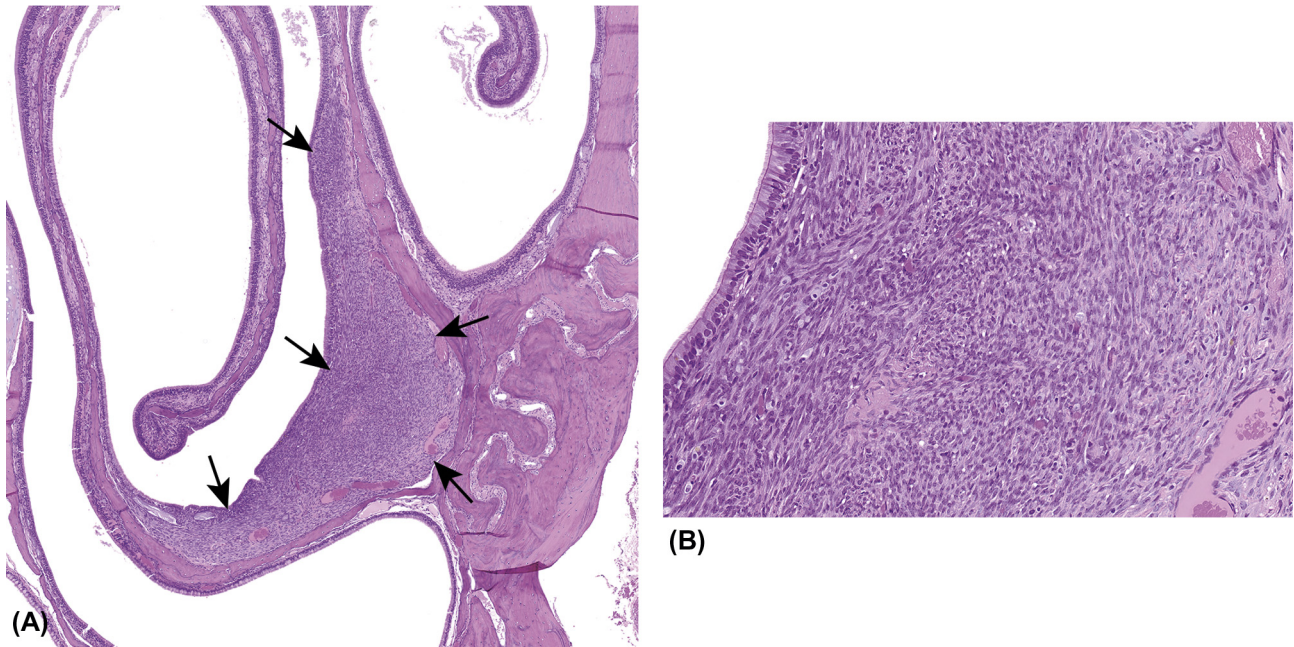
FIGURE 22.63   (A) Fibroma in the olfactory epithelial mucosa associated with ethmoturbinate (arrows). (B) Magnified view of the fibroma demonstrating spindle-shaped neoplastic cells.

regenerative, proliferative, and inflammatory lesions resulting from inhalation exposure to chemicals are common in the larynx, but less so in the trachea. When observed, the lesions are morphologically similar to those that occur in the nasal cavity. In the larynx, lesions are most often observed in the epithelium at the base of the epiglottis.

Dilation of the submucosal glands at the base of the epiglottis of the larynx and the trachea is perhaps the most common age-related lesion and frequently occurs in association with other chemically induced changes in the larynx. This lesion is characterized by variable dilation of the glands, which may be lined by flattened epithelium (Figures 22.45 and 22.46). A mixture of inflammatory cells and secretory material may be present in the lumen of affected glands.

Degeneration may consist of one or more changes including small irregular cytoplasmic vacuoles, increased cellular eosinophilia, cellular swelling, rounding, blebbing, loss of cilia, nuclear pyknosis, loss of cell-to-cell contact, loss of cells, and overall disorganization of the epithelium. Necrosis may also be present (Figures 22.67 and 22.68). As in other sites of the upper respiratory tract, regeneration may occur after epithelial injury and is characterized by replacement of damaged or lost epithelial cells by a single layer of flattened to low cuboidal epithelial cells that cover the affected site (Figures 22.69 and 22.70). Sometimes, immature polyhedral cells are a component of the regenerating epithelium.

Inflammatory cells, primarily lymphocytes, in the submucosa of the larynx at the base of the epiglottis may occur as a normal finding. Inflammation frequently accompanies injury to the laryngeal epithelium, and the nature of inflammatory lesions observed varies with the exposure duration and potency of the inhaled agent. Hemorrhage in laryngeal tissue is usually related to trauma or may accompany inflammation, degeneration, and necrosis. The nature of inflammatory lesions observed varies with the exposure duration and potency of the inhaled agent.

Hyperplasia of the respiratory epithelium of the larynx and trachea may be focal, multifocal, or diffuse. The epithelium appears thickened, crowded, and disorganized due to increased numbers of epithelial cells (Figures 22.71 and 22.72). The hyperplastic cells may be nonciliated or ciliated, and the epithelium may occasionally form papillary structures that extend into the laryngeal lumen. Minimal cellular and nuclear pleomorphism and atypia may be evident.

Focal, segmental, or diffuse hyperplasia of the squamous epithelium lining the medial and lateral aspects of the arytenoid cartilages is a common exposure-related change in the larynx. The hyperplastic epithelium is generally well-differentiated, variably keratinized, and may be quite thickened (Figure 22.73). Slight nuclear pleomorphism and cellular atypia may be present. Squamous hyperplasia of the epithelium lining the arytenoid cartilage is often accompanied by squamous metaplasia of the
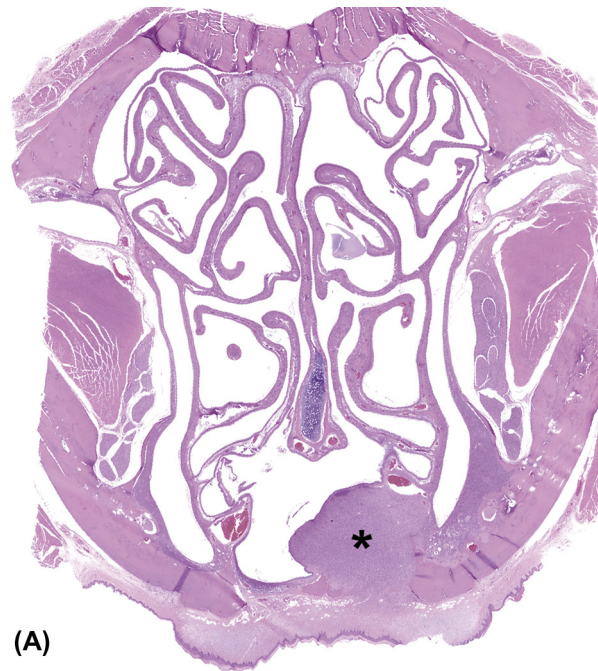
(A)
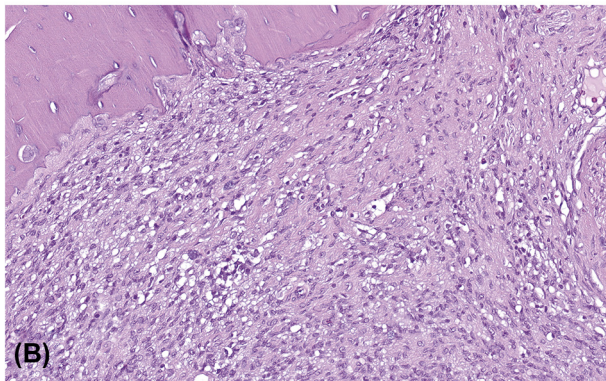
(B)
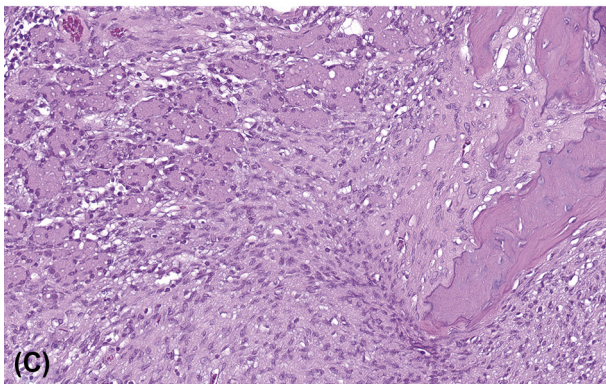
(C)

FIGURE 22.64   (A) Fibrosarcoma (asterisk) at the level of nasopharyngeal duct. (B) and (C) Higher magnifications of the neoplasm showing its infiltrative nature and cellular detail.

epithelium lining the base and lateral aspects of the epiglottis (Figure 22.73A). In subchronic and chronic inhalation studies conducted by the National Toxicology Program, squamous metaplasia is a commonly observed
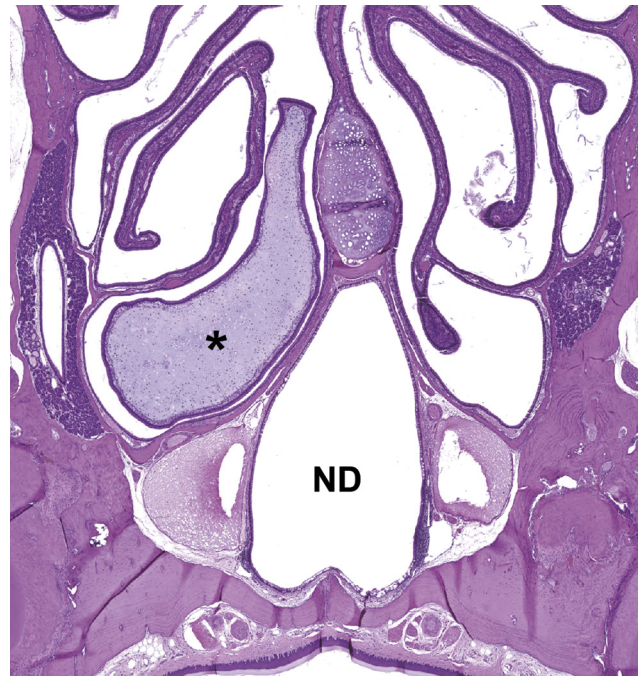
FIGURE 22.65   Chondroma (asterisk) associated with ethmoid turbinates and adjacent to nasopharyngeal duct (ND).

epithelial response to inhaled irritants in the laryngeal and tracheal epithelia, and is typically observed in association with, or as a consequence of, inflammation, degeneration, necrosis, and ulceration. Squamous metaplasia is generally considered an adaptive/protective response to repeated irritation rather than a preneoplastic lesion; progression to squamous cell neoplasia in the larynx and trachea is extremely rare. In the larynx, squamous metaplasia is most common and severe in the respiratory epithelium lining the base and lateral aspects of the epiglottis. However, it is not unusual to see squamous metaplasia in other regions of the larynx that are lined by respiratory type epithelium, particularly when metaplasia is severe at the base of the epiglottis. The submucosal glands are seldom affected; however, squamous metaplasia may occur in the ducts as an extension of metaplasia in the overlying epithelium.

Squamous metaplasia is characterized by focal, segmental, or diffuse replacement of the respiratory epithelium by typically well-differentiated, variably keratinized, squamous epithelium (Figure 22.74). The metaplastic epithelium may have minimal cellular and nuclear pleomorphism or atypia.

Spontaneous and chemically induced neoplasms of the larynx and trachea are rare. Those that have been observed are most commonly metastatic or extensions of neoplasms in adjacent tissues. Granular cell tumor (Figure 22.75) is a rare spontaneous neoplasm that has been reported in the trachea. The tumor is composed of

(A)

(B)
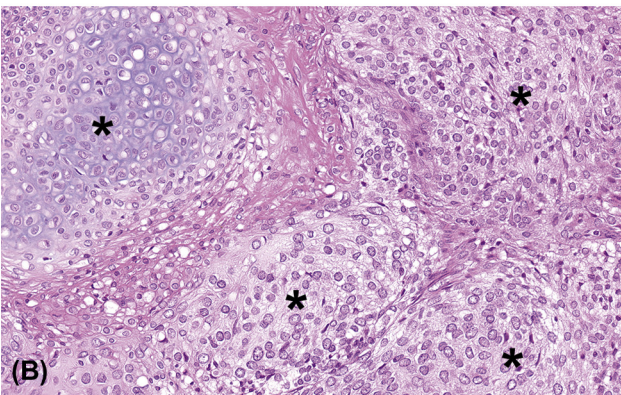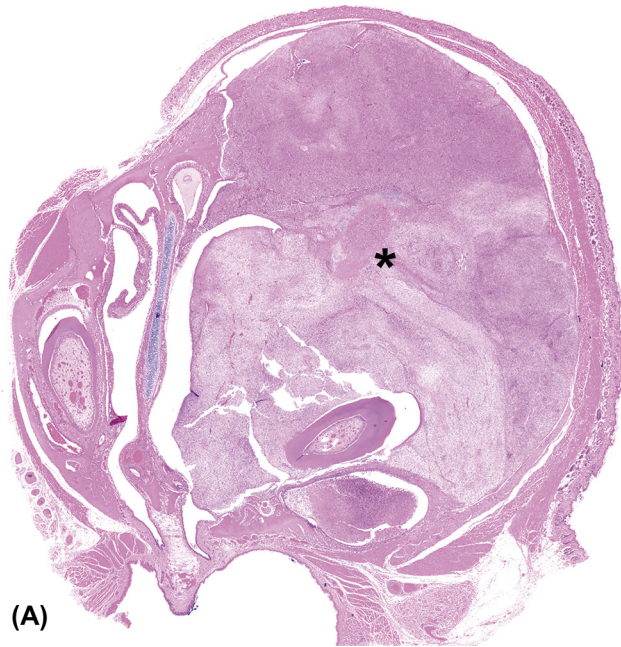
FIGURE 22.66   (A) Chondrosarcoma (asterisk) has effaced the nasal cavity with invades the surrounding tissues. (B) Higher magnification of the neoplasm showing neoplastic chondrocytes (asterisks).
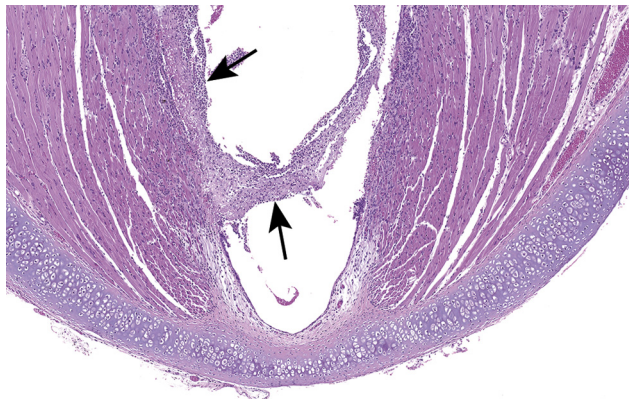
FIGURE 22.67   Necrosis of laryngeal mucosa (arrows) with accumulation of inflammatory cells and cellular and karyorrhectic debris in the tissue and lumen.
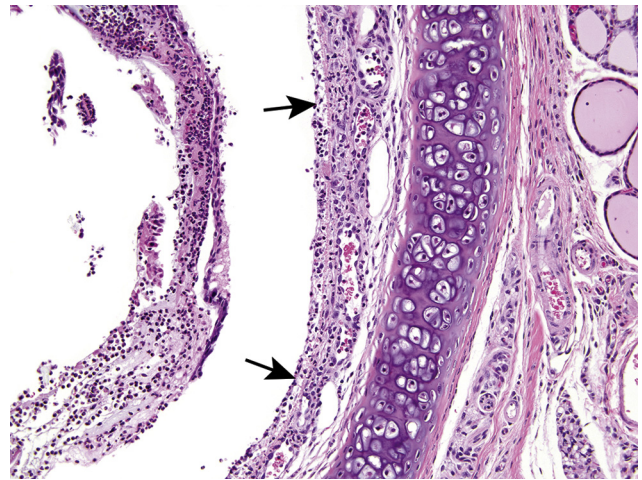
FIGURE 22.68   Necrosis of tracheal mucosa (arrows) with accumulation of degenerate neutrophils and cellular and karyorrhectic debris in the lumen.

large, uniform, ovoid, or polyhedral cells that have abundant eosinophilic and PAS-positive cytoplasm.

7. MISCELLANEOUS

7.1. Nasal Cavity

Lesions in nasal bones, including turbinates, are usually related to other systemic bone changes in the animal. These changes may be secondary to advanced renal disease or may follow long-term exposure to a chemical that produces necrosis of the mucosa. In aging rats, inflammation of incisors and molars may result in tooth dysplasia with distortion of structures in the nasal cavity.

Hyperostosis is a rare spontaneous nasal lesion in rats, but has been a treatment-related lesion in inhalation studies. This lesion is more common in females and has been observed in chronic studies with marked degeneration, necrosis, and inflammation in the nasal cavity. The naso-, maxilla- and ethmoid turbinates may be affected, but hyperostosis is most common in the anterior nasal cavity. Microscopically, there is thickening of the turbinate by dense woven bone that is lined by increased numbers of osteoclasts (Figure 22.76). The affected turbinates are wide, short, and blunt.

Gastric reflux associated with gavage administration of test material can result in inflammatory lesions in the nose. Reflux-induced lesions are usually unilateral, often involve the nasopharyngeal duct, and tend to be more severe posteriorly, ventrally, and laterally in the nasal cavity. The lesions are often suppurative, and have acute changes superimposed on chronic changes, especially if the reflux is a repetitive event.
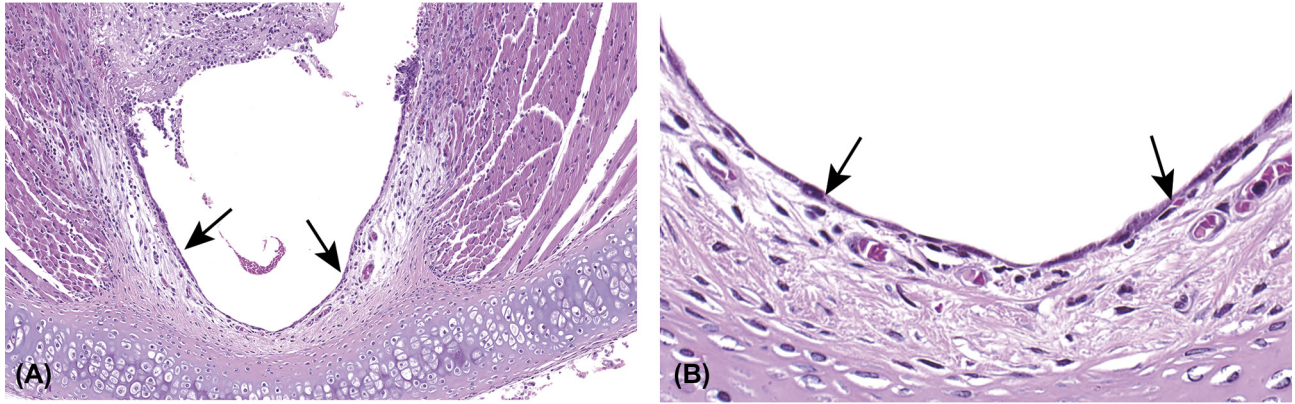
FIGURE 22.69   Regeneration of laryngeal epithelium (arrows) (A). (B) Magnified view demonstrating mucosa lined by a single layer of flattened epithelium (arrows).
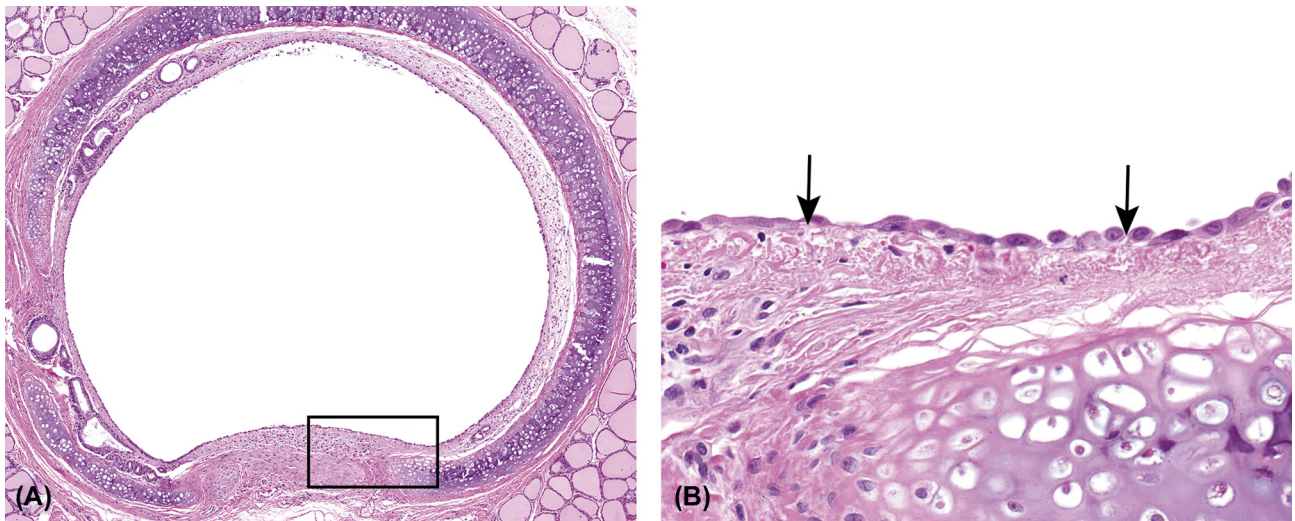
FIGURE 22.70   Regeneration of tracheal epithelium (A). (B) Higher magnification of (A). The mucosa lined by a single layer of flattened epithelial cells (arrows).
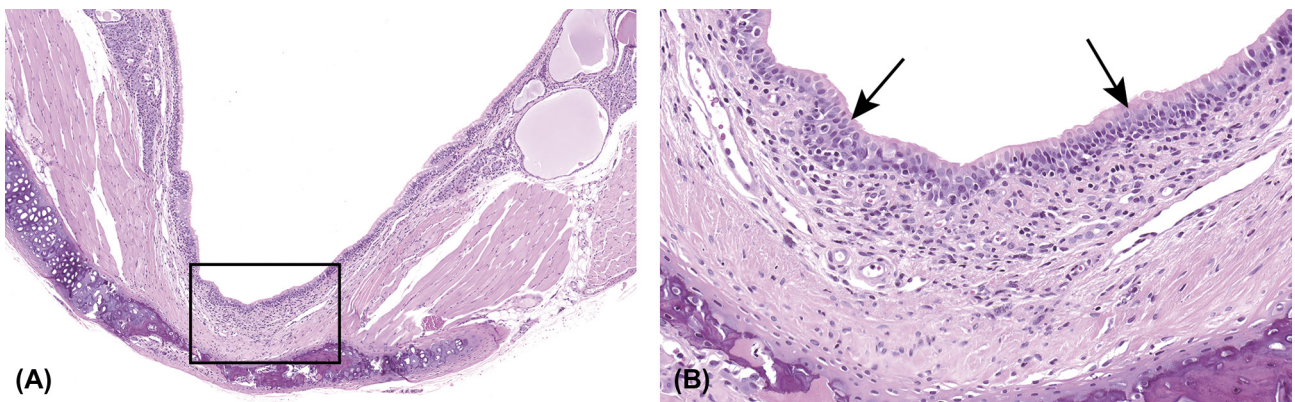
FIGURE 22.71   Hyperplasia of laryngeal respiratory epithelium (A). (B) Higher magnification of the (A) showing increased thickness of the epithelium with disorganized piling up of the epithelial cells (arrows). Compare to the normal epithelium in Figures 22.14 and 22.15.
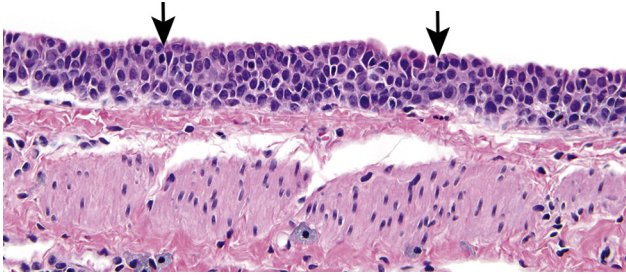
FIGURE 22.72 Hyperplasia of tracheal epithelium. Compare to normal epithelium in Figure 22.16.
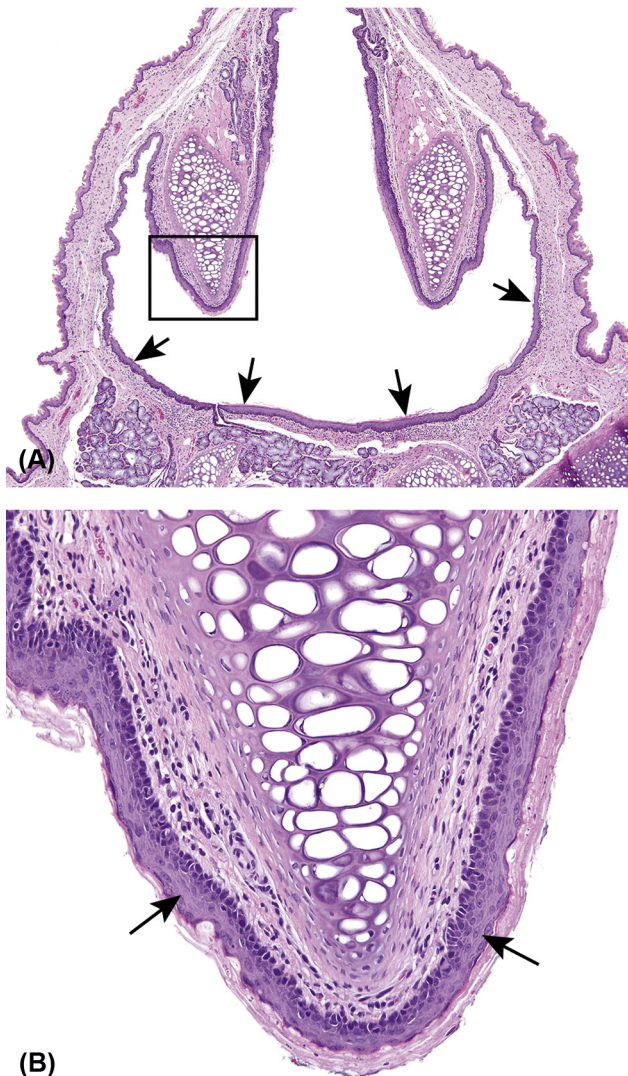
FIGURE 22.73 Hyperplasia of squamous epithelium lining the arytenoid cartilage (boxed area) (A). Note squamous metaplasia in the epithelium lining the base and lateral aspects of the epiglottis (arrows). (B) Higher magnification of boxed area in (A) (arrows).

8. TOXICOLOGIC LESIONS

As indicated in section IIB, for studies conducted by the National Toxicology Program, a standard set of transverse sections of the nasal cavity are routinely prepared for examination of the nasal cavity. In inhalation studies, location of lesions is generally dependent on regional deposition of inhaled agents or on regional cell susceptibility. Nasal uptake, regional deposition, and cellular responses are influenced by the airflow dynamics of the upper respiratory tract, the physical and chemical properties of the agent (volatility, water solubility, reactivity, size), the ambient concentration of the agent, the extent of local metabolism, the duration of exposure, and the effectiveness of the local defense mechanisms.

Areas of air turbulence in the anterior regions of the nose would be expected to increase contact of the mucosal surface with vapors and aerosols. Particles, depending on size, will be deposited at or near bends in the airways and produce site-specific responses. The physiologic characteristics of the nasal epithelium, such as mucociliary function, may also account for site-specific response. Mucociliary function is a sensitive indicator of nasal toxicity; treatment-induced upper airway lesions may be associated with areas of ciliostasis. Local cellular susceptibility may result from cell-specific metabolism. The transitional, respiratory and olfactory epithelia possess cytochrome P-450 and other metabolic and biotransformational enzyme systems that are important for metabolism and detoxification of inhaled toxicants. Cytochrome P-450 enzymes are present at higher levels in the olfactory epithelium than in the transitional and respiratory epithelia. Metabolism by these enzymes is largely responsible for injury to the olfactory epithelium, not only from inhaled xenobiotics, but also from parenterally administered xenobiotics that require metabolism by P-450 enzymes.

Many of the inhaled chemicals studied are classified as irritants and induced lesions result from regional epithelial cytotoxicity. Some chemicals are selectively toxic to specific cell populations, probably as a result of regional metabolism. In inhalation studies, lesions in the upper respiratory tract may show a steep anterio-posterior severity gradient. Regardless of the mechanism of toxicity, the response of epithelia of the upper respiratory tract generally proceeds through a characteristic and somewhat predictable sequence of events, depending on the degree of tissue damage and the presence or absence of continued toxic exposure. Exposure typically induces a spectrum of lesions that may include epithelial degeneration, necrosis, exfoliation of the epithelial cells, and ulcers or erosions, accompanied by vascular changes, edema, and acute to chronic inflammation. With chronic exposure, attempts at repair of the damaged epithelium may ensue,
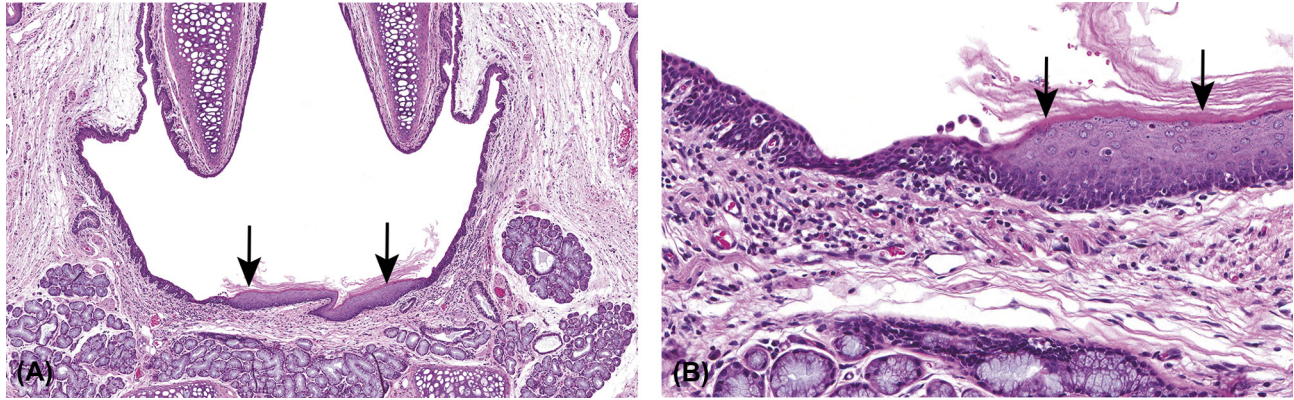
FIGURE 22.74 (A) Squamous metaplasia (arrows) of the laryngeal epithelium lining the lateral aspects and base of the epiglottis (A). (B) Squamous epithelium (arrows) has replaced the ciliated columnar epithelium that normally lines the base of the epiglottis.

including regeneration, hyperplasia, metaplasia, or fibrosis. Progression to neoplasia is rare. On cessation of exposure, restoration to the normal morphology may occur.

8.1. Nasal Passages and Associated Structures

Chemically induced lesions can occur along the length of the nasal cavity. Transverse sections through the most rostral aspects of the nose are not usually prepared possibly because this region of the nose is lined by keratinized stratified, squamous epithelium that is generally resistant to inhaled xenobiotics. However, high concentrations of highly volatile, water-soluble, irritant chemicals will induce toxicologically significant lesions (focal acute erosions or ulceration) in the squamous epithelium lining the vestibule or the ventral meatus, with or without inflammation. Ulceration may be severe on the tips of the more anterior turbinates, resulting in severe degeneration, necrosis or even loss of these structures. Prolonged exposure to irritants may induce epithelial hyperplasia and squamous metaplasia with or without hyperkeratosis, which are considered adaptive or protective responses and, less commonly, preneoplastic changes. Therefore, routine examination of the rostral aspects of the nose may be prudent in inhalation studies.

In the standard transverse sections at Levels I and II, the nasal passages are lined by transitional and respiratory epithelium, which are very sensitive to irritants. In both epithelial types, the degree of irritation, sensitivity of the mucosa to the irritant, and integrity of the mucociliary apparatus generally determine the course of the toxic response to inhaled chemicals and particles. The transitional epithelium may be especially sensitive. The increased sensitivity may be due in part to its anterior location in the nasal passage, to the thinner mucous blanket covering this epithelium, or to the paucity of ciliated

cells in this region, which results in a more slowly moving mucous blanket. Exposure to irritants such as ozone will cause proliferative and metaplastic responses in the transitional epithelium at concentrations that have little effect on the squamous, respiratory, or olfactory epithelia. The lesions may be superficial, or involve the full thickness of the epithelium extending to the lamina propria. If the irritant is relatively mild and the exposure is of short duration, goblet cell metaplasia and mucous secretion may be the only response. A purely serous inflammation is often seen in the nasal cavity in response to mild irritants; microscopically, the serous exudate contains few or no inflammatory cells. Highly irritant chemicals will elicit a more varied and extensive response in the epithelium and associated glands. This may include epithelial cell vacuolation and loss of cilia, or more severe forms of degeneration, inflammation, epithelial necrosis and ulceration, and necrosis, atrophy, or hyperostosis of the turbinates. During the reparative response, a single layer of flattened regenerating cells or, with continued injury, two or more layers of undifferentiated polyhedral cells, may replace the ciliated and secretory cells. These lesions may progress to hyperplasia, squamous metaplasia and hyperkeratosis, with persistent injury. Hyperplasia, particularly when atypical, may be an indication of incipient neoplasia. However, chemically induced neoplasia is rare in the upper respiratory tract.

The epithelium lining the ethmoid turbinates at Level III is predominantly olfactory epithelium and responds to irritants in a manner that is generally similar to that of the transitional and respiratory epithelia. However, there are some aspects of the response that are unique for this epithelium. Lesions may include epithelial cell vacuolation, degeneration, and/or necrosis, loss of sustentacular and neuroepithelial cells, and consequently, decreased thickness or atrophy of the epithelium. Regeneration follows and may be accompanied by epithelial and basal cell hyperplasia and, frequently, respiratory epithelial and

(A)

(B)
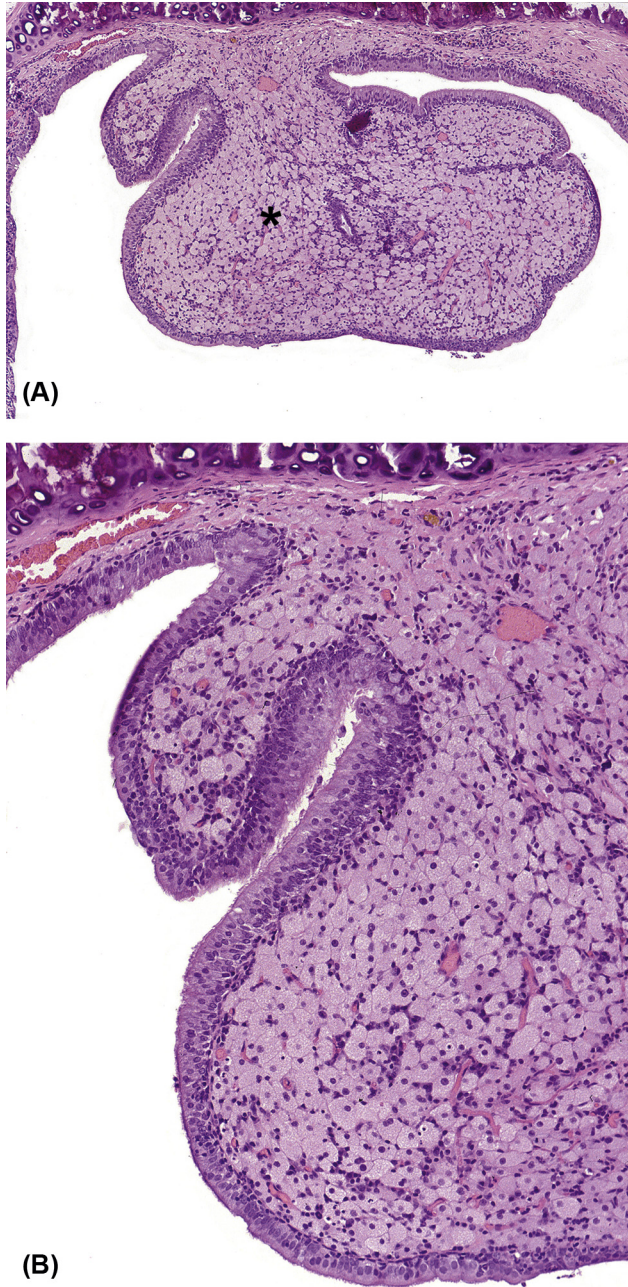
FIGURE 22.75   (A) Granular cell tumor (asterisk) of trachea forming a polypoid mass that extends into the lumen. (B) Higher magnification of (A). The neoplasm consists of polyhedral cells that have granular, eosinophilic cytoplasm.

(A)

(B)

FIGURE 22.76   (A) Hyperostosis in the ethmoid turbinates (arrows). The turbinate bone is irregularly thickened by increased amounts of woven bone (asterisk). (B) Higher magnification of (A).

squamous metaplasia. These epithelial responses may involve the submucosal (Bowman's) glands. These glands are often a prime target because the P-450 metabolizing enzyme content in these cells may produce metabolites that are toxic to the glandular epithelium. Atrophy and/or loss of the nerve bundles in the lamina propria is a common finding. The regenerative or hyperplastic epithelium is often quite disorganized, which may simply be due to a

lack of structural support normally maintained by the sustentacular cells. Respiratory epithelial metaplasia is a unique but common response to irritants. In addition to the epithelium of the ethmoid turbinates, this change is often found in the olfactory epithelium that lines the dorsal meatus in the Level II section of the nasal cavity. The olfactory neurons are extremely sensitive to the effects of noxious gases. The protection offered by the metaplastic respiratory epithelium may be due to a thicker mucus blanket.

The metabolic properties of the olfactory epithelium predispose this epithelium to toxicity following inhalation or systemic exposure to certain chemicals. This enzyme rich epithelium has carboxylesterases and aldehyde dehydrogenases that hydrolyze the components of certain chemicals to highly toxic acidic metabolites.

8.2. Larynx

The responses of the laryngeal epithelium to chemical exposure are generally similar to those that occur in the nasal cavity. Lesions are most commonly caused by inhalation exposure, but may also be seen with systemic toxicity. The lesions show distinct site specificity.

The respiratory type epithelium lining the base of the epiglottis in the transition zone from squamous to respiratory epithelium is the most sensitive site. Other commonly affected sites include the respiratory epithelium of the ventral pouch and the poorly keratinized squamous epithelium lining the medial aspects of the vocal processes of the arytenoid cartilages. Squamous metaplasia is by far the most common response followed by hyperplasia of the squamous epithelium lining the arytenoid cartilages. Although most common and severe in the standard section that contains the epiglottis, these lesions may occur at other sites in the laryngeal epithelium. Progression to neoplasia at predilection sites of injury in the larynx is extremely rare.

8.3. Trachea

The responses of the tracheal epithelium to chemical exposure are generally similar to those that occur in the nasal cavity and larynx, but are less common. Epithelial hyperplasia and squamous metaplasia are the most commonly observed chemically induced lesions. The anatomic structure of the tracheobronchial tree determines in part the effect of the irritant in the trachea. Experimental studies have established that the tracheal bifurcation (carina) is a common site for lesions and may respond to irritants with goblet cell hyperplasia, metaplasia, and dysplasia. Neoplasia is extremely rare.

9. MOLECULAR PATHOLOGY OF THE UPPER RESPIRATORY TRACT

The upper respiratory tract is one of the principal portals of entry into the body and is exposed to one of the highest concentrations of environmental toxicants in gaseous, vapor or particulate forms. The lining epithelium of the nasal respiratory and olfactory epithelium have abundant xenobiotic metabolizing capacity and assist in detoxifying the inhaled xenobiotics. More frequently, the inhaled xenobiotics are metabolized into greater reactive forms that can cause tissue injury. Chronic exposure to these xenobiotics can result in inflammation, tissue repair that may include proliferative lesions (regeneration and hyperplasia) and ultimately neoplasia.

Specific sites in the nasal epithelium are differentially susceptible to chemically induced toxicity and carcinogenicity (Harkema et al., 2006). The lesions may arise in the squamous, respiratory, transitional, or olfactory epithelium. Chemicals such as acetaminophen, coumarin, naphthalene, and phenacetin are metabolized to more toxic forms in the nasal epithelium (Genter, 2010). The respiratory and olfactory epithelia are very rich in both phase I and II metabolic enzymes and are thus the potential sites of injury or carcinogenesis after chemical exposure. Nasal epithelium expresses several xenobiotic metabolizing enzymes such as CYP1A1, CYP1A2, CYP2A5, CYP2B, CYP2C, CYP2E1, epoxide hydrolase, metallothioneins, superoxide dismutases, heme oxygenases, among others (Genter, 2010). Thus, the nose is one of the major extrahepatic sites for xenobiotic metabolism and is often the site of chemical-induced cytotoxicity and neoplasia in the upper respiratory tract (Jeffrey et al., 2006).

Within the olfactory epithelium, the distribution of metabolic enzymes varies with the anatomic location and as a result certain xenobiotic-induced toxicities are site specific. For example, in rats, alachlor causes respiratory epithelial metaplasia of the olfactory epithelium that subsequently progresses to neoplasia, primarily in the ethmoid turbinate region (Genter et al., 2000). In addition to alachlor, hydrogen sulfide, naphthalene, and vinyl acetate specifically cause cytotoxicity of the olfactory epithelium while relatively sparing the respiratory epithelium (Dodd et al., 2010; Lantz et al., 2003; Moulin et al., 2002). Formaldehyde causes squamous metaplasia and squamous cell carcinoma in the respiratory and transitional epithelium along the nasal septum and ventral meatus of the turbinates while relatively sparing the olfactory epithelium (St Clair et al., 1990).

Several molecular disturbances underlie xenobiotic-induced proliferative and neoplastic lesions. These may include alterations in gene expression and protein levels, formation of DNA adducts, and somatic mutations.

9.1. Alterations in Gene Expression

The global gene expression profiles of the various types of nasal epithelia have been described in the F344 (Hester et al., 2002) and Sprague-Dawley (Roberts et al., 2007) rats. The gene expression changes due to cigarette smoke exposure in the bronchial epithelium are reflected in the nasal epithelium. In Sprague-Dawley rats, acute inhalation exposure (3 h) to cigarette smoke caused alterations in genes encoding the oxidative stress-response pathways (Nrf2 signaling) and phase I and II metabolizing enzymes in the nasal epithelium and lungs. However, the same exposure over a 3-week period resulted in a markedly reduced oxidative stress and phase II responsive genes but not in phase I gene expression pattern indicating an adaptive response in both nasal epithelium and lungs (Gebel et al., 2004). Formaldehyde targets the respiratory epithelium causing dose dependent epithelial degeneration, respiratory cell hypertrophy, squamous metaplasia, cell proliferation and nasal tumors in the rat (Monticello et al., 1996). The toxic effects of endogenous and exogenous formaldehyde on the nasal cavity have been reported (Schroeter et al., 2014). At 2 ppm formaldehyde, pathways associated with cellular stress, thiol transport/reduction, inflammation and cellular proliferation were

upregulated, whereas, at 6 ppm and greater, pathways associated with cell cycle, DNA repair and apoptosis, ERBB, EGFR, WNT, TGF-beta, Hedgehog and Notch signaling were enriched. Formaldehyde exposure also altered miRNA expression in the nose (Andersen et al., 2010). Based on gene expression and toxicokinetic data, along with histological examination for cell proliferation, the authors suggested that there are dose/duration transitions for the formaldehyde-induced toxicity and carcinogenicity in the nasal tissues.

A total of 108 miRNAs were recognized to be formaldehyde-responsive in the rat nose; however, their expression was dose and duration dependent and most were present at only one-time point (Rager et al., 2014). Of these miRNAs, let-7a, let-7c, let-7f, and miR-10b were decreased in expression in nasopharyngeal carcinoma tissue in comparison to healthy tissue, suggesting that these miRNAs could potentially serve as biomarkers of preneoplasia (Li et al., 2011). These let-7 family of miRNAs act on apoptosis and cell proliferation pathways, suggesting that they may play a tumor suppressor role in formaldehyde exposure (Rager et al., 2014).

Alachlor is an herbicide that causes tumors in the nasal cavity, liver, thyroid and stomach in the rat. In the nasal cavity, the tumors arise primarily from the olfactory epithelium. Transcriptomic analysis revealed disruption of pathways associated with the extracellular matrix homeostasis (MMP-2, MMP-9), and olfactory mucosal oxidative stress (Heme oxygenase). Progression from the adenoma to adenocarcinoma was associated with alterations in the wnt/beta-catenin signaling pathway (Genter et al., 2002).

9.2. Alterations in Protein Expression

Examination of the protein expression in the nasal tissue is usually performed as a part of the validation of the transcriptomic studies and to examine the enzyme induction, to determine the cell of origin in cytotoxicity and neoplasia within the nasal epithelium. One of the major challenges for immunolocalization of the proteins in nasal epithelium is the tissue processing. The typical decalcification processes using either 5−10% formic acid or 10% hydrogen chloride may degrade the native protein structure within the nasal epithelium, and immunohistochemical localization of proteins in these decalcified tissues is typically not successful. Gentler decalcification methods such as 14% ethylenediaminetetraacetic acid (EDTA) at pH 7−7.6 for 2−3 weeks, RapidCal · Immuno (BBC biochemical, Mount Vernon, WA) for 2 h, or Immunocal (Decal Chemical Corporation, Congers, NY) for 6 days are preferred for rat nasal immunohistochemical studies. In spite of these gentler decalcification processes, independent optimization of the immunohistochemical parameters is still often

necessary for successful localization of proteins in nasal tissues (Harris et al., 2013). Alternatively, dissection of the respective nasal epithelium from various regions allows for direct measurement of the CYP enzymes and metabolic intermediates of nasal toxins (Dunston et al., 2013).

In response to chemical exposure (systemic or by inhalation route), the alterations in phase I and II enzymes can be monitored by various methods to gain an understanding of the mechanisms of cytotoxicity (Genter, 2006; Harkema et al., 2006). Based on the differential distribution of these biotransformation enzymes, differential regional susceptibility to various nasal toxins has been demonstrated (Morris and Shusterman, 2010). Naphthalene is metabolized within the nasal epithelium by CYP enzymes to an unstable 1,2-epoxide that undergoes further epoxidation and/or glutathione conjugation. Upon saturation of the CYP metabolic pathway, tissue injury occurs. Parenteral administration of naphthalene causes diffuse cytotoxicity of the nasal olfactory mucosa whereas with inhalation exposure, tissue injury is confined to dorsal medial meatus. Measuring the CYP enzymes and naphthalene metabolites within the nasal epithelium from the dorsal medial meatus and the ethmoturbinates from the distal regions demonstrated that the differential susceptibility of parenteral versus inhalation exposure was due to the differences in extent of naphthalene distribution within the tissues (Lee et al., 2005).

In inhalation studies, respiratory epithelial metaplasia is a common lesion in the olfactory epithelium. Identification of the native cytokeratins for each of the nasal epithelial types is essential to gain a greater understanding of the early metaplastic changes. Differential cytokeratin localization has been demonstrated in the various nasal epithelial cells and in the epithelial cells of the larynx, trachea and lungs of control and cigarette smoke exposed rats (Schlage et al., 1998).

9.3. DNA Adducts and Mutations in Nasal Tumors

DNA adducts resulting from xenobiotic exposure contribute to mutagenesis and carcinogenesis in the nose, as in other tissues. In general, the concentrations of DNA adducts within various tissues correlate with the target sites of neoplasia (Genter, 2010). For example, rodent nasal carcinogens such as 2,6-dimethylaniline, 2-methylaniline, dimethyl sulfate, propylene oxide, formaldehyde, tobacco-specific nitrosamines, beta-propiolactone, methylmethane sulfonate, and dimethylcarbamyl chloride form DNA adducts within the nasal epithelium. However, other rodent nasal carcinogens such as alachlor, wood dust extracts, and nickel subsulfide do not form DNA adducts.

These agents may cause nasal tumors through other mechanisms.

Formaldehyde is one of the most studied genotoxic nasal carcinogen in rodents. In rats, formaldehyde causes nasal squamous cell carcinomas in a concentration-dependent manner that parallels the formation of DNA-protein crosslinks and adducts (Heck et al., 1990; Kerns et al., 1983). Formaldehyde can cause inter- and intra-DNA crosslinks, base adducts and DNA-protein crosslinks. It induces *N*-hydroxymethyl mono-adducts primarily on guanine, adenine and cytosine, and *N*-methylene crosslinks between adjacent purines in DNA resulting in DNA damage (Kawanishi et al., 2014). Examination of *Tp53* mutations from formaldehyde-induced rat nasal squamous cell carcinomas indicated G:C to T:A/C:G transversions, and G:C to A:T transitions (Recio et al., 1992). The subsequent unrepaired DNA damage causes cytotoxicity, inflammation, and regenerative hyperplasia that eventually results in neoplasia (Monticello et al., 1991; Recio et al., 1992).

In summary, the lining epithelium of the nasal respiratory and olfactory epithelium have abundant xenobiotic metabolizing capacity and assist in detoxifying the inhaled xenobiotics. In some cases, however, these xenobiotic enzymes metabolize some chemicals to intermediates that cause a higher degree of cytotoxicity, and may result in neoplasia with prolonged exposure. The site specificity and the type of the cellular injury within the nose provide some indication on the mechanism of toxicity. However, examination of the molecular alterations within the specific cell types provides a more thorough understanding of the mechanisms of tissue injury.

REFERENCES

Andersen, M.E., Clewell 3rd, H.J., Bermudez, E., Dodd, D.E., Willson, G.A., Campbell, J.L., et al., 2010. Formaldehyde: integrating dosimetry, cytotoxicity, and genomics to understand dose-dependent transitions for an endogenous compound. Toxicol. Sci. 118, 716−731.

Bojsen-Møller, F., 1964. Topography of the nasal glands in rats and some other mammals. The Anat. Rec. 150, 11−24.

Bojsen-Møller, F., 1975. Demonstration of terminalis, olfactory, trigeminal and perivascular nerves in the rat nasal septum. J. Compar. Neurol. 159, 245−256.

Bojsen-Moller, F., Fahrenkrug, J., 1971. Nasal swell-bodies and cyclic changes in the air passage of the rat and rabbit nose. J. Anat. 110, 25−37.

Cesta, M.F., 2006. Normal structure, function, and histology of mucosa-associated lymphoid tissue. Toxicol. Pathol. 34, 599−608.

Corr, S.C., Gahan, C.C., Hill, C., 2008. M-cells: origin, morphology and role in mucosal immunity and microbial pathogenesis. FEMS Immunol. Med. Microbiol. 52, 2−12.

Dodd, D.E., Gross, E.A., Miller, R.A., Wong, B.A., 2010. Nasal olfactory epithelial lesions in F344 and SD rats following 1- and 5-day inhalation exposure to naphthalene vapor. Int J Toxicol. 29, 175−184.

Dunston, D., Ashby, S., Krosnowski, K., Ogura, T., Lin, W., 2013. An effective manual deboning method to prepare intact mouse nasal tissue with preserved anatomical organization. J. Visual. Exp. JoVE.

Gebel, S., Gerstmayer, B., Bosio, A., Haussmann, H.J., Van Miert, E., Muller, T., 2004. Gene expression profiling in respiratory tissues from rats exposed to mainstream cigarette smoke. Carcinogenesis. 25, 169−178.

Genter, M., 2010. Biomarkers of Nasal Toxicity in Experimental Animals, Toxicology of the Nose and Upper Airways. CRC Press, Boca Raton, pp. 151−166.

Genter, M.B., 2006. Molecular biology of the nasal airways: how do we assess cellular and molecular responses in the nose? Toxicol. Pathol. 34, 274−280.

Genter, M.B., Burman, D.M., Dingeldein, M.W., Clough, I., Bolon, B., 2000. Evolution of alachlor-induced nasal neoplasms in the Long-Evans rat. Toxicol. Pathol. 28, 770−781.

Genter, M.B., Burman, D.M., Vijayakumar, S., Ebert, C.L., Aronow, B.J., 2002. Genomic analysis of alachlor-induced oncogenesis in rat olfactory mucosa. Physiol. Genomics. 12, 35−45.

Graziadei, P.P.C., Graziadei, G.A.M., 1979. Neurogenesis and neuron regeneration in the olfactory system of mammals. I. Morphological aspects of differentiation and structural organization of the olfactory sensory neurons. J. Neurocytol. 8, 1−18.

Gross, E.A., Swenberg, J.A., Fields, S., Popp, J.A., 1982. Comparative morphometry of the nasal cavity in rats and mice. J. Anat. 135, 83−88.

Harkema, J., Morgan, K., 1996. Normal morphology of the nasal passages in laboratory rodents. In: Jones, T., Dungworth, D., Mohr, U. (Eds.), Respiratory System. Springer, Berlin Heidelberg, pp. 3−17.

Harkema, J.R., Carey, S.A., Wagner, J.G., 2006. The nose revisited: a brief review of the comparative structure, function, and toxicologic pathology of the nasal epithelium. Toxicol. Pathol. 34, 252−269.

Harris, N., Carter, C.A., Misra, M., Maronpot, R., 2013. Immunohistochemistry on decalcified rat nasal cavity: trials and successes. J. Histotechnol. 36, 92−99.

Hebel, R., Stromberg, M., 1976. Anatomy of the Laboratory Rat. The Williams and Wilkins Company, Baltimore.

Heck, H.D., Casanova, M., Starr, T.B., 1990. Formaldehyde toxicity-new understanding. Crit. Rev. Toxicol. 20, 397−426.

Hester, S.D., Benavides, G.B., Sartor, M., Yoon, L., Wolf, D.C., Morgan, K.T., 2002. Normal gene expression in male F344 rat nasal transitional and respiratory epithelium. Gene 285, 301−310.

Huard, J.M.T., Schwob, J.E., 1995. Cell cycle of globose basal cells in rat olfactory epithelium. Dev. Dyn. 203, 17−26.

Jang, W., Chen, X., Flis, D., Harris, M., Schwob, J.E., 2014. Label-retaining, quiescent globose basal cells are found in the olfactory epithelium. J. Compar. Neurol. 522, 731−749.

Jeffery, P.K., Reid, L., 1975. New observations of rat airway epithelium: a quantitative and electron microscopic study. J. Anatomy 120, 295−320.

Jeffrey, A.M., Iatropoulos, M.J., Williams, G.M., 2006. Nasal cytotoxic and carcinogenic activities of systemically distributed organic chemicals. Toxicol. Pathol. 34, 827−852.

Jenkins, P.M., McEwen, D.P., Martens, J.R., 2009. Olfactory cilia: linking sensory cilia function and human disease. Chem. Senses. 34, 451−464.

Katz, S., Merzel, J., 1977. Distribution of epithelia and glands of the nasal septum mucosa in the rat. Cells Tissues Organs. 99, 58−66.

Kawanishi, M., Matsuda, T., Yagi, T., 2014. Genotoxicity of formaldehyde: molecular basis of DNA damage and mutation. Front. Environ. Sci. 2.

Kerns, W.D., Pavkov, K.L., Donofrio, D.J., Gralla, E.J., Swenberg, J.A., 1983. Carcinogenicity of formaldehyde in rats and mice after long-term inhalation exposure. Cancer Res. 43, 4382−4392.

Lantz, R.C., Orozco, J., Bogdanffy, M.S., 2003. Vinyl acetate decreases intracellular pH in rat nasal epithelial cells. Toxicol. Sci. 75, 423−431.

Lee, M.G., Phimister, A., Morin, D., Buckpitt, A., Plopper, C., 2005. In situ naphthalene bioactivation and nasal airflow cause region-specific injury patterns in the nasal mucosa of rats exposed to naphthalene by inhalation. J. Pharmacol. Exp. Ther. 314, 103−110.

Lewis, D.J., 1981. Factors affecting the distribution of tobacco smoke-induced lesions in the rodent larynx. Toxicol. Lett. 9, 189−194.

Lewis, D.J., 1991. Morphological assessment of pathological changes within the rat larynx. Toxicol. Pathol. 19, 352−357.

Li, T., Chen, J.X., Fu, X.P., Yang, S., Zhang, Z., Chen, K.H., et al., 2011. microRNA expression profiling of nasopharyngeal carcinoma. Oncol. Rep. 25, 1353−1363.

Marin, M.L., Lane, B.P., Gordon, R.E., Drummond, E., 1979. Ultrastructure of rat tracheal epithelium. Lung 156, 223−236.

Menco, B.P.M., 1997. Ultrastructural aspects of olfactory signaling. Chem. Senses. 22, 295−311.

Mendoza, A.S., 1993. Morphological studies on the rodent main and accessory olfactory systems: the regio olfactoria and vomeronasal organ. Ann. Anatomy Anatomischer Anzeiger. 175, 425−446.

Mery, Sp, Gross, E.A., Joyner, D.R., Godo, M., Morgan, K.T., 1994. Nasal diagrams: a tool for recording the distribution of nasal lesions in rats and mice. Toxicol. Pathol. 22, 353−372.

Monteiro-Riviere, N.A., Popp, J.A., 1984. Ultrastructural characterization of the nasal respiratory epithelium in the rat. Am. J. Anat. 169, 31−43.

Monticello, T.M., Miller, F.J., Morgan, K.T., 1991. Regional increases in rat nasal epithelial cell proliferation following acute and subchronic inhalation of formaldehyde. Toxicol. Appl. Pharmacol. 111, 409−421.

Monticello, T.M., Swenberg, J.A., Gross, E.A., Leininger, J.R., Kimbell, J.S., Seilkop, S., et al., 1996. Correlation of regional and nonlinear formaldehyde-induced nasal cancer with proliferating populations of cells. Cancer Res. 56, 1012−1022.

Morgan, K.T., Monticello, T.M., 1990. Airflow, gas deposition, and lesion distribution in the nasal passages. Environ. Health Perspect. 85, 209−218.

Morgan, K.T., Monticello, T.M., Patra, A.L., Fleishman, A., 1989. Preparation of rat nasal airway casts and their application to studies of nasal airflow. In: Crapo, J.D., Smolko, E.D., Miller, F.J., Graham, J.A., Hayes, W.A. (Eds.), Extrapolation of Dosimetric Relationships for Inhaled Particles and Gases. Academic Press, Inc, San Diego, California, pp. 45−58.

Morris, J., Shusterman, D., 2010. Nasal enzymology and its relevance to nasal toxicity and disease pathogenesis. Toxicology of the Nose and Upper Airways. CRC Press, Boca Raton, pp. 82−98.

Moulin, F.J., Brenneman, K.A., Kimbell, J.S., Dorman, D.C., 2002. Predicted regional flux of hydrogen sulfide correlates with distribution of nasal olfactory lesions in rats. Toxicol. Sci. 66, 7−15.

Naguro, T., Iwashita, K., 1992. Olfactory epithelium in young adult and aging rats as seen with high-resolution scanning electron microscopy. Microscopy Res. Tech. 23, 62−75.

Nomura, T., Takahashi, S., Ushiki, T., 2004. Cytoarchitecture of the normal rat olfactory epithelium: light and scanning electron microscopic studies. Arch. Histol. Cytol. 67, 159−170.

NTP, 1978. Bioassay of 1,4-dioxane for possible carcinogenicity. Natl. Cancer Inst. Carcinogenesis Tech. Rep. Ser. 80, 1−123.

NTP, 1979. Bioassay of p-cresidine for possible carcinogenicity. Natl. Cancer Inst. Carcinogenesis Tech. Rep. Ser. 142, 1−123.

NTP, 1982a. Carcinogenesis bioassay of 1,2-dibromo-3-chloropropane (CAS No. 96-12-8) in F344 rats and B6C3F1 mice (inhalation study). Natl. Toxicol. Program Tech. Rep. Ser. 206, 1−174.

NTP, 1982b. Carcinogenesis bioassay of 1,2-dibromoethane (CAS No. 106-93-4) in F344 rats and B6C3F1 mice (inhalation study). Natl. Toxicol. Program Tech. Rep. Ser. 210, 1−163.

NTP, 1985. NTP toxicology and carcinogenesis studies of propylene oxide (CAS no. 75-56-9) in F344/N rats and B6C3F1 mice (inhalation studies). Natl. Toxicol. Program Tech. Rep. Ser. 267, 1−168.

NTP, 1986. NTP toxicology and carcinogenesis studies of dimethylvinyl chloride (1-chloro-2-methylpropene) (CAS No. 513-37-1) in F344/N rats and B6C3F1 mice (gavage studies). Natl. Toxicol. Program Tech. Rep. Ser. 316, 1−238.

NTP, 1988. NTP toxicology and carcinogenesis studies of 1,2-epoxybutane (CAS No. 106-88-7) in F344/N rats and B6C3F1 mice (inhalation studies). Natl. Toxicol Program Tech Rep Ser. 329, 1−176.

NTP, 1990. NTP toxicology and carcinogenesis studies of 2,6-Xylidine (2,6-dimethylaniline) (CAS No. 87-62-7) in Charles river CD rats (feed studies). Natl Toxicol Program Tech Rep Ser. 278, 1−138.

NTP, 1993. NTP toxicology and carcinogenesis studies of 2,3-dibromo-1-propanol (CAS No. 96-13-9) in F344/N rats and B6C3F1 mice (dermal studies). Natl. Toxicol. Program Tech. Rep. Ser. 400, 1−202.

NTP, 1999a. NTP toxicology and carcinogenesis studies of pentachlorophenol (CAS NO. 87-86-5) in F344/N rats (feed studies). Natl. Toxicol. Program Tech. Rep. Ser. 483, 1−182.

NTP, 1999b. Toxicology and carcinogenesis studies of furfuryl alcohol (CAS No. 98-00-0) in F344/N rats and B6C3F1 mice (inhalation studies). Natl. Toxicol. Program Tech. Rep. Ser. 482, 1−248.

NTP, 2000. Toxicology and carcinogenesis studies of naphthalene (cas no. 91-20-3) in F344/N rats (inhalation studies). Natl. Toxicol. Program Tech. Rep. Ser. 1−173.

NTP, 2008. Toxicology and carcinogenesis studies of propargyl alcohol (CAS No. 107-19-7) in F344/N rats and B6C3F1 mice (inhalation studies). Natl. Toxicol. Program Tech. Rep. Ser. 1−172.

NTP, 2009. Toxicology and carcinogenesis studies of cumene (CAS No. 98-82-8) in F344/N rats and B6C3F1 mice (inhalation studies). Natl. Toxicol. Program Tech. Rep. Ser. 1−200.

NTP, 2012. Toxicology and carcinogenesis studies of N,N-dimethyl-p-toluidine (CAS No. 99-97-8) in F344/N rats and B6C3F1/N mice (gavage studies). Natl. Toxicol. Program Tech. Rep. Ser. 1−211.

Parent, R.A., 2015. Appendix 1 - architecture of nasal passages and larynx. In: Parent, R.A. (Ed.), Comparative Biology of the Normal Lung, second ed. Academic Press, San Diego, pp. 731−746.

Plopper, C.G., Mariassy, A.T., Wilson, D.W., Alley, J.L., Nishio, S.J., Nettesheim, P., 1983. Comparison of nonciliated tracheal epithelial cells in six mammalian species: ultrastructure and population densities. Exp. Lung Res. 5, 281−294.

Rager, J.E., Moeller, B.C., Miller, S.K., Kracko, D., Doyle-Eisele, M., Swenberg, J.A., et al., 2014. Formaldehyde-associated changes in microRNAs: tissue and temporal specificity in the rat nose, white blood cells, and bone marrow. Toxicol. Sci. 138, 36−46.

Recio, L., Sisk, S., Pluta, L., Bermudez, E., Gross, E.A., Chen, Z., et al., 1992. p53 mutations in formaldehyde-induced nasal squamous cell carcinomas in rats. Cancer Res. 52, 6113−6116.

Renne, R., Brix, A., Harkema, J., Herbert, R., Kittel, B., Lewis, D., et al., 2009. Proliferative and nonproliferative lesions of the rat and mouse respiratory tract. Toxicol. Pathol. 37, 5S−73S.

Renne, R.A., Gideon, K.M., 2006. Types and patterns of response in the Larynx following inhalation. Toxicol. Pathol. 34, 281−285.

Renne, R.A., Gideon, K.M., Miller, R.A., Mellick, P.W., Grumbein, S. L., 1992. Histologic methods and interspecies variations in the laryngeal histology of F344/N rats and B6C3F1 mice. Toxicol. Pathol. 20, 44−51.

Reynolds, S.D., Pinkerton, K.E., Mariassy, A.T., 2015. Chapter 6 - Epithelial Cells of Trachea and Bronchi A2 - Parent, Richard A, Comparative Biology of the Normal Lung. Second Edition Academic Press, San Diego, pp. 61−81.

Roberts, E.S., Soucy, N.V., Bonner, A.M., Page, T.J., Thomas, R.S., Dorman, D.C., 2007. Basal gene expression in male and female Sprague-Dawley rat nasal respiratory and olfactory epithelium. Inhal. Toxicol. 19, 941−949.

Schlage, W.K., Bulles, H., Friedrichs, D., Kuhn, M., Teredesai, A., Terpstra, P.M., 1998. Cytokeratin expression patterns in the rat respiratory tract as markers of epithelial differentiation in inhalation toxicology. II. Changes in cytokeratin expression patterns following 8-day exposure to room-aged cigarette sidestream smoke. Toxicol. Pathol. 26, 344−360.

Schreider, J.P., Raabe, O.G., 1981. Anatomy of the nasal-pharyngeal airway of experimental animals. Anat. Rec. 200, 195−205.

Schroeter, J.D., Campbell, J., Kimbell, J.S., Conolly, R.B., Clewell, H.J., Andersen, M.E., 2014. Effects of endogenous formaldehyde in nasal tissues on inhaled formaldehyde dosimetry predictions in the rat, monkey, and human nasal passages. Toxicol. Sci. 138, 412−424.

Smith, G., 1977. Structure of the normal rat larynx. Lab. Anim. 11, 223−228.

Spit, B.J., Hendriksen, E.G.J., Bruijntjes, J.P., Kuper, C.F., 1989. Nasal lymphoid tissue in the rat. Cell Tissue Res. 255, 193−198.

St Clair, M.B., Gross, E.A., Morgan, K.T., 1990. Pathology and cell proliferation induced by intra-nasal instillation of aldehydes in the rat: comparison of glutaraldehyde and formaldehyde. Toxicol. Pathol. 18, 353−361.

Uraih, L.C., Maronpot, R.R., 1990. Normal histology of the nasal cavity and application of special techniques. Environ. Health Perspect. 85, 187−208.

Vaccarezza, O.L., Sepich, L.N., Tramezzani, J.H., 1981. The vomeronasal organ of the rat. J. Anatomy 132, 167−185.

Vollrath, M., Altmannsberger, M., Weber, K., Osborn, M., 1985. An ultrastructural and immunohistological study of the rat olfactory epithelium: unique properties of olfactory sensory cells. Differentiation 29, 243−253.

Ward, J.M., Yoon, M., Anver, M.R., Haines, D.C., Kudo, G., Gonzalez, F.J., et al., 2001. Hyalinosis and Ym1/Ym2 gene expression in the stomach and respiratory tract of 129S4/SvJae and wild-type and CYP1A2-Null B6,129 mice. Am. J. Pathol. 158, 323−332.

Weiler, E., Farbman, A.I., 2003. The septal organ of the rat during postnatal development. Chem. Senses. 28, 581−593.

Winkelmann, A., Noack, T., 2010. The Clara cell: a "Third Reich eponym"? European Respir. J. 36, 722−727.

FURTHER READING—MOLECULAR PATHOLOGY

Crosby, R.M., Richardson, K.K., Craft, T.R., Benforado, K.B., Liber, H. L., Skopek, T.R., 1988. Molecular analysis of formaldehyde-induced mutations in human lymphoblasts and *E. coli*. Environ. Mol. Mutagen. 12, 155−166.

Dunnick, J.K., Merrick, B.A., Brix, A., Morgan, D.L., Gerrish, K., Wang, Y., et al., 2016. Molecular changes in the nasal cavity after N, N-dimethyl-p-toluidine exposure. Toxicol Pathol. 44, 835−847.

Green, T., Lee, R., Toghill, A., Meadowcroft, S., Lund, V., Foster, J., 2001. The toxicity of styrene to the nasal epithelium of mice and rats: studies on the mode of action and relevance to humans. Chemico-biol. Interact. 137, 185−202.

Rager, J.E., Smeester, L., Jaspers, I., Sexton, K.G., Fry, R.C., 2011. Epigenetic changes induced by air toxics: formaldehyde exposure alters miRNA expression profiles in human lung cells. Environ. Health Perspect. 119, 494−500.

Roberts, E.S., Thomas, R.S., Dorman, D.C., 2008. Gene expression changes following acute hydrogen sulfide (H2S)-induced nasal respiratory epithelial injury. Toxicol. Pathol. 36, 560−567.

Sridhar, S., Schembri, F., Zeskind, J., Shah, V., Gustafson, A.M., Steiling, K., et al., 2008. Smoking-induced gene expression changes in the bronchial airway are reflected in nasal and buccal epithelium. BMC Genomics 9, 259.